INVESTIGATIONS ON ELASTIC AND INELASTIC NUCLEAR SCATTERING AND POLARISATION

by

FRIEDRICH JOHANNES WILHELM HAHNE

Thesis submitted for the degree of

DOCTOR OF PHILOSOPHY

in the Faculty of Science, University of Cape Town

March, 1967

Cape Town

ACKNOWLEDGEMENTS

I wish to express my gratitude to:

Professor W.E. Frahn, my promoter, for his guidance and for many profitable discussions

The South African Council for Scientific and Industrial Research for making my stay at the University of Cape Town possible, and in particular to Drs. A. Strasheim and W.L. Rautenbach for their interest

The staff of the University Computer Department, Mr. W.B. de Villiers-Smit and Mrs. W. Ensor, for their cooperation

The South African Mutual Life Assurance Society (The Old Mutual) for computing facilities on the Orion II and in particular Messrs. E.P.H. Bieber, S.H.J. Leprini, M.J. Swanepoel and Mrs. G.J.S. Hartsuiker for help rendered

Dr. G. Wiechers and Mr. J.M. Potgieter for discussions and for the use of some of their computer programmes

Mrs. E.B. Prosser for typing the manuscript

I wish to thank my wife for her help and encouragement.

CONTENTS

ABSTRACT

Elastic and inelastic scattering of nuclear particles are treated in a partial wave formalism. It is assumed that only a few partial waves having large angular momenta contribute significantly to the scattering amplitude. Parameterised elastic S-matrix elements are used in the Austern-Blair theory to obtain the inelastic S-matrix elements. Relations between elastic and inelastic cross sections and polarisations are derived. The resulting phase rules are discussed. A modification of the Austern-Blair theory makes it possible to describe angular correlation measurements. The theory is compared with optical model and distorted wave Born approximation calculations.

1. INTRODUCTION

The method most widely used for the description of elastic and inelastic scattering is the extended optical model. The inelastic cross sections are either calculated by coupled channel methods (Buc 61) or in distorted wave Born approximation (DWBA). The interactions are described by potentials, and wave functions are calculated in coordinate space. These are subsequently used in the calculation of other direct reactions.

It has been pointed out (Igo 59, Dri 63) that, for elastic scattering of strongly absorbed particles (e.g. α-particles), only the surface properties of the potentials are of importance. The potential in the nuclear interior is not unique, which implies that the interior parts of the wave function are ambiguous.

Scattering cross sections and polarisations are determined only by the asymptotic properties of the wave functions. These are fully described by the S-matrix. Instead of describing the interactions by means of potentials one can try to determine directly the S-matrix elements. At low energies this is done by direct phase shift analyses. However, with increasing energy the number of partial waves increases and this method becomes impracticable. For composite particles the absorption is strong enough to ensure that the low angular momentum partial waves are purely ingoing. This is borne out by optical model (OM) calculations. On the other hand, the high angular momentum partial waves are excluded from the interaction by the centrifugal barrier and become standing waves. In an intermediate region in ℓ-space, called the surface region, we have a gradual transition from ingoing to standing waves.

The simplest description of this situation is the Blair

model (Bla 54) which assumes that the elastic S-matrix elements η_ℓ change discontinuously from zero to unity. This model was generalised by Frahn and Venter (Fra 63, Ven 63, Fra 64a) whose strong absorption model (SAM) describes η_ℓ as a smooth function of ℓ and contains earlier formulations of a similar nature as special cases.

Austern and Blair have derived, in the adiabatic approximation, simple relations between elastic and inelastic S-matrix elements in ℓ-space.

The present work is based on these two theories. Polarisation effects in elastic and inelastic scattering are particularly emphasised. Like Austern and Blair we approach the problem of finding an S-matrix description by using potential model arguments. For inelastic scattering we use the DWBA formalism and study radial integrals, which are actually inelastic S-matrix elements. Furthermore, we assume certain properties of potentials and derive relations for the S-matrix elements. Alternatively, we could have postulated these S-matrix properties without the recourse to a potential model. At the moment our present approach appears to be the safer one. Easy comparison with OM and DWBA calculations is also facilitated.

In section 2 the formalism for elastic and inelastic scattering is briefly summarised. For inelastic scattering we confine ourselves to one-phonon excitations in the macroscopic collective model. Both the complex and the spin-orbit potentials are deformed.

The structure of the S-matrix elements calculated from the OM and DWBA is considered in section 3.

In section 4, fairly general analytic forms are assumed for η_ℓ as a function of ℓ. From these, cross sections and polarisations of elastically scattered spin-o, $\frac{1}{2}$ and 1 particles are calculated.

In section 5, the Austern-Blair theory is used to calculate inelastic cross sections and polarisations of spin-o and spin-$\frac{1}{2}$ particles. The relations between the elastic and inelastic expressions are discussed.

The Austern-Blair theory is slightly modified in section 6. This makes it possible to give an improved description of angular correlation measurements. The modified theory is also compared with DWBA calculations, particularly with regard to the deformation distances.

2. FORMALISM FOR ELASTIC AND INELASTIC SCATTERING

In this section we summarise partial wave expressions for elastic and inelastic scattering. The results are presented in a convenient form for the use in subsequent sections.

We consider the scattering of a light projectile of arbitrary spin from a heavy target nucleus, assuming either target spin to be zero or interactions which are independent of the target spin.

2.1 Density matrix

For the description of polarisation phenomena it is convenient to introduce the density matrix $\underset{\sim}{\rho}$ in spin space. If the density matrix of the incident beam and the scattering matrix are known the cross section and the polarisation in the final state are obtained by a straight-forward calculation. The results for multiple scattering are also easily obtained.

The wave function $|\psi\rangle$ of an assembly is given by

$$|\Psi\rangle = \Sigma\, a_n |n\rangle \quad , \qquad \Sigma |a_n|^2 = 1 \quad , \tag{2.1}$$

where $|n\rangle$ are a given set of basis vectors. The density matrix is then defined by

$$\rho_{nn'} = a_n a^*_{n'} \quad , \qquad tr(\underset{\sim}{\rho}) = 1 \quad . \tag{2.2}$$

Normally, however, we are only interested in the density matrix defined in a certain subspace. In our case this is defined by the spin projection eigenvalues m. We denote the other quantum numbers by ν and define the density matrix by

$$\rho_{m\,m'} = \frac{1}{N} \sum_{\nu=1}^{N} a_m(\nu)\, a^*_{m'}(\nu) \quad . \tag{2.3}$$

The expectation value of an operator $\underset{\sim}{o}$ is given by

$$\langle \underset{\sim}{o} \rangle = tr(\underset{\sim}{\rho}\, \underset{\sim}{o}) \quad . \tag{2.4}$$

The density matrix can be expanded in terms of statistical tensors t_{kq} by

$$\rho_{mm'} = (2s+1)^{-1} \sum_{kq} t_{kq}\, \hat{k} \langle s\, k\, m\, q \,|\, s\, m' \rangle \tag{2.5}$$

and by inversion, we obtain

$$t_{kq} = \hat{k} \sum_{m} \rho_{m\,m'} \langle s\, k\, m\, q \,|\, s\, m' \rangle \quad , \tag{2.6}$$

where $\hat{x} \equiv (2x+1)^{\frac{1}{2}}$ and s is the spin of the particles.

The triangular condition limits the range of k to $o \leq k \leq 2s$. For spin-$\frac{1}{2}$ particles we have only the scalar component t_{oo} and the vector components t_{iq}. For spin-1 partilces we have, in addition, the tensor (or alignment) components t_{2q}.

An unpolarised beam is defined by

$$t_{kq} = 0 \qquad \forall \qquad k \neq 0 \quad , \tag{2.7}$$

and this implies (eq. (2.5)) that

$$\rho_{m\,m'} = (2s+1)^{-1}\, \delta_{m\,m'} \quad . \tag{2.8}$$

From the definition (2.2) or (2.3) it is seen that $\underset{\sim}{\rho}$ is Hermitian. It thus follows that

$$t_{kq} = (-1)^q\, t^*_{k\,-q} \quad . \tag{2.9}$$

From eq. (2.5) we have

$$t_r(\underset{\sim}{\rho}) = t_{00} = 1 \,. \tag{2.10}$$

The components t_{kq} can be interpreted in terms of spin expectation values. By inserting eq. (2.5) in eq. (2.4) and applying the Wigner-Eckart theorem to $\langle sm|S_q|sm'\rangle$ we obtain

$$\langle S_q \rangle = \tfrac{1}{\sqrt{3}}\left[s(s+1)\right]^{\frac{1}{2}} t_{1q} \,, \tag{2.11}$$

$$\langle S_q S_{q'} \rangle = s(s+1)\hat{s} \sum_{KQ} \hat{K}\, t_{KQ} (-1)^Q \begin{pmatrix} K & 1 & 1 \\ Q & -q & -q' \end{pmatrix} \cdot$$
$$\cdot W(s\,1\,s\,;\,s\,K) \,, \tag{2.12}$$

where

$$S_0 = S_z \,; \quad S_{\pm 1} = \mp \tfrac{1}{\sqrt{2}} (S_x \pm i S_y) \,. \tag{2.13}$$

In eq. (2.12) the round brackets represent a Wigner 3j-symbol and W denotes a Racah coefficient (Bri 62).

From eqs. (2.9), (2.11) and (2.13) it follows that

$$\begin{aligned} \langle S_y \rangle &= -\left[\tfrac{2}{3} s(s+1)\right]^{\frac{1}{2}} \mathrm{Im}\, t_{11} \,, \\ \langle S_x \rangle &= \left[\tfrac{2}{3} s(s+1)\right]^{\frac{1}{2}} \mathrm{Re}\, t_{11} \,, \\ \langle S_z \rangle &= \langle S_0 \rangle = \left[\tfrac{1}{3} s(s+1)\right]^{\frac{1}{2}} t_{10} \,. \end{aligned} \tag{2.14}$$

For spin-1 particles we can easily identify

$$t_{20} = \frac{1}{\sqrt{2}} \left[3 \langle S_0 S_0 \rangle - 2 \right] \quad ,$$

$$t_{2\pm1} = \sqrt{\frac{3}{2}} \left[\langle S_0 S_{\pm1} \rangle + \langle S_{\pm1} S_0 \rangle \right] \quad , \qquad (2.15)$$

$$t_{2\pm2} = \sqrt{3} \langle S_{\pm1} S_{\pm1} \rangle \quad .$$

In a scattering process, an amplitude $f_{mm'}(\theta\phi)$ is defined. Its properties for elastic and direct inelastic scattering are discussed in sections 2.2 and 2.3. If the incoming beam is described by the density matrix $\underset{\sim}{\rho}^{(1)}$, the angular distribution of the outgoing particles is given by (Gol 64)

$$\sigma(\theta) = \mathrm{tr} \left(\underset{\sim}{f}(\theta) \, \underset{\sim}{\rho}^{(1)} \, \underset{\sim}{f}^{+}(\theta) \right) \quad , \qquad (2.16)$$

and the density matrix for the scattered beam becomes (Gol 64)

$$\underset{\sim}{\rho}^{(2)} = \frac{\underset{\sim}{f}(\theta) \, \underset{\sim}{\rho}^{(1)} \, \underset{\sim}{f}^{+}(\theta)}{\sigma(\theta)} \quad , \qquad (2.17)$$

where $\underset{\sim}{\rho}^{(1)}$ and $\underset{\sim}{\rho}^{(2)}$ are described in the same system of axes. Eq. (2.17) can be used for multiple scattering by repetition, but one must always transform to the relevant system of axes. When the axes are turned through the Euler angles (α, β, γ), the density matrix in the new system is given by (Bri 62)

$$\rho'_{m\,m'} = \sum_{\mu\mu'} D^{s\,*}_{\mu\,m}(\alpha\beta\gamma) \, \rho_{\mu\mu'} \, D^{s}_{\mu'\,m}(\alpha\beta\gamma) \quad . \qquad (2.18)$$

2.2 Elastic scattering

In a time-independent description, the total wave function in the asymptotic region is given by

$$\psi_{m_s} \cong \chi_{m_s} e^{i\underset{\sim}{k}\cdot\underset{\sim}{r}} + \sum_{m_s'} f_{m_s' m_s}(\theta,\varphi)\, \chi_{m_s'}\, \frac{e^{ikr}}{r} \quad .$$

The first term represents the incident plane wave, while the second term represents the scattered wave. If the quantisation axis is chosen along the incident beam direction ($\underset{\sim}{k}$), and the y-axis perpendicular to the scattering plane, the scattering amplitude $f_{m_s' m_s}(\theta,o)$ takes the form (Bla 52)

$$f_{m_s' m_s}(\theta) = \frac{i\sqrt{\pi}}{k} \sum_{j\ell\ell'\mu'} i^{\ell-\ell'}\, \hat{\ell}\, \langle \ell s\, o\, m_s | j\, m_s\rangle \langle \ell' s\, \mu' m_s' | j\, m_s\rangle \cdot \left(\delta_{\ell\ell'} - S^{j}_{\ell'\ell}\right) Y_{\ell'}^{\mu'}(\theta,0) \quad , \tag{2.19}$$

where $s^{j}_{\ell',\ell} = \eta^{j}_{\ell',\ell}\, e^{i(\sigma_\ell + \sigma_{\ell'})}$.

Here σ_ℓ are the point-charge Coulomb phase shifts and $\eta^{j}_{\ell',\ell}$ are the "nuclear" reflection coefficients. Parity conservation requires that $\ell'-\ell$ = even, while time reversal requires that $S^{j}_{\ell',\ell} = S^{j}_{\ell\ell'}$.

For s = o, we have

$$f(\theta) = f_c(\theta) + \frac{i\sqrt{\pi}}{k} \sum_{\ell} \hat{\ell}\, (1-\eta_\ell)\, e^{2i\sigma_\ell}\, Y_\ell^{o}(\theta,0) \quad , \tag{2.20}$$

$$\sigma(\theta) = |f(\theta)|^2 .$$

Here, $f_c(\theta)$ is the Coulomb scattering amplitude.

For s = $\frac{1}{2}$, we have

$$f_{m_s' m_s} = \begin{pmatrix} A & B \\ -B & A \end{pmatrix} ,$$

$$A(\theta) = f_c(\theta) + \frac{i\sqrt{\pi}}{k} \sum_{\ell} \left[(\ell+1)\alpha_\ell^+ + \ell\alpha_\ell^- \right] e^{2i\sigma_\ell} \hat{\ell}^{-1} Y_\ell^0(\theta,0) , \tag{2.21}$$

$$B(\theta) = - \frac{i\sqrt{\pi}}{k} \sum_{\ell} (\alpha_\ell^+ - \alpha_\ell^-) e^{2i\sigma_\ell} \hat{\ell}^{-1} \{\ell(\ell+1)\}^{\frac{1}{2}} Y_\ell^1(\theta,0) ,$$

with $\alpha_\ell^\pm = 1 - \eta_\ell^{\ell \pm \frac{1}{2}}$. In the case of an unpolarised incident beam,

$$\sigma(\theta) = |A|^2 + |B|^2 ,$$

$$\sigma(\theta) P_y(\theta) = 2 \mathrm{Im}(AB^*) , \quad P_x = P_z = 0 . \tag{2.22}$$

Here, $P_y(\theta)$ represents the polarisation of the scattered beam along the direction $\underset{\sim}{k}_i \times \underset{\sim}{k}_f$.

For s = 1, $\underset{\sim}{f}$ is a 3 × 3 matrix and we have

$$f_{m'm} = \begin{pmatrix} B & C & E \\ -D & A & D \\ E & -C & B \end{pmatrix} ,$$

$$A = f_c + \frac{i\sqrt{\pi}}{k} \sum_{\ell} \Big[\{\ell\alpha_\ell^- + (\ell+1)\alpha_\ell^+\} e^{2i\sigma_\ell} \hat{\ell}^{-1} Y_\ell^0 - \beta_\ell \{\ell(\ell+1)\}^{\frac{1}{2}} \{ \hat{\ell+1}^{-1} Y_{\ell+1}^0 + \hat{\ell-1}^{-1} Y_{\ell-1}^0 \} \Big] ,$$

$$B = f_c + \frac{i\sqrt{\pi}}{k} \sum_{\ell} \Big[\tfrac{1}{2} \{ (\ell-1)\alpha_\ell^- + (2\ell+1)\alpha_\ell^0 + (\ell+2)\alpha_\ell^+ \} e^{2i\sigma_\ell} \hat{\ell}^{-1} Y_\ell^0 + \tfrac{1}{2} \beta_\ell \{\ell(\ell+1)\}^{\frac{1}{2}} \{ \hat{\ell+1}^{-1} Y_{\ell+1}^0 + \hat{\ell-1}^{-1} Y_{\ell-1}^0 \} \Big] ,$$

$$C = \frac{i\sqrt{\pi}}{k}\sum_{\ell}\frac{1}{\sqrt{2}}\Big[(\alpha_\ell^- - \alpha_\ell^+)\, e^{2i\sigma_\ell}\,\{\ell(\ell+1)\}^{\frac{1}{2}}\,\hat{\ell}^{-1}\,Y_\ell^1 - \beta_\ell\{[\ell(\ell+2)]^{\frac{1}{2}}\,\hat{\ell+1}^{-1}\,Y_{\ell+1}^1 - [(\ell+1)(\ell-1)]^{\frac{1}{2}}\,\hat{\ell-1}^{-1}\,Y_{\ell-1}^1\}\Big]\,, \tag{2.23}$$

$$D = \frac{i\sqrt{\pi}}{k}\sum_{\ell}\frac{1}{\sqrt{2}}\Big[\{(\ell^2-1)\alpha_\ell^- + (2\ell+1)\alpha_\ell^0 - (\ell^2+2\ell)\alpha_\ell^+\}\, e^{2i\sigma_\ell}\,\{\ell(\ell+1)\}^{\frac{1}{2}}\,\hat{\ell}^{-1}\,Y_\ell^1 + \beta_\ell\{[\ell(\ell+2)]^{\frac{1}{2}}\,\hat{\ell+1}^{-1}\,Y_{\ell+1}^1 - [(\ell+1)(\ell-1)]^{\frac{1}{2}}\,\hat{\ell-1}^{-1}\,Y_{\ell-1}^1\}\Big]\,,$$

$$E = \frac{i\sqrt{\pi}}{k}\sum_{\ell}\frac{1}{2}\Big[\{(\ell+1)\alpha_\ell^- - (2\ell+1)\alpha_\ell^0 + \ell\alpha_\ell^+\}\, e^{2i\sigma_\ell}\,\{\ell(\ell+1)\}^{-1}\left\{\frac{(\ell+2)!}{(\ell-2)!}\right\}^{\frac{1}{2}}\hat{\ell}^{-1}\,Y_\ell^2 + \frac{1}{2}\beta_\ell\{[(\ell+2)(\ell+3)]^{\frac{1}{2}}\,\hat{\ell+1}^{-1}\,Y_{\ell+1}^2 + [(\ell-2)(\ell-1)]^{\frac{1}{2}}\,\hat{\ell-1}^{-1}\,Y_{\ell-1}^2\}\Big]\,,$$

where

$$\alpha_\ell^{\pm} = 1 - \eta_\ell^{\ell\pm1}\,,\quad \alpha_\ell^0 = 1-\eta_\ell^\ell\,,\quad \beta_\ell = \eta^\ell_{\ell+1,\ell-1}\, e^{i(\sigma_{\ell+1}+\sigma_{\ell-1})}\,.$$

The five amplitudes of eq. (2.23) are not independent, they are connected by

$$E + A - B = \sqrt{2}\,(C-D)\,\mathrm{cotg}(\theta)\,. \tag{2.24}$$

For an unpolarised incident beam, we have

$$\sigma(\theta) = \tfrac{1}{3}[|A|^2 + 2(|B|^2+|C|^2+|D|^2+|E|^2)]\,,$$

$$\sigma(\theta)P_y(\theta) = \tfrac{2\sqrt{2}}{3}\,\mathrm{Im}(AC^* + BD^* + DE^*)\,,\quad P_x = P_z = 0\,, \tag{2.25}$$

$$t_{20}(\theta) = \frac{1}{\sqrt{2}}\left[1 - \frac{|A|^2+2|D|^2}{\sigma(\theta)}\right]\,,$$

$$t_{21}(\theta) = -\sqrt{\tfrac{2}{3}}\;\frac{\mathrm{Re}(AC^* - DB^* + DE^*)}{\sigma(\theta)}\,,$$

$$t_{22}(\theta) = \frac{1}{\sqrt{3}}\;\frac{2\,\mathrm{Re}(BE^*) - |C|^2}{\sigma(\theta)}\,.$$

For s = o, the η_ℓ-coefficients can be obtained in a local potential model by solving the radial Schrödinger equation,

$$\left[\frac{d^2}{dr^2} + \frac{2\mu}{\hbar^2}\{E - V_c(r) - U(r)\} - \frac{\ell(\ell+1)}{r^2}\right] u_\ell(kr) = 0 \quad , \tag{2.26}$$

for all significant ℓ-values, with the boundary conditions

$$\begin{aligned} u_\ell(0) &= 0 \quad , \\ u_\ell(kr_M) &= F_\ell(kr_M) + iG_\ell(kr_M) + \eta_\ell\{F_\ell(kr_M) - iG_\ell(kr_M)\} \\ &\xrightarrow[\infty]{r_M} \sin\{kr_M - \tfrac{1}{2}\ell\pi - n\ln(2kr_M) + \sigma_\ell + \delta_\ell\} \quad . \end{aligned} \tag{2.27}$$

Here, F_ℓ and G_ℓ are the regular and irregular Coulomb functions (Frö 55, Hod 63) , $\eta_\ell = e^{2i\delta_\ell}$,μ is the reduced mass, E is the energy, $V_C(r)$ is the Coulomb potential and U(r) the nuclear potential. The matching radius r_M is chosen well outside the interaction region so that $U(r_M) \approx o$.

For spin-$\frac{1}{2}$ particles, the potential is in general not central. Its radial form depends on ℓ and j, and the Schrödinger equation becomes

$$\left[\frac{d^2}{dr^2} + \frac{2\mu}{\hbar^2}\{E - V_c(r) - U(r) - U_{\ell j}(r)\} - \frac{\ell(\ell+1)}{r^2}\right] u^j_\ell(kr) = 0 \quad . \tag{2.28}$$

For each ℓ-value, two differential equations have to be solved.

For spin-1 particles the situation is more complicated. Potentials which are not diagonal in ℓ-space (see eqs.(4.34)) have to be included. They determine β_ℓ . If non-diagonal interactions are neglected, we have three uncoupled differential

equations for each ℓ-value. In this case, we have $\beta_\ell = 0$. Small non-diagonal interactions can for instance be treated in DWBA.

2.3 Inelastic scattering

In the DWBA the transition amplitude for inelastic scattering by spin-0 targets is given by (Mes 62, Sat 64)

$$T^{M_f m_f m_i}$$

$$= \sum_{m_i' m_f'} \int d\underset{\sim}{r}\, \chi^{(-)*}_{m_f' m_f}(\underset{\sim}{k}_f, \underset{\sim}{r}) \langle s m_f' I_f M_f | V(\underset{\sim}{r}, \xi_p, \xi_t) | s m_i' 0 0 \rangle \chi^{(+)}_{m_i' m_i}(\underset{\sim}{k}_i, \underset{\sim}{r}) \quad , \tag{2.29}$$

where $V(\underset{\sim}{r}, \xi_t, \xi_p)$ is the inelastic scattering potential (assumed local), ξ_t and ξ_p are the internal coordinates of the target and projectile, i and f denote initial and final channels, and m and M are spin projection quantum numbers for projectile and target, respectively. The matrix $X^{(\pm)}_{m'm}(\underset{\sim}{k}, \underset{\sim}{r})$ acts as wave function for the relative motion. It carries two indices, because the spin projection is not conserved in the elastic channels. The superscripts (+),(-) denote ingoing- and outgoing- wave boundary conditions.

The matrix $X^{(+)}_{m'm}(\underset{\sim}{k}, \underset{\sim}{r})$ can be written as

$$\chi^{(+)}_{m'm}(\underset{\sim}{k}, \underset{\sim}{r}) = \langle s m' | \psi^{(+)}(\underset{\sim}{k}, \underset{\sim}{r}, \underset{\sim}{\xi}) | s m \rangle \quad , \tag{2.30}$$

where $\psi^{(+)}$ is the wave function for relative motion. It is spin-dependent and can be expanded in terms of

$$\phi_{j\ell n} = \sum_{\sigma\mu} \langle \ell s \mu \sigma | j n \rangle \chi_\sigma i^\ell Y^\mu_\ell \quad , \tag{2.31}$$

where $\phi_{j\ell n}$ is the generalisation, in the s=o case, of Y_ℓ^m . This yields

$$\chi^{(+)}_{m'_s\, m_s}(\underset{\sim}{k},\underset{\sim}{r}) = \frac{4\pi}{kr}\sum_{j\ell m}\langle \ell s\, m\, m_s | j\, m+m_s\rangle\langle \ell s\; m+m_s-m'_s\;\; m'_s \,|\, j\;\; m+m_s\rangle$$
$$\cdot Y_\ell^{m\,*}(\Omega_k)\; Y_\ell^{m+m_s-m'_s}(\Omega_r)\; i^\ell u_\ell^j(kr)\; e^{i\sigma_\ell} \quad , \qquad (2.32)$$

where u_ℓ^j is given by eq. (2.28). In deriving eq. (2.32) it is assumed that the elastic interaction is diagonal in ℓ-space.

Time reversal relates $X^{(-)*}$ and $X^{(+)}$ by

$$\chi^{(-)*}_{m'm}(\underset{\sim}{k},\underset{\sim}{r}) = (-1)^{m-m'}\,\chi^{(+)}_{-m'\,-m}(-\underset{\sim}{k},\underset{\sim}{r}) . \qquad (2.33)$$

We now consider the interaction potential $V(\underset{\sim}{r},\xi_t,\xi_p)$. We list four possible situations.

(i) In its simplest form, V is spin-independent. The polarisation of the projectile is then only due to the spin-dependent distortions.

(ii) The interaction can depend on the coupling of ξ_t and ξ_p. This case is normally considered in impulse approximation. The relevant formalism was given by Satchler (Sat 64a). In the absence of spin-dependent distortions, this contribution to the vector polarisation vanishes for $k_i = k_f$ (Sat 60).

(iii) The interaction depends on the coupling of the spin of the target nucleus and the relative motion. These effects are normally neglected.

(iv) The projectile spin can couple with the relative motion. We shall only consider this type of interaction. It is the logical extension of the extended OM where spin-orbit effects are included. The interaction is written in the form

$$V(\underset{\sim}{r},\xi_t,\xi_p) = \sum_{LM} \alpha_{LM}(\xi_t)\left\{V(r)\,Y_L^{M*}(\Omega_r) + \tfrac{1}{2}V_{s.o.}(r)\left[Y_L^{M*}(\Omega_r)\,\underset{\sim}{s}\cdot\underset{\sim}{l} + \underset{\sim}{s}\cdot\underset{\sim}{l}\,Y_L^{M*}(\Omega_r)\right]\right\}, \tag{2.34}$$

$$V(r) = \frac{dU(r,R)}{dR} .$$

Here, U(r,R) is the <u>complex</u> OM potential for elastic scattering. The form (2.34) was chosen in order to preserve Hermiticity in angular and spin space. This type of interaction was also recently considered by Fricke et al. (Fri 66) for the inelastic scattering of 40 MeV protons.

From eqs. (2.29), (2.32)-(2.34) the transition matrix can be calculated in a partial-wave form. We obtain

$$\begin{aligned} T_L^{M_f m_f m_i} = {} & \delta_{J_f,L}\,\langle J_f \| \mathcal{M}_L \| 0\rangle\,\frac{4\pi}{k_i k_f}\sum_{\ell\ell' jj'} i^{\ell-\ell'}\,\beta_{\ell\ell'}^{jj'}\,e^{i(\sigma_\ell+\sigma_{\ell'})} \\ & \cdot \hat{S}^{-1}\,\hat{\ell}\,\hat{\ell}'\,\hat{L}\,\hat{j}'\,(-)^{\ell'+j+L-s}\,W(j\,\ell\,j'\ell';\,sL)\,Y_{\ell'}^{-m}(\theta,0) \\ & \cdot \langle j' L\, m_f-m\;\; m-m_f+m_i \,|\, j m_i\rangle\langle \ell' s\;\; -m\;\; m_f \,|\, j'\, m_f-m\rangle \\ & \cdot \langle \ell s\, 0\, m_i \,|\, j m_i\rangle\langle \ell' L\, 0\, 0 \,|\, \ell 0\rangle , \end{aligned} \tag{2.35}$$

where $m = M_f - m_i + m_f$. We have again chosen the z-axis along $\underset{\sim}{k}_i$ and the y-axis along $\underset{\sim}{k}_i \times \underset{\sim}{k}_f$. The radial integrals $\beta_{\ell\ell'}^{jj'}$ are defined by

$$\beta_{\ell\ell'}^{jj'} = \int_0^\infty dr\; u_\ell^j(k_i r)\, V_{\ell\ell'}^{jj'}\, u_{\ell'}^{j'}(k_f r) . \tag{2.36}$$

The interaction form factor depends on the quantum numbers of the partial waves in the entrance and exit channels. This is, of course, due to the fact that our inelastic interaction contains an $\underset{\sim}{l}\cdot\underset{\sim}{s}$ term. The form factor can be calculated from

$$V_{\ell\ell'}^{jj'}(r) = V(r) + \tfrac{1}{4}\left[j'(j'+1) + j(j+1) - \ell'(\ell'+1) - \ell(\ell+1) - 2s(s+1)\right] V_{s.o.}(r) . \tag{2.37}$$

We note that, in eq. (2.35), only excitations to natural parity levels (i.e. 0^+, 1^-, 2^+ etc.) are allowed. This is due to the fact that (i) we have assumed local potentials and (ii) for $s \neq 0$, we have neglected coupling of the spin of the projectile to the internal coordinates of the target nucleus.

The differential cross section for unpolarised projectiles is given by

$$\sigma(\theta) = \left(\frac{\mu}{2\pi\hbar^2}\right)^2 \frac{k_f}{k_i} \frac{1}{2s+1} \sum_{M_f m_f m_i} \left| T^{M_f m_f m_i} \right|^2 , \qquad (2.38)$$

and the polarisation of the scattered particles (using eqs. (2.6) and (2.14)) is

$$P_y(\theta) = \frac{\sum [(s-m_f)(s+m_f+1)]^{\frac{1}{2}} I_m \{ T^{M_f m_f m_i} T^{M_f m_f+1 m_i *} \}}{s \sum |T^{M_f m_f m_i}|^2} . \qquad (2.39)$$

The summations extend over M_f, m_f and m_i. We sum over M_f because it is assumed that the polarisation of the excited level is not measured.

Higher order tensor polarisation can again be calculated by similar techniques. However, for inelastic scattering we shall confine ourselves to vector polarisation.

3. REFLECTION COEFFICIENT AND RADIAL INTEGRALS FROM COMPLEX POTENTIALS

For composite particles the physical significance of the OM potentials is not clear. However, the OM is still a useful method of parameterising the η_ℓ-coefficients. With the view to find a simpler method of parameterisation, we investigate the η_ℓ-functions obtained from successful OM fits. For this purpose a computer programme was written to calculate η_ℓ for a general class of OM potentials. The programme also included calculation of radial integrals for inelastic scattering. Some features of the programme are discussed in appendix A. In this section the numerical results are discussed and compared with WKB predictions.

3.1 Potentials

The central potential U(r) which appears in the radial Schrödinger equation (2.28) has the form

$$U(r) = -V f_V(r) - i W f_W(r) - i W_S f_S(r) \quad , \tag{3.1}$$

and the Coulomb potential $V_C(r)$ for a uniformly charged sphere of radius $R_C = r_C A^{\frac{1}{3}}$ is given by

$$\begin{aligned} V_C(r) &= \tfrac{1}{2} Z_1 Z_2 e^2 (3 R_C^2 - r^2)/R_C^3 \quad , \; r \le R_C \; , \\ &= Z_1 Z_2 e^2/r \quad , \; r \ge R_C \; , \end{aligned} \tag{3.2}$$

Z_1 and Z_2 being the charges (in units of e) of the projectile and target, respectively. For f_V and f_W the Woods-Saxon (WS) shape

$$f_{V,W}(r) = \left[1 + \exp\left(\frac{r-R}{a}\right)\right]^{-1} , \tag{3.3}$$

was used. For the surface absorption form $f_s(r)$, the derivative of the WS shape

$$f_s(r) = -\frac{1}{4}\frac{d}{dx}\left[1 + \exp(x)\right]^{-1}, \qquad x = \frac{r-R}{a}, \tag{3.4}$$

or a Gaussian shape was used. The two shapes are closely related (Hod 63) if a (Gauss) = 2.1 a(WS).

In the radial equation, the spin-orbit term takes the form

$$U_{lj} = \frac{1}{2}\left(V_{s.o.} + iW_{s.o.}\right) f_{s.o.}(r)\left[j(j+1) - l(l+1) - s(s+1)\right],$$
$$f_{s.o.}(r) = \frac{1}{r}\frac{d}{dr}\left[1 + \exp\left(\frac{r-R}{a}\right)\right]^{-1}. \tag{3.5}$$

3.2 WKB calculations

To facilitate comparison with numerical calculations, the η_l-coefficients are derived in WKB approximation.

The wave function which satisfies the boundary condition (2.27) at r = o is given in WKB approximation by

$$u_l(kr) = A\left\{k(r)\right\}^{-\frac{1}{2}} \sin\left\{\int_{r_t}^{r} k(r)\,dr + \tfrac{1}{4}\pi\right\} \tag{3.6}$$

for $r > r_t$. Here k(r) is the local wave number

$$k(r) = \left[k^2 - \frac{2\mu}{\hbar^2}\left(U(r) + V_c(r)\right) - \left(\frac{l+\frac{1}{2}}{r}\right)^2\right]^{\frac{1}{2}}, \tag{3.7}$$

and r_t is defined by Re $\{k(r_t)\} = 0$.

From eqs. (3.6) and (3.7) and the boundary condition at infinity, eq. (2.27), the phase shifts $\sigma_\ell + \delta_\ell$ and σ_ℓ can be calculated for the full potential and a point charge, respectively. It then immediately follows that

$$\delta_\ell = \int_{r_2}^{\infty} \left\{ k^2 - \frac{2\mu}{\hbar^2}\left(U(r) + V_c(r)\right) - \left(\frac{\ell+\frac{1}{2}}{r}\right)^2 \right\}^{\frac{1}{2}} dr - \int_{r_1}^{\infty} \left\{ k^2 - \frac{2\mu Z_1 Z_2 e^2}{\hbar^2 r} - \left(\frac{\ell+\frac{1}{2}}{r}\right)^2 \right\}^{\frac{1}{2}} dr \,. \qquad (3.8)$$

If the potential U(r) is small in comparison with the energy E $\left(= \frac{\hbar^2 k^2}{2\mu}\right)$, eq. (3.8) can be approximated further to yield

$$\delta_\ell = -\frac{\mu}{\hbar^2 k} \int_{t/k}^{\infty} \frac{U(r) + V_c - Z_1 Z_2 e^2/r}{\left(1 - \frac{t}{kr}\right)^{\frac{1}{2}}} \, dr \,, \qquad (3.9)$$

where $t = \ell + \frac{1}{2}$.

In approximation (3.9), the total phase shift is the sum of contributions obtained from different terms of the potential. If the Coulomb interaction is neglected, eq. (3.9) is identical with the "high energy approximation" which is obtained by a different method (see for instance (Hod 63)) from the Klein-Gordon or Dirac equations.

3.3 Neutral particle scattering

We are now in a position to discuss the dependence of η_ℓ on the OM potential parameters. In order to avoid Coulomb complications, we confine ourselves to neutral particle scattering. The potential parameters do not necessarily correspond to actual physical situations.

In some scattering processes (e.g. deuteron scattering) surface absorption is normally assumed and in other cases (e.g. high energy nucleon scattering) the absorptive potential is assumed to extend over the volume of the nucleus. To investigate the effect of these assumptions on the η_ℓ-coefficients, we consider the scattering of 182 MeV neutrons by ^{197}Au. (The geometrical parameters are r_o = 1.3 fm and a = 0.6 fm.) The OM calculations for pure surface absorption (W_S = 20 MeV, V = o) are illustrated in figs. 1(a) and 1(b). The curves show that the minimum of $|\eta_\ell| \approx \mathrm{Re}\,\eta_\ell$ occurs at an ℓ-value slightly smaller than kR and $|\eta_\ell|$ increases again for decreasing ℓ. We also see that arg η_ℓ is small and positive for small ℓ-values. All these features are predicted by eq. (3.8). However, the peculiar behaviour of arg η_ℓ around $\ell \approx 20$ is not described by eq. (3.8).

Figs. 1(c)-1(e) show the results for the volume absorption (W = 15 MeV) case with real potentials V = o, and V = 20 MeV. Here we note four points. (i) The main variation of $|\eta_\ell|$ occurs in the surface region. (ii) The curves for $|\eta_\ell|$ depend on the real potential. Attractive potentials tend to increase the cut-off ℓ-value and also slightly increase the value of $|\eta_o|$. (iii) The curve for arg η_ℓ, with V = 20 MeV, varies rapidly in the surface region but becomes fairly flat for low ℓ-values. (iv) For V = o, arg η_ℓ is small and positive for low ℓ-values, but has a negative dip in the surface region. Except for this negative dip, all the features mentioned are qualitatively in accordance with the WKB predictions (3.8).

We now turn our attention to the spin-orbit interaction. To the central potentials with volume absorption as discussed above, a spin-orbit potential ($V_{s.o.}$ = 4 MeV/fm^2) was added. The results for V = o are illustrated in figs. 1(f) and 1(g)

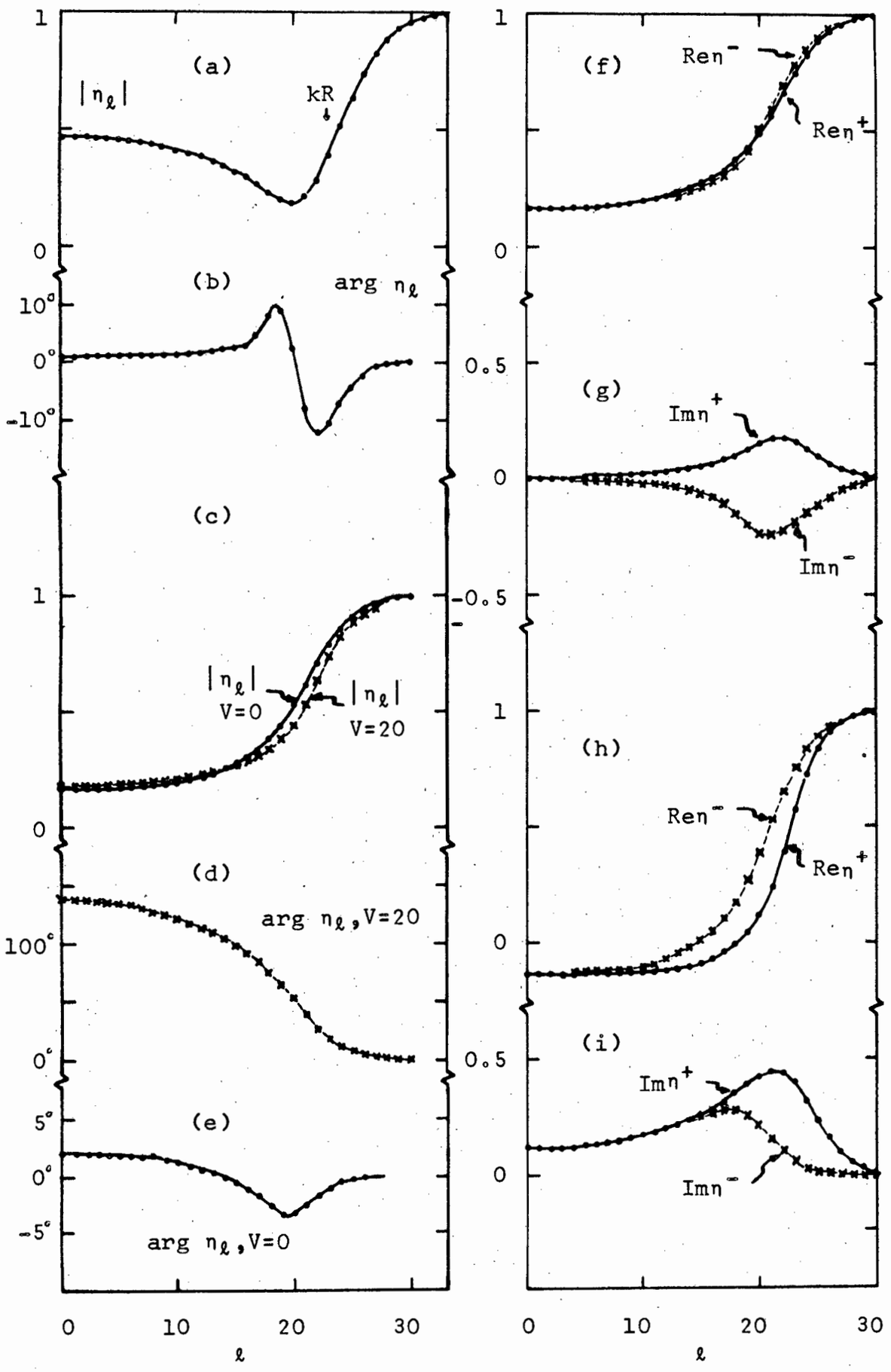

Fig.1. Structure of η_ℓ for neutral particle scattering. For OM parameters, see text.

while those for V = 20 MeV are shown in figs. 1(h) and 1(i). From these curves we see that for V = o, the main difference between η_ℓ^+ and η_ℓ^- occurs in the imaginary parts. This is in accordance with the "ν-model" of Frahn and Venter (Fra 64). (This model is discussed in section 4.2.) On the other hand, the real parts of η_ℓ^+ and η_ℓ^- differ appreciably in the case of V = 20 MeV. (This is due to the fact that arg $\eta_\ell^\pm$ is so large that cos (arg $\eta_\ell^\pm$) varies rapidly.) In this case η_ℓ^+ and η_ℓ^- take the form of a combined "τ- and ν-model" (Fra 64). However, the "ν-model" could be recovered from the OM by including a suitable absorptive part $W_{s.o.}$ (with sign opposite to $V_{s.o.}$) in the spin-orbit interaction.

So far we have considered the case of incomplete absorption, $\eta_o \neq o$. Except for the behaviour of arg η_ℓ in the surface region, the calculations are in agreement with WKB predictions. We now consider stronger absorptive potentials. In fig. 2 $|\eta_\ell|$ is represented as a function of W for 180 MeV neutrons scattered by ^{208}Pb. (The other parameters are r_o = 1.3 fm, a = 0.5 fm and V = o.) We see from fig. 2 that, for small ℓ, $|\eta_\ell|$ desceases exponentially with W up to about W = 50 MeV and increases again from about W = 80 MeV. Furthermore, it is shown in fig. 3 that curves for arg η_ℓ as a function of ℓ are notably different for W = 50 MeV and W = 80 MeV. For W = 160 MeV (not shown) arg η_ℓ has the same qualitative behaviour as fig. 3(b), and except for the oscillations at low ℓ-values fig. 3(a) is similar to fig. 1(e). The functions η_ℓ can thus be divided into two groups depending on W.

In order to understand the behaviour of η_ℓ for increasing W, we consider a square well absorption of radius R. For small ℓ-values we then find, to first order in W/E,

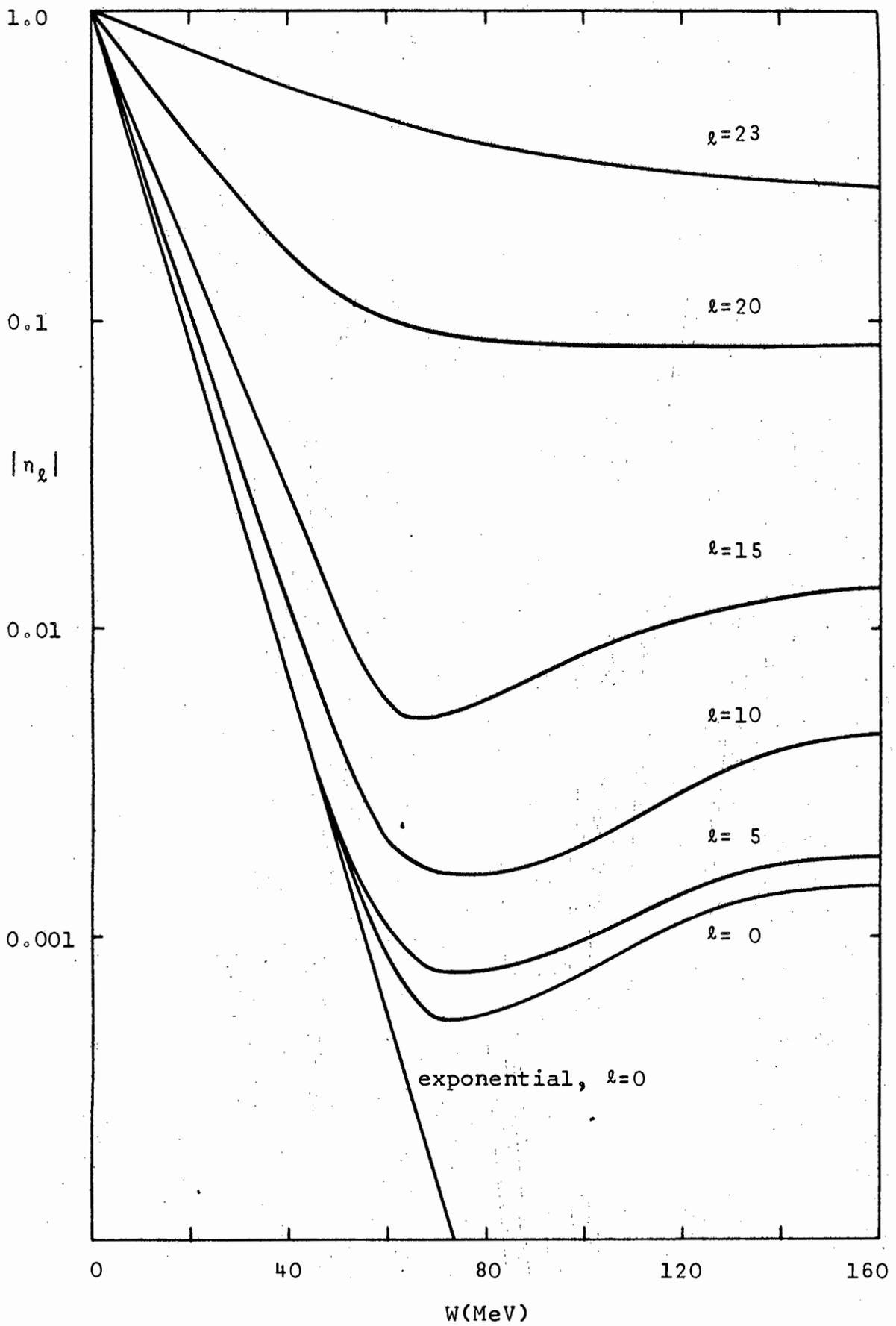

Fig. 2. Curves for $|\eta_\ell|$ as a function of the absorptive potential W (see text).

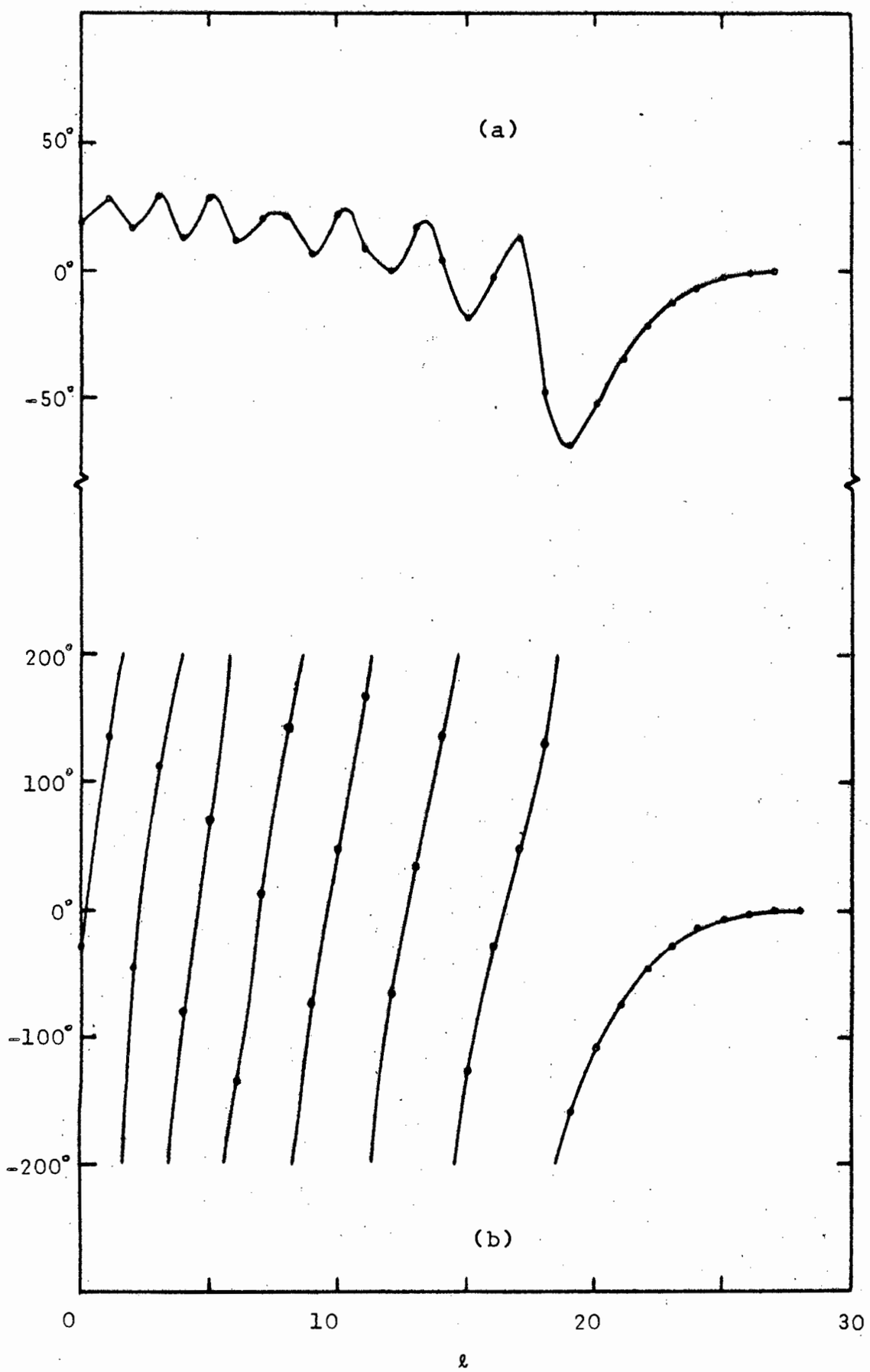

Fig. 3. Curves for arg η_ℓ as a function of ℓ (a) W=50 MeV and (b) W=80 MeV (see text).

$$\eta_\ell = e^{-\frac{WkR}{E}} + \frac{iW}{4E-iW}\, e^{i(2kR-\ell\pi)} \quad . \qquad (3.10)$$

From eq. (3.10) we see that, for small W, $|\eta_\ell|$ decreases exponentially with W. However, for large W the second term in eq. (3.10) dominates and $|\eta_\ell|$ increases with increasing W. (For Woods-Saxon potentials, these curves depend, of course, on the width a and for non-vanishing real potentials also on the additional parameters.) It is now also clear why the phase of η_ℓ varies rapidly for small ℓ-values for the case W = 80 MeV. From fig. 3(b) it can be seen that the difference of arg η_ℓ for consecutive small ℓ-values is about π as predicted by eq. (3.10). We note also the odd-even variation for small ℓ in fig. 3(a) which is due to the contribution of the second term in eq. (3.10).

We have seen that the characteristic behaviour of the η_ℓ-function obtained from a complex potential can be divided into two groups depending on W. We define the extreme absorption condition (EAC) as the condition under which the η_ℓ-functions have the main characteristics of the second term in eq. (3.10).

3.4 Coulomb effects

We now investigate in what way the results of section 3.3 change in the presence of a Coulomb interaction.

In the neutral case the phase shifts are obtained relative to the free particle solution while for charged particles the "nuclear" phase shifts are calculated relative to the point charge solutions. Our object is to show that the nuclear

phase shifts still depend on the Coulomb parameter in a two-fold way.

(i) For increasing repulsive Coulomb forces the absorption of high-ℓ partial waves decreases. We see this in WKB approximation by noting that the classical turning point is displaced towards larger radii. In parameterised η-functions this effect is taken care of by replacing the neutral angular momentum "cut-off" value T(o) by

$$T(\eta) = T(0)\left[1 - 2\eta/T(0)\right]^{\frac{1}{2}} , \qquad (3.11)$$

$$\eta = \frac{\mu Z_1 Z_2 e^2}{\hbar^2 k} . \qquad (3.12)$$

This effect is illustrated in fig. 5 which is discussed in section 3.5.

(ii) The charge of the nucleus extends over the whole volume and for low-ℓ partial waves the point charge approximation is insufficient. By assuming that the nucleus is a uniformly charged sphere we calculate a phase shift $\Delta\delta_\ell$ which is due to the difference between a point charge and an extended charge distribution. In WKB approximation $\Delta\delta_\ell$ is given by

$$\Delta\delta_\ell = \int_{\rho_1}^{\rho_c}\left[1 - \frac{\eta}{\rho_c}\left\{3 - \left(\frac{\rho}{\rho_c}\right)^2\right\} - \frac{t^2}{\rho^2}\right]^{\frac{1}{2}} d\rho - \int_{\rho_2}^{\rho_c}\left[1 - \frac{2\eta}{\rho} - \frac{t^2}{\rho^2}\right]^{\frac{1}{2}} d\rho , \qquad (3.13)$$

where $\rho_c = kR_c$, and ρ_1 and ρ_2 are the values of ρ for which the respective integrands vanish.

The correction $\Delta\delta_\ell$ is unnecessary if we use, for matching purposes, extended charge wave functions instead of Coulomb

functions. However, we must then also use "extended charge phase shifts" instead of the normal Coulomb phase shifts σ_ℓ in the calculation of cross sections etc..

For small Coulomb parameters we can compensate, to some extent, for the errors made in neglecting $\Delta\delta_\ell$, by calculating the cross section in a neutral formalism. Fig. 4 shows cross sections calculated for 182 MeV protons scattered by ^{197}Au with (i) extended charge distribution η_ℓ-coefficients and charged formalism for $\sigma(\theta)$, (ii) point charge η_ℓ-coefficients and neutral formalism for $\sigma(\theta)$ and (iii) point charge η_ℓ-coefficients and charged formalism for $\sigma(\theta)$. (For the calculations, the central potentials of ref. (Sat 64b) were taken.) Although curves (i) and (ii) have different slopes and oscillation amplitudes, they have approximately the same oscillation period. The fact that curves (i) and (iii) bear little resemblance to each other shows that $\Delta\delta_\ell$ is very important in the case of incomplete absorption of low-ℓ partial waves.

In order to test approximation (3.13) and to study its applicability to radial integrals, the phase shift differences $\Delta\delta_\ell$ were calculated for 182 MeV protons scattered by ^{197}Au (Coulomb parameter $n = 0.922$) by the following four methods: (i) numerical solution of the Schrödinger equation with no nuclear potentials, (ii) WKB approximation (3.13), (iii) difference between point charge and extended charge distribution calculations of arg η_ℓ with OM parameters from ref. (Sat 64b), and (iv) differences between the respective diagonal radial integrals $\beta_{\ell\ell}$ with $Q = 0$. The results are shown in table 1.

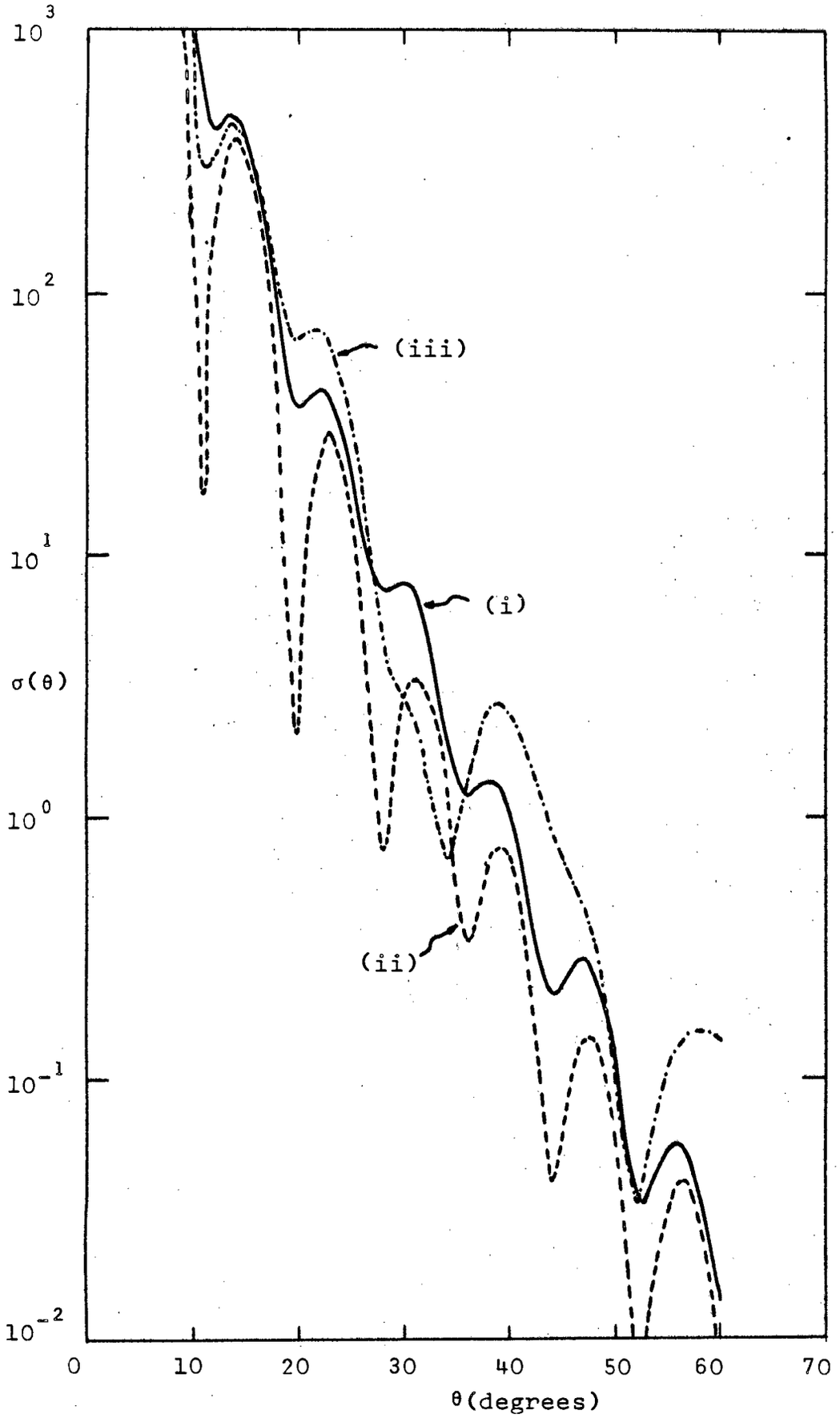

Fig. 4. Effect of the Coulomb interaction on the differential cross section for the elastic scattering of 182 MeV protons by ^{197}Au. Methods (i),(ii) and (iii) are described on page 23.

Table 1 Calculation of $2\Delta\delta_\ell$ for 182 MeV protons scattered by ^{197}Au (see text)

ℓ	Method			
	(i)	(ii)	(iii)	(iv)
0	279.6	283.3	272.9	272.8
1	194.7	196.1	191.1	191.0
2	146.1	146.9	144.6	145.1
3	113.2	113.7	113.4	112.9
4	89.0	89.3	90.1	90.7
5	70.3	70.6	72.2	72.0
6	55.4	55.5	57.7	57.9
7	43.4	43.6	46.1	46.3
8	33.6	33.6	36.4	36.3
9	25.6	25.7	28.4	28.7
10	19.0	19.1	21.9	22.0
11	13.8	13.8	16.5	16.4
12	9.7	9.7	12.0	12.2
13	6.5	6.4	8.3	8.5

The most striking feature in table 1 is the good agreement between methods (iii) and (iv). The fact that arg η_ℓ and arg $\beta_{\ell\ell}$ behave similarly can be readily understood by observing that σ_ℓ appears in the inelastic amplitude (2.35) and again no correction is necessary if extended charge phase shifts are used. In general, the agreement between methods (i) -(iv) is quite good. Remembering that the

uniformly charged sphere is an idealisation and that R_c is chosen fairly arbitrarily, we conclude that approximation (3.13), which can be integrated exactly, should suffice for parameterised η-functions.

In the case under consideration, $\Delta\delta_{l3}$ is already small while Re $\eta_\ell \approx \frac{1}{2}$ for $\ell \approx 20$. It follows for strong absorption (e.g. α-scattering) that $|\eta_\ell|$ is sufficiently small for ℓ-values for which $\Delta\delta_\ell$ becomes important, and therefore $\Delta\delta_\ell$ may be neglected in such cases.

3.5 Radial integrals

We now discuss the radial integrals $\beta_{\ell\ell'}$ for neutral particle scattering. In the preceeding section we have seen how some of these results can be extended to the charged case.

First of all we consider the diagonal elements $\ell = \ell'$. For vanishing Q-value, Austern and Blair (Aus 65) have derived the exact relation

$$\beta_{\ell\ell}(k_i k_i) = \frac{iE}{2k} \frac{d\eta_\ell}{dR} \quad , \tag{3.14}$$

where R is the OM radius. As these authors point out, an increment δR in the OM radius will result in an increment $\delta\ell_o \approx k\delta R$ in the cut-off angular momentum. (This assumption is expected to be quite accurate at high energies where WKB arguments are valid.) By assuming that η_ℓ is a function of $\ell - \ell_o$ in the surface region it is found that

$$\beta_{\ell\ell}(k_i k_i) \approx -\frac{iE}{2} \frac{d\eta_\ell}{d\ell} \quad . \tag{3.15}$$

Eq. (3.15) is not valid for low ℓ-values. By calculating η_o in WKB approximation and applying eq. (3.14) we can estimate β_{oo}. The result is

$$\beta_{oo} \approx \frac{iE}{2kR}\,\eta_o \ln \eta_o \approx \frac{iE}{2T}\,\eta_o \ln \eta_o \;, \qquad (3.16)$$

where $T = \ell_o + \frac{1}{2}$. We thus have expressions for low ℓ-values and for surface ℓ-values. It is, at present, not clear how the intermediate region in ℓ-space should be treated. However, for strong absorption we have $\eta_o = o$ and therefore $\beta_{oo} = o$ and only surface elements are important.

In order to calculate the off-diagonal radial integrals with $K \equiv \ell' - \ell = \pm 1$, we use the integral expressions of Fradkin and Calogero (Fra 66) for phase shift differences and assume that U(r) is a function of (r-R). We obtain

$$\beta_{\ell+1\,\ell}(k_i k_i) = -i\,\tfrac{1}{2}E\,(\eta_{\ell+1} - \eta_\ell) \;. \qquad (3.17)$$

We note that there is a resemblance between eqs. (3.17) and (3.15), but eq. (3.17) is valid for all ℓ-values and greater ℓ-space localisation is expected for $\beta_{\ell+1,\ell}$. It then follows that, for incomplete absorption ($\eta_o \neq o$), the S-matrix description of inelastic scattering by a 1^- state will be the simplest case.

For $\ell' - \ell = \pm 2$ we have no simple relations between phase shifts and radial integrals. Austern and Blair (Aus 65) assume that all off-diagonal elements can be approximated by

$$\beta_{\ell'\ell}(k_i k_i) = \beta_{\bar{\ell}\bar{\ell}}(k_i k_i) \;, \qquad (3.18)$$

$$\bar{\ell} = \tfrac{1}{2}(\ell + \ell') \;.$$

We shall use approximation (3.18) in section 5. An improved approximation is proposed in section 6.

We now consider the relative sign between radial integrals for different $\ell' - \ell$. For low ℓ-values, the wave function in the r-space surface region is approximately given by

$$u_\ell(kr) \approx e^{-i(kr - \frac{1}{2}\ell\pi)} + \eta_\ell(r)\, e^{i(kr - \frac{1}{2}\ell\pi)} \quad , \qquad (3.19)$$

where $\eta_\ell(r)$ satisfies the Calogero equation (Cal 63, Kla 66). The reflection coefficient is then given by $\eta_\ell = \eta_\ell(r\to\infty) = \eta_\ell(r = r_M)$. If we assume that $\eta_\ell(R) \approx \eta_{\ell'}(R)$ (remembering that $\eta_\ell(r_M) \approx \eta_{\ell'}(r_M)$ for low ℓ- and ℓ'-values, fig. 1) we find

$$\beta_{\ell+2\,\ell}(k_i k_i) = \beta_{\ell\,\ell+2}(k_i k_i) \approx -\beta_{\ell+1\,\ell+1}(k_i k_i) \qquad (3.20)$$

for small ℓ. By the same procedure we also find, for low ℓ-values, that $|\beta_{\ell+1\,\ell}| \ll |\beta_{\ell+2\,\ell}|, |\beta_{\ell\ell}|$. On the other hand, η_ℓ approaches unity for large ℓ-values. This implies that the main contribution to the wave function is the term containing the Bessel function $j_\ell(kr)$. For $\ell > kR$, these functions are predominantly positive in the inelastic interaction region. We therefore expect that the radial integrals with different $\ell'-\ell$ have the same sign in the ℓ-space surface region. These results will be used in section 6.

Fig. 5 illustrates some of the points discussed in this section. For the calculations, the scattering of 182 MeV neutrons and protons by ^{197}Au was considered. (The central potential parameters were taken from ref. (Sat 64b)). We note four points.

(i) The curves for K = o,2 have opposite signs at low ℓ-values as predicted by eq. (3.20). For the neutron case we

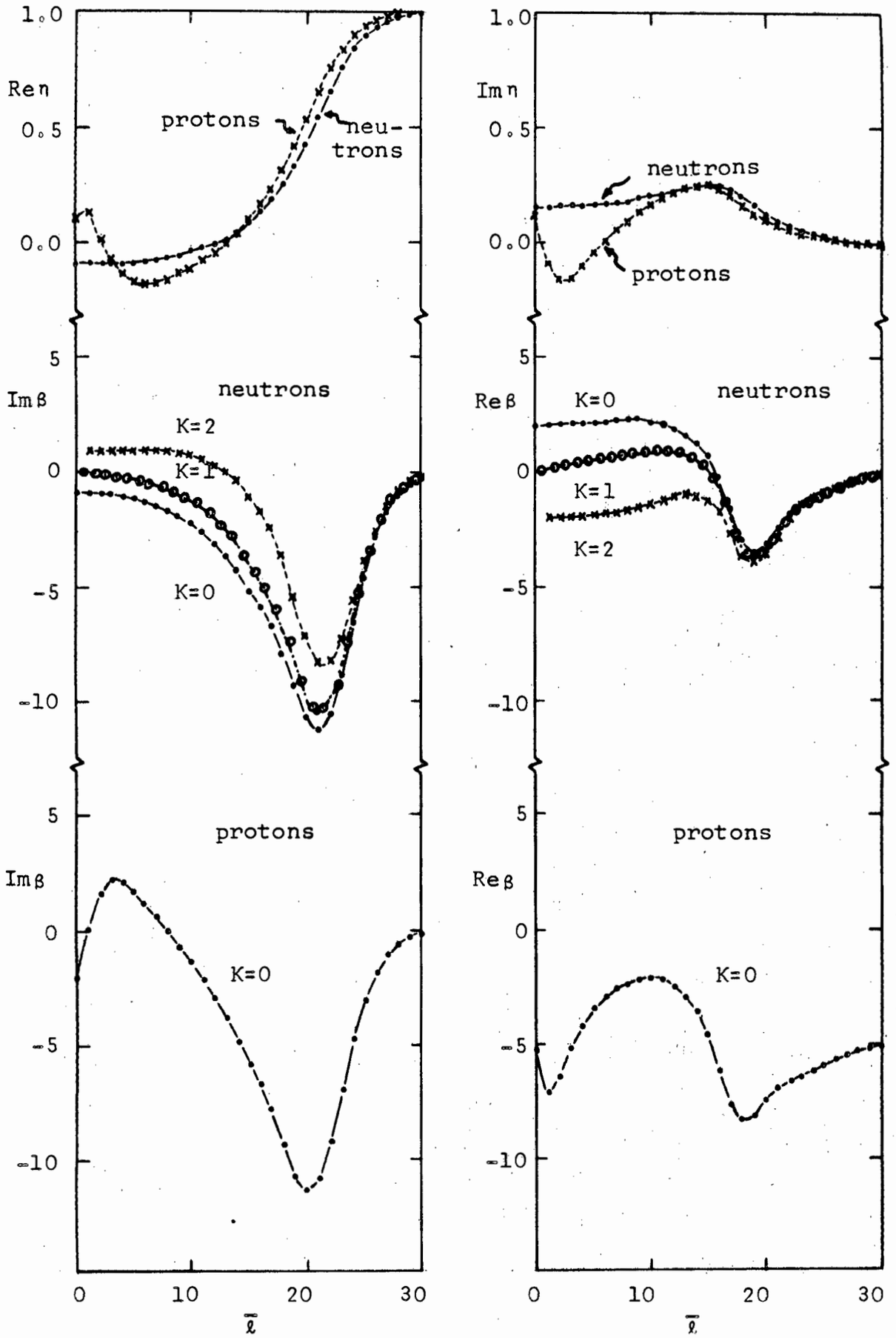

Fig. 5. Reflection coefficients and radial integrals for 182 MeV neutrons and protons scattered by ^{197}Au.

have Re β_{11} = 2.039, Im β_{11} = -0.916, Re β_{20} = Re β_{02} = -2.035 and Im β_{20} = Im β_{02} = 0.914. Therefore eq. (3.20) is seen to be well satisfied in this case. (ii) The values of $\beta_{\ell,\ell+1}$ are small for small ℓ in agreement with eq. (3.17). (iii) By taking T = 20 and calculating β_{oo} from eq. (3.16), we obtain Re β_{oo} = 2.151, Im β_{oo} = -0.739. The correct values are Re β_{oo} = 2.047, Im β_{oo} = -0.902. This shows that eq. (3.16) gives a satisfactory estimate of the contribution from low ℓ-values. (iv) For protons the cut-off angular momentum ℓ_o is smaller than the one for neutrons. This is also true for the ℓ-value at which the imaginary parts of the radial integrals have maximum magnitude. In the surface region the neutral expressions for η_ℓ and $\beta_{\ell\ell'}$ can thus be adapted for charged particles by using eq. (3.11) which is also quantitatively correct.

3.6 Alpha-particle scattering

We have now collected enough background material to discuss typical η_ℓ-functions and radial integrals for α-particle scattering. Here we consider one example only.

Optical model analyses of 65 MeV α-particle scattering by ^{92}Zr have been performed by Bingham, Halbert and Bassel (Bin 66). These authors give three different four-parameter potentials. Figs. 6 and 7 illustrate calculations of η_ℓ and $\beta_{\ell\ell'}$ for potentials 1 and 3. (The potential parameters are V = 34.36 MeV, W = 18.92 MeV, r_o = 1.554 fm and a = 0.662 fm for potential 1, and V = 200 MeV, W = 97.68 MeV, r_o = 1.227 fm and a = 0.665 fm for potential 3.)

For potential 1, fig. 7 shows that arg η_ℓ increases with decreasing ℓ (starting at ℓ = 30) as a result of the real

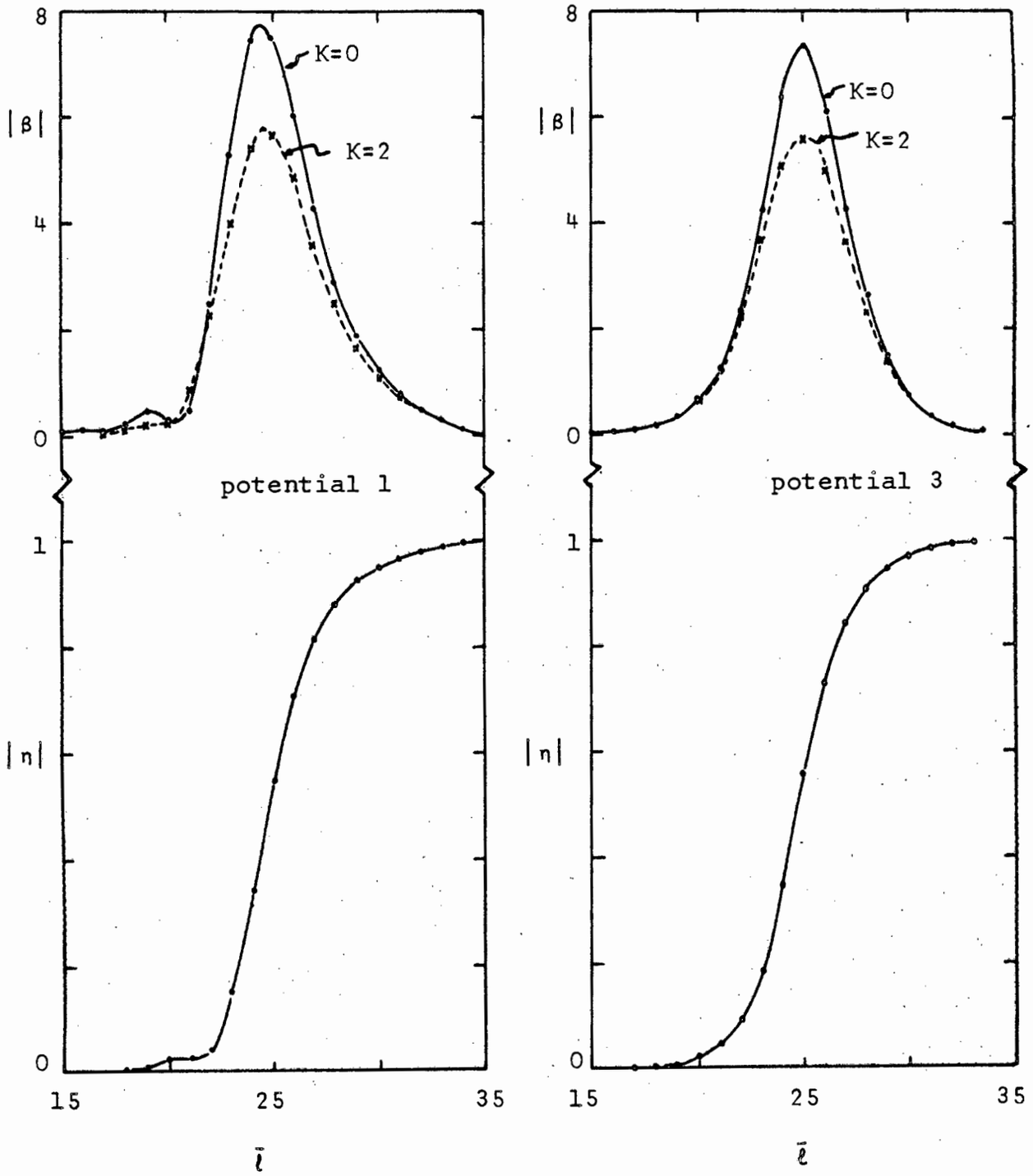

Fig. 6. Absolute values of reflection coefficients and radial integrals for the scattering of 65 MeV α-particles by ^{92}Zr. The potential parameters are given on page 28.

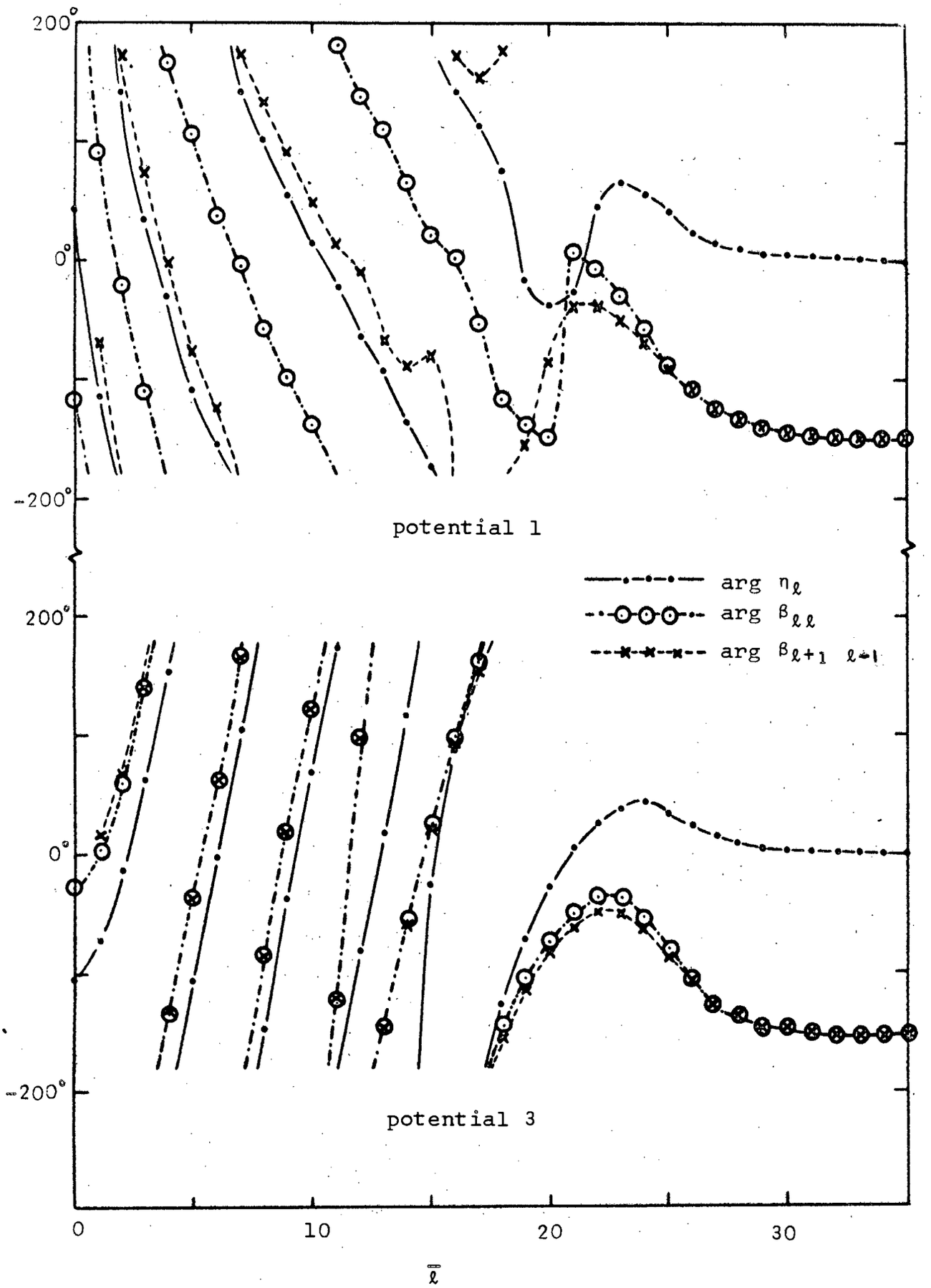

Fig.7. Arguments of the reflection coefficients and radial integrals shown in fig.6.

potential V. Below ℓ = 23, arg η_ℓ drops to negative values as a result of the imaginary potential (as discussed in section 3.3). Below ℓ = 20, arg η_ℓ increases again with decreasing ℓ under the influence of V and $\Delta\delta_\ell$. The phases of $\beta_{\ell\ell}$, follow a similar pattern but in this case arg $\beta_{\ell\ell}$ and arg $\beta_{\ell+1,\ell-1}$ are not simply related in the surface region. Fig. 6 shows that, for potential 1, $|\beta_{\ell\ell}|$ is not symmetrical and both $|\beta_{\ell\ell}|$ and $|\eta_\ell|$ have a peculiar behaviour near ℓ = 20.

Judging by the form of arg η_ℓ shown in fig. 7, potential 3 satisfies the EAC (section 3.3). Again, the behaviour of arg $\beta_{\ell\ell}$ and arg $\beta_{\ell+1,\ell-1}$ is similar to that of arg η_ℓ. In this case the former seem to be related in a simple way. Furthermore, the functions $|\eta_\ell|$ and $|\beta_{\ell\ell}|$ are fairly anti-symmetric and symmetric, respectively. They are also quite smooth. Considering all these facts, it seems that this case is suitable for a simple S-matrix parameterisation. (Although no comparison with ingoing wave boundary condition calculations (IWB) (Raw 66) has been made, it is believed that under EAC, IWB and normal OM calculations are very similar.) However, most OM potentials quoted in the literature produce η_ℓ-functions which are similar to those obtained for potential 1.

With decreasing α-particle energy the irregular behaviour of $|\eta_\ell|$ below the cut-off ℓ-value increases. Austern (Aus 61) has shown that this effect is due to the interference between waves reflected at the nuclear surface and waves reflected from the centrifugal barrier. Curves for $\beta_{\ell,\ell}$ for 28 MeV α-particle scattering are discussed in section 6.1 (fig.11).

3.7 Helium-3 scattering

We now extend the Austern-Blair relation (3.15) to the scattering of strongly absorbed spin-$\frac{1}{2}$ particles in the presence of a spin-orbit interaction.

By deforming the complex central and spin-orbit potentials in the extended OM as suggested in section 2.3, we again obtain, in direct analogy to the spin-independent expressions (3.14), the exact relations

$$\beta_{ll}^{++}(k_i k_i) = \frac{iE}{2k} \frac{\partial \eta_l^+}{\partial R} \,, \qquad \beta_{ll}^{--}(k_i k_i) = \frac{iE}{2k} \frac{\partial \eta_l^-}{\partial R} \,, \tag{3.21}$$

where $\beta_{\ell\ell}^{++}$ and $\beta_{\ell\ell}^{--}$ are the radial integrals for $j-\ell = j'-\ell' = +\frac{1}{2}$ and $j-\ell = j'-\ell' = -\frac{1}{2}$, respectively. Using the assumptions that lead from eq. (3.14) to eq. (3.15) we obtain in this case

$$\beta_{ll}^{++}(k_i k_i) = -\frac{iE}{2} \frac{\partial \eta_l^+}{\partial l} \,, \qquad \beta_{ll}^{--}(k_i k_i) = -\frac{iE}{2} \frac{\partial \eta_l^-}{\partial l} \,. \tag{3.22}$$

In order to illustrate the relations (3.22), the phase shifts and radial integrals for 60 MeV ^{3}He projectiles scattered by ^{58}Ni, are calculated. (For the central potential the parameters are assumed to be V = 40 MeV, W = 20 MeV, r_o = 1.5 fm and a = 0.6 fm. These are similar to the α-particle potentials (Dar 64). A real spin-orbit potential $V_{s.o.}$ = 10 MeV/fm^2 is included.) The numerical results are illustrated in fig. 8. From the curves we see that, apart from the difference between Im η^+ and Im η^-, the real spin-orbit effect has a pronounced effect on the cut-off and the

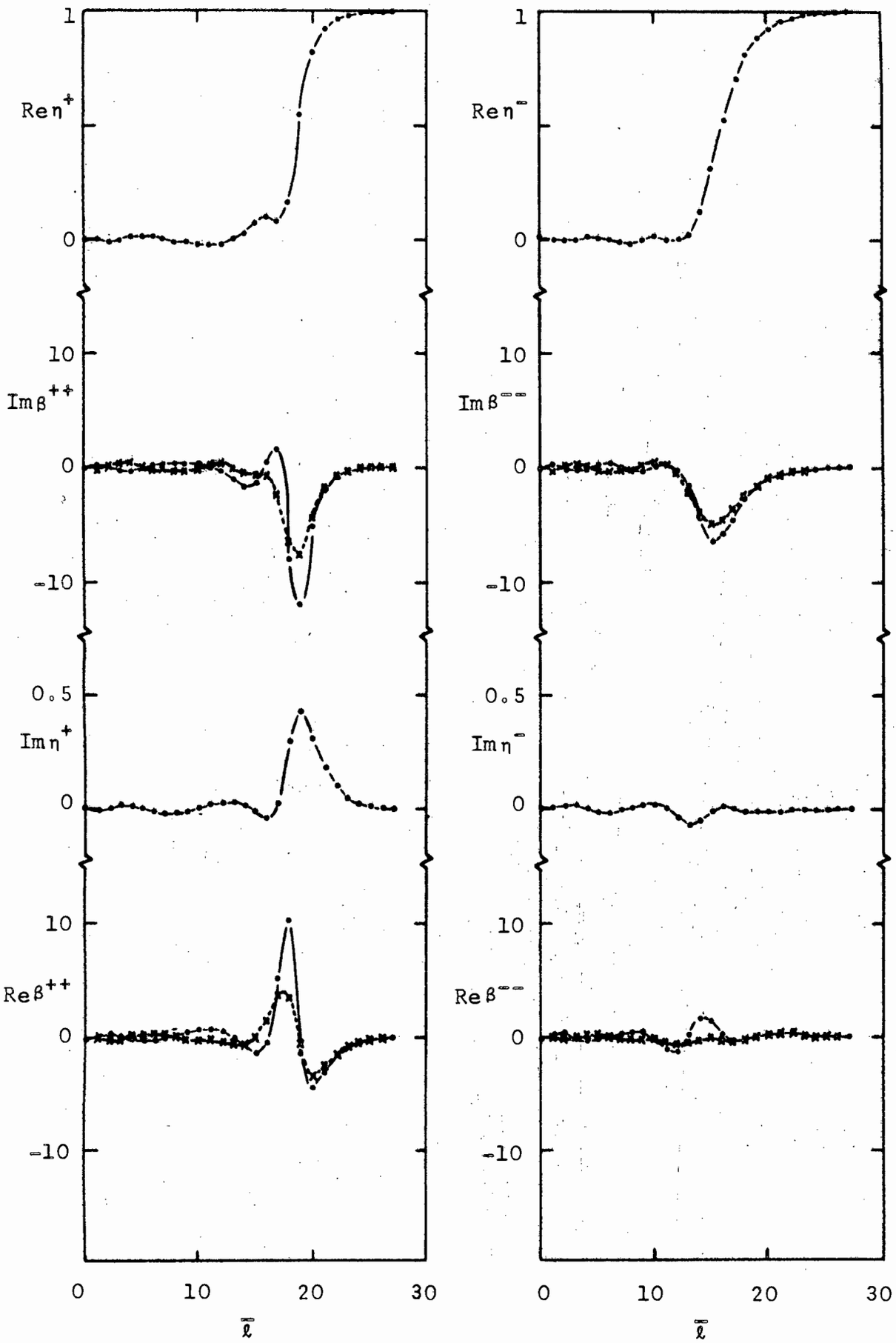

Fig. 8. Reflection coefficients and radial integrals for 60 MeV ^{3}He-scattering. For radial integrals points and crosses denote curves for K=0 and K=2, respectively.

"widths" of Re η^+ and Re η^-. However, the shapes of η^+ and η^- should not be taken too seriously at this stage because the potentials are not a result of actual analyses of $\sigma(\theta)$ and $P(\theta)$. Our spin-orbit potential was chosen rather large in order to illustrate clearly the relations (3.22). In fig. 8 the radial integrals for $K = \ell' - \ell = \pm 2$ are also shown. As in the spin-o case, the relations

$$\beta^{++}_{\ell\ell'} = \beta^{++}_{\bar{\ell}\bar{\ell}} \quad , \quad \beta^{--}_{\ell\ell'} = \beta^{--}_{\bar{\ell}\bar{\ell}} \quad , \quad \bar{\ell} = \tfrac{1}{2}(\ell+\ell') \quad ; \qquad (3.23)$$

are not as accurate as expressions (3.22). However, eqs. (3.22) and (3.23) will both be used in section 5.5 to derive an extension of the Blair phase rule (Bla 59).

4. STRONG ABSORPTION FORMALISM FOR ELASTIC SCATTERING OF PARTICLES WITH SPIN 0, $\frac{1}{2}$ AND 1

In the previous section we have discussed OM reflection coefficients. At high energies these were found to be reasonably smooth functions of ℓ. Therefore, it is possible to parameterise η_ℓ in a simple way. The simplest form is the unit step function (Bla 54). Frahn and Venter (Fra 63) give a review of other forms. These authors suggest a parameterisation of which we consider only the simplified version

$$\eta_\ell = q(t) + i\mu \frac{dq(t)}{dt} \quad , \tag{4.1}$$

where $t = \ell+\frac{1}{2}$ and $g(t)$ is a smoothed generalisation of the unit step function. One possible choice for $g(t)$ is the Woods-Saxon shape

$$q(t) = \left[1 + \exp\{ (t-T)/\Delta \} \right]^{-1} . \tag{4.2}$$

The parameters of this model are T, Δ and μ. Springer and Harvey (Spr 65) have extended eq. (4.1) by assuming

$$\eta_\ell = q(t) + \gamma \frac{dq}{dt} + i\left\{ \mu_1 \frac{dq}{dt} + \mu_2 \frac{dq}{dt} \right\} . \tag{4.3}$$

For spin-$\frac{1}{2}$ particles the parameters for $j = \ell+\frac{1}{2}$ and $j = \ell-\frac{1}{2}$ have different values in general (Fra 64). The formalism can easily be extended to spin-1 particle scattering.

With these η_ℓ-functions, cross sections and polarisations can be directly calculated by means of a computer. However, in order to exhibit the main features of the model, it is instructive to derive closed-form expressions for the angular distributions. Frahn and Venter give the expressions for

spin-o (Fra 63, Ven 63) and spin-$\frac{1}{2}$ particles (Fra 64a). Here we shall only consider the scattering of charged particles in the asymptotic diffraction region which is defined by $\theta >> \theta_c$, where θ_c is the Coulomb grazing angle given by

$$\theta_c = 2 \arctg (n|T) \quad . \tag{4.4}$$

4.1 Spin-o particles

To derive the scattering amplitude $f(\theta)$ for spin-o particles, Frahn and Venter (Fra 63, Ven 63) replace the summation in eq. (2.20) by an integral and approximate the spherical harmonics by

$$Y_l^0(\theta,0) = \tfrac{1}{2}\pi^{-1}(\sin\theta)^{-\frac{1}{2}} \left\{ e^{i(l\theta - \frac{1}{4}\pi)} + e^{-i(l\theta - \frac{1}{4}\pi)} \right\} , \tag{4.5}$$

and obtain, for η_l of the form (4.1),

$$f(\theta) = -i\lambda(\theta) \left[\frac{1+\mu(\theta_c+\theta)}{\theta_c+\theta} F_+ e^{i(T\theta - \frac{1}{4}\pi)} + \frac{1+\mu(\theta_c-\theta)}{\theta_c-\theta} F_- e^{-i(T\theta - \frac{1}{4}\pi)} \right] ,$$

$$\lambda(\theta) = \left(\frac{T}{2\pi k^2 \sin\theta} \right)^{\frac{1}{2}} e^{2i\sigma_{l_0}} , \tag{4.6}$$

$$F_\pm = \int_{-\infty}^{+\infty} \frac{dq}{dt} e^{\pm i(t-T)(\theta_c \pm \theta)} \, dt \quad .$$

For the Woods-Saxon form (4.2), we have

$$F_{\pm} = \frac{\pi \Delta (\theta_c \pm \theta)}{\sinh [\pi \Delta (\theta_c \pm \theta)]} \quad . \tag{4.7}$$

Eq. (4.6) is valid if the $d\eta/dt$ is well localised and the cut-off is large enough so that terms of order $1/\ell_0$ can be neglected. Venter (Ven 63) gives the strong absorption conditions (SAC)

$$\text{(i)} \quad 2\pi T \gg 1 \quad ,$$
$$\text{(ii)} \quad \frac{\pi \Delta}{2T} \ll 1 \quad . \tag{4.8}$$

We can easily generalise eq. (4.6) for more complicated forms of η_ℓ (such as eq. (4.3)) and obtain

$$f(\theta) = -i\lambda(\theta) \left[H_+ e^{i(T\theta - \frac{1}{4}\pi)} + H_- e^{-i(T\theta - \frac{1}{4}\pi)} \right] \quad , \tag{4.9}$$

where

$$H_{\pm} = (\theta_c \pm \theta)^{-1} \int_{-\infty}^{+\infty} \frac{d\eta(t)}{dt} \; e^{\pm i(t-T)(\theta_c \pm \theta)} \, dt \, . \tag{4.10}$$

The differential cross section is given by

$$\sigma(\theta) = \frac{T}{2\pi k^2 \sin\theta} \left[|H_+|^2 + |H_-|^2 + 2\,\mathrm{Im}\left(H_+ H_-^* e^{2iT\theta}\right) \right] . \tag{4.11}$$

If Re $\eta(t)$ and Im $\eta(t)$ are antisymmetric and symmetric functions of t-T, respectively, it follows from eq. (4.10) that H_+ and H_- are real functions. This implies that

$$\sigma(\theta) = \frac{T}{2\pi k^2 \sin\theta} \left[H_+^2 + H_-^2 + 2 H_+ H_- \sin(2T\theta) \right] . \tag{4.12}$$

The effects of the different parameters on the elastic

cross section have been discussed (Fra 63). Similar expressions are obtained for inelastic cross sections. These will be discussed in section 5.

4.2 Spin-$\frac{1}{2}$ particles

For spin-$\frac{1}{2}$ particles the calculations of the non-spin-flip amplitude $A(\theta)$ is similar to the calculations of $f(\theta)$ of section 4.1. By comparison, we find

$$A(\theta) \approx -i\,\lambda(\theta)\left\{ H_+(\bar{\eta})\, e^{i(T\theta - \frac{1}{4}\pi)} + H_-(\bar{\eta})\, e^{-i(T\theta - \frac{1}{4}\pi)} \right\}, \qquad (4.13)$$

where

$$\bar{\eta}(t) = \tfrac{1}{2}\left\{ \eta^+(t) + \eta^-(t) \right\}, \qquad (4.14)$$

$$H_\pm(\bar{\eta}) = \tfrac{1}{2}\left\{ H_\pm(\eta^+) + H_\pm(\eta^-) \right\}$$

$$= \frac{1}{\theta_c \pm \theta} \int_{-\infty}^{+\infty} \frac{d\bar{\eta}}{dt}\; e^{\pm i(t-\bar{T})(\theta_c \pm \theta)}\, dt\,. \qquad (4.15)$$

For the calculation of the spin-flip amplitude $B(\theta)$ we use the approximation

$$Y_l^1(\theta,0) \approx \tfrac{1}{2}\pi^{-1}(\sin\theta)^{-\frac{1}{2}}\left\{ e^{i(l\theta + \frac{1}{4}\pi)} + e^{-i(l\theta + \frac{1}{4}\pi)} \right\}, \qquad (4.16)$$

and obtain

$$B(\theta) = -\tfrac{1}{2}\lambda(\theta)\left[H_+(\xi)\, e^{i(T\theta - \frac{1}{4}\pi)} - H_-(\xi)\, e^{-i(T\theta - \frac{1}{4}\pi)} \right], \qquad (4.17)$$

where

$$\zeta(t) = \eta^+(t) - \eta^-(t) \,, \tag{4.18}$$

$$H_\pm(\zeta) = H_\pm(\eta^+) - H_\pm(\eta^-)$$

$$= \frac{1}{\theta_c \pm \theta} \int_{-\infty}^{+\infty} \frac{d\zeta}{dt}\, e^{\pm i(t-T)(\theta_c \pm \theta)}\, dt. \tag{4.19}$$

The angular distributions of the cross section and polarisation are calculated from eq. (2.22), giving

$$\sigma(\theta) \approx \frac{T}{2\pi k^2 \sin\theta}\Big[|H_+(\bar\eta)|^2 + |H_-(\bar\eta)|^2 + 2\,\mathrm{Im}\left\{H_+(\bar\eta)\, H_-^*(\bar\eta)\, e^{2iT\theta}\right\}$$

$$+ \tfrac{1}{4}\left\{ |H_+(\zeta)|^2 + |H_-(\zeta)|^2 - 2\,\mathrm{Im}\left(H_+(\zeta)\, H_-^*(\zeta)\, e^{2iT\theta}\right)\right\}\Big] \,, \tag{4.20}$$

$$\sigma(\theta) P(\theta) \approx \frac{T}{2\pi k^2 \sin\theta}\Big[\mathrm{Re}\left\{ H_+(\bar\eta)\, H_+^*(\zeta) - H_-(\bar\eta)\, H_-^*(\zeta)\right\}$$

$$- \mathrm{Im}\left\{ H_+(\bar\eta)\, H_-^*(\zeta)\, e^{2iT\theta} + H_-(\bar\eta)\, H_+^*(\zeta)\, e^{-2iT\theta}\right\}\Big] \,. \tag{4.21}$$

Expressions (4.20) and (4.21) are the main result of this subsection. They will be compared to the inelastic expressions in section 5.5. We now consider specific forms of η^+ and η^- and discuss the resultant polarisation.

The polarisation of 182 MeV protons (Ven 64) and 29 MeV ^{3}He-particles (Fra 65a) has been described in terms of the "ν-model". In this model, it is assumed that the $\eta^\pm$-functions in parameterisation (4.1) differ only in their μ-values. Defining $\mu = \frac{1}{2}(\mu^+ + \mu^-)$ and $\nu = \mu^+ - \mu^-$, we obtain

$$H_\pm(\bar\eta) = \left[\frac{1}{\theta_c \pm \theta} + \bar\mu\right] F_\pm \,, \tag{4.22}$$

$$H_{\pm}(\xi) = \nu F_{\pm} \quad . \tag{4.23}$$

For small Coulomb parameters, the "ν-model" gives an angular distribution for the polarisation which is positive for positive ν-values and oscillates in phase with the cross section.

Hüfner and de Shalit (Hüf 65) have reproduced a Rodberg-type relation (Rod 69) between $\sigma(\theta)$ and the polarisation, $\sigma(\theta)P(\theta) = K(\theta)\, d\sigma(\theta)/d\theta$ where $K(\theta)$ is a slowly varying function of θ. The extended Rodberg relation is also obtained (Fra 66) by assuming that μ_2 in eq. (4.3) is the only variable depending on the spin state of the projectile. By taking $\mu_1 = o$, $\gamma = o$, $\bar{\mu}_2 = \frac{1}{2}(\mu_2^+ + \mu_2^-)$ and $\nu_2 = \mu_2^+ - \mu_2^-$, we find

$$\begin{aligned} H_{\pm}(\bar{\eta}) &= \left[(\theta_c \pm \theta)^{-1} - i\,\bar{\mu}_2(\theta_c \pm \theta)\right] F_{\pm} \quad , \\ H_{\pm}^{*}(\xi) &= i\,\nu_2(\theta_c \pm \theta)\, F_{\pm} \quad . \end{aligned} \tag{4.24}$$

By inserting eqs. (4.24) in eq. (4.21) and taking $\theta_c = o$, we obtain

$$\sigma(\theta)P(\theta) = -2\,|\lambda(\theta)|^2\,\nu_2\,(F)^2\cos(2T\theta) \quad . \tag{4.25}$$

For $\bar{\mu}_2 = o$, we see from eq. (4.12) that the oscillation in the differential cross section is proportional to $\sin(2T\theta)$. The rapid oscillations of eq. (4.25) are thus of the Rodberg form $d\sigma(\theta)/d\theta$.

The criterion for the type of polarisation can be stated as follows. If $H_{\pm}(\bar{\eta})$ is predominantly real (i.e. $\sigma(\theta)$ oscillates like $\sin(2T\theta)$), the generalised Rodberg relation is obtained for predominantly imaginary $H_{\pm}(\xi)$, while

polarisation of the "ν-model" type is obtained if $H_\pm(\xi)$ is predominantly real.

Frahn and Venter (Fra 64) have shown that the Coulomb interaction suppresses the polarisation for $\theta << \theta_c$. This is due to the fact that the major contribution to small angle scattering comes from the spin-independent Coulomb interaction. For $\theta >> \theta_c$, the Coulomb interaction damps out the diffraction oscillations in the "ν-model". We wish to point out one other interesting feature. If $\eta^+(t)$ and $\eta^-(t)$ are real functions, we have no polarisation for neutral particle scattering, but polarisation is possible for charged particles. If η^+ and η^- differ only in their cut-off value ($\tau = T_+ - T_-$) the polarisation is enhanced by the Coulomb interaction. The calculation yields

$$
\begin{aligned}
H_\pm(\bar{\eta}) &= \mathcal{H}_\pm \cos\{\tfrac{1}{2}\tau(\theta_c \pm \theta)\} \,, \\
H_\pm(\xi) &= -i\,\mathcal{H}_\pm \sin\{\tfrac{1}{2}\tau(\theta_c \pm \theta)\} \,, \\
\mathcal{H}_\pm &= (\theta_c \pm \theta)^{-1} \int_{-\infty}^{+\infty} \frac{d\bar{\eta}}{dt}(t,\bar{T})\; e^{\pm i(t-\bar{T})(\theta_c \pm \theta)}\, dt \,, \\
\bar{T} &= \tfrac{1}{2}(T_+ + T_-) \,.
\end{aligned}
\tag{4.26}
$$

Again $H_\pm(\xi)$ is imaginary if $H_\pm(\bar{\eta})$ is real and a Rodberg-type relation follows. (Even if $\mathcal{H}_\pm$ is complex we obtain a generalised Rodberg relation because the phase of $H_\pm(\bar{\eta})$ and $H_\pm(\xi)$ differ by $\pm \frac{\pi}{2}$.) For real $\mathcal{H}_\pm$, insertion of eq. (4.26) in (4.21) yields

$$
\sigma(\theta) P(\theta) \approx |\lambda(\theta)|^2\, \mathcal{H}_+ \mathcal{H}_-\, \sin(\tau\theta_c)\, \cos(2T\theta) \,. \tag{4.27}
$$

If $\theta_c = 0$, we find $P(\theta) \approx 0$.

We have found different ways of obtaining the generalised Rodberg relation. To distinguish between these, actual

analyses of $\sigma(\theta)$, $P(\theta)$ and the Wolfenstein rotation parameter (Wol 54, Hod 63) are necessary.

4.3 Spin-1 particles

For spin-1 particles the amplitudes A-E of eq. (2.23) can be calculated by methods similar to those used in sections 4.1 and 4.2.

To achieve this we define the quantities $\bar{\alpha}_\ell = 1 - \bar{\eta}_\ell$, ξ_ℓ, ψ_ℓ and γ_ℓ by

$$\begin{aligned} \alpha_\ell^{\pm} &= \bar{\alpha}_\ell \mp \tfrac{1}{2}\xi_\ell \,, \\ \alpha_\ell^{0} &= \bar{\alpha}_\ell - \psi_\ell \,, \\ \beta_\ell &= \gamma_\ell e^{i(\sigma_{\ell+1}+\sigma_{\ell-1})} \approx \gamma_\ell e^{2i\sigma_\ell} \,, \end{aligned} \tag{4.28}$$

(the latter approximation is possible because $|\beta_\ell|$ is confined to the vicinity of ℓ_0) and make use of the approximate relations

$$\begin{aligned} &\hat{\ell+1}^{-1} Y^0_{\ell+1} + \hat{\ell+1}^{-1} Y^0_{\ell-1} \approx \{\ell(\ell+1)\}^{-1} \hat{\ell} \cos\theta\, Y^0_\ell \,, \\ &\left[\frac{\ell(\ell+2)}{2\ell+3}\right]^{\frac{1}{2}} Y^1_{\ell+1} - \left[\frac{(\ell+1)(\ell-1)}{2\ell-1}\right]^{\frac{1}{2}} Y^1_{\ell-1} \approx \hat{\ell} \sin\theta\, Y^0_\ell \,, \\ &\left[\frac{(\ell+3)(\ell+2)}{2\ell+3}\right]^{\frac{1}{2}} Y^2_{\ell+1} + \left[\frac{(\ell-2)(\ell-1)}{2\ell-1}\right]^{\frac{1}{2}} Y^2_{\ell-1} \approx \hat{\ell} \cos\theta\, Y^2_\ell \,, \end{aligned} \tag{4.29}$$

where Y^m_ℓ stands for $Y^m_\ell(\theta,0)$. After neglecting terms of order ℓ^{-1}, we obtain

$$A \approx f_c + \frac{i\sqrt{\pi}}{k} \sum_\ell (\bar{\alpha}_\ell - \gamma_\ell \cos\theta)\, e^{2i\sigma_\ell}\, \hat{\ell}\, Y_\ell^0 \quad ,$$

$$B \approx f_c + \frac{i\sqrt{\pi}}{k} \sum_\ell (\bar{\alpha}_\ell - \tfrac{1}{2}\psi_\ell + \tfrac{1}{2}\gamma_\ell \cos\theta)\, e^{2i\sigma_\ell}\, \hat{\ell}\, Y_\ell^0 \quad ,$$

$$C \approx \frac{i\sqrt{\pi}}{k} \sum_\ell \frac{1}{\sqrt{2}} \left\{ \tfrac{1}{2}\xi_\ell Y_\ell^1 - \gamma_\ell \sin\theta\, Y_\ell^0 \right\} \hat{\ell}\, e^{2i\sigma_\ell} \quad , \qquad (4.30)$$

$$D \approx \frac{i\sqrt{\pi}}{k} \sum_\ell \frac{1}{\sqrt{2}} \left\{ \tfrac{1}{2}\xi_\ell Y_\ell^1 + \gamma_\ell \sin\theta\, Y_\ell^0 \right\} \hat{\ell}\, e^{2i\sigma_\ell} \quad ,$$

$$E \approx \frac{i\sqrt{\pi}}{k} \sum_\ell \frac{1}{2} \left\{ \psi_\ell + \gamma_\ell \cos\theta \right\} e^{2i\sigma_\ell}\, \hat{\ell}\, Y_\ell^2 \quad .$$

By using the asymptotic form of the spherical harmonics

$$Y_\ell^m(\theta,0) = (4\pi^2 \sin\theta)^{-\frac{1}{2}} \left[e^{i(t\theta - \frac{1}{4}\pi)}\, i^m + e^{-i(t\theta - \frac{1}{4}\pi)}\, i^{-m} \right] \quad , \qquad (4.31)$$

replacing the summations in eqs. (4.30) by integrals and taking Fourier transforms, we obtain in the asymptotic diffraction region $\theta >> \theta_c$ the expressions

$$A(\theta) = -i\,\lambda(\theta) \left[Z(\bar{\eta}) + Z(\gamma)\cos\theta \right] \quad ,$$

$$B(\theta) = -i\,\lambda(\theta) \left[Z(\bar{\eta}) + \tfrac{1}{2} Z(\psi) - \tfrac{1}{2} Z(\gamma)\cos\theta \right] \quad ,$$

$$C(\theta) = i\,\lambda(\theta) \tfrac{1}{\sqrt{2}} \left[\tfrac{1}{2} Z(\xi) - Z(\gamma)\sin\theta \right] \quad , \qquad (4.32)$$

$$D(\theta) = i\,\lambda(\theta) \tfrac{1}{\sqrt{2}} \left[\tfrac{1}{2} Z(\xi) + Z(\gamma)\sin\theta \right] \quad ,$$

$$E(\theta) = -\tfrac{1}{2} i\,\lambda(\theta) \left[Z(\psi) + Z(\gamma)\cos\theta \right] \quad ,$$

where $\lambda(\theta)$ is given by eq. (4.6). The quantities Z are

defined by

$$Z(\bar{\eta}, \psi, \gamma) = H_+(\bar{\eta}, \psi, \gamma)\, e^{i\phi} + H_-(\bar{\eta}, \psi, \gamma)\, e^{-i\phi},$$

$$Z(\xi) = i\left[H_+(\xi)\, e^{i\phi} - H_-(\xi)\, e^{-i\phi}\right], \qquad (4.33)$$

$$\phi = T\theta - \tfrac{1}{4}\pi,$$

and the functions $H_\pm$ are expressed in terms of Fourier transforms, similar to eqs. (4.15) and (4.19).

Before we write down expressions for vector and tensor polarisation, it is instructive to interpret the quantities ξ_ℓ and ψ_ℓ in terms of OM potentials. Satchler (Sat 60c) has shown that, apart from the normal spin-orbit interaction, $V_{s.o.}(r)\ \underset{\sim}{\ell}\cdot\underset{\sim}{s}$, we can have three types of tensor interaction in the scattering of spin-1 particles by spin-0 targets. These are

$$V_1(\underset{\sim}{r}) = V_1(\underset{\sim}{r})\, T_r = V_1(\underset{\sim}{r})\left[(\underset{\sim}{S}\cdot\underset{\sim}{r})^2 - \tfrac{2}{3}r^2\right]\frac{1}{r^2},$$

$$V_2(\underset{\sim}{r}) = V_2(\underset{\sim}{r})\, T_p = V_2(\underset{\sim}{r})\left[(\underset{\sim}{S}\cdot\underset{\sim}{p})^2 - \tfrac{2}{3}p^2\right], \qquad (4.34)$$

$$V_3(\underset{\sim}{r}) = V_3(\underset{\sim}{r})\, T_L = V_3(\underset{\sim}{r})\left[(\underset{\sim}{\ell}\cdot\underset{\sim}{S})^2 + \tfrac{1}{2}\,\underset{\sim}{\ell}\cdot\underset{\sim}{S} - \tfrac{2}{3}\ell^2\right].$$

The operators $\underset{\sim}{\ell}\cdot\underset{\sim}{s}$ and T_L are diagonal in the partial wave representation, but T_r and T_p are not. The latter are responsible for the off-diagonal S-matrix elements γ_ℓ. For $V_2 = V_3 = 0$, we have $\gamma_\ell = 0$.

For small non-central interactions we can calculate η_ℓ^j in DWBA and obtain

$$\eta_\ell^j - \eta_\ell \propto \lambda_\ell^j \int_0^\infty u_\ell(r)\, V(r)\, u_\ell(r)\, dr, \qquad (4.35)$$

where η_ℓ and $u_\ell(r)$ are reflection coefficients and wave functions for the central part of the interaction.

For an $\underset{\sim}{\ell}.\underset{\sim}{s}$ interaction we have $\lambda_\ell^j = \ell, \ell-1, -(\ell+1)$ for $j = \ell+1, \ell, \ell-1$, respectively. If ℓ is large it follows that $\psi_\ell << \xi_\ell$. For the T_L interaction we have $\lambda_\ell^j = \frac{1}{6}(\ell+1)(\ell+3), -\frac{1}{6}(2\ell-1)(2\ell+3), \frac{1}{6}\ell(\ell+1)$ for $j = \ell+1, \ell, \ell-1$, respectively. Although $\bar{\eta}_\ell = \frac{1}{2}(\eta_\ell^+ + \eta_\ell^-)$ is different from η_ℓ , we readily see that $\xi_\ell << \psi_\ell$, for large ℓ. (Similar expressions can also be obtained for the diagonal element of T_r (Ray 65).) We can therefore approximately identify ξ_ℓ with vector interactions, ψ_ℓ with diagonal tensor interactions, and γ_ℓ with off-diagonal tensor interactions. The identification is valid for large ℓ-values and in first order pertubation theory.

We now return to the closed form calculations of polarisation. For the vector polarisation, we obtain from eqs. (4.32) and (2.25) the expression

$$\sigma(\theta) P(\theta) = -\tfrac{2}{3} \left|\lambda(\theta)\right|^2 \mathrm{Im}\left[Z(\bar{\eta}) Z^*(\xi)\right] . \qquad (4.36)$$

It is seen from eq. (4.36) that, apart from the tensor contributions to $\bar{\eta}_\ell$ and to $\sigma(\theta)$, the vector polarisation of strongly absorbed particles (for $\theta >> \theta_c$) depends only on the vector interaction. This result may prove useful in OM search programmes.

Tensor polarisation can easily be calculated from eqs. (2.25) and (4.32). Here we give only the expressions for the special case where no off-diagonal tensor interactions are present (i.e. $Z(\gamma) = 0$). They are

$$\sigma(\theta)\, t_{20}(\theta) \approx \frac{\sqrt{2}}{3} |\lambda(\theta)|^2 \left[-\tfrac{1}{8} |Z(\xi)|^2 + \tfrac{1}{2} |Z(\psi)|^2 + \mathrm{Re}\{ Z(\bar{\eta})\, Z^*(\psi) \} \right] ,$$

$$\sigma(\theta)\, t_{21}(\theta) \approx 0 \quad , \qquad (4.37)$$

$$\sigma(\theta)\, t_{22}(\theta) \approx \frac{1}{\sqrt{3}} |\lambda(\theta)|^2 \left[-\tfrac{1}{8} |Z(\xi)|^2 + \tfrac{1}{2} |Z(\psi)|^2 + \mathrm{Re}\{ Z(\bar{\eta})\, Z^*(\psi) \} \right] .$$

In our approximation we thus find two interesting results: (i) in the absence of off-diagonal tensor interactions, $t_{21} \approx o$ and $t \approx \sqrt{273}\, t_{22}$, and (ii) if only central and $\underset{\sim}{\ell} \cdot \underset{\sim}{s}$ interactions are present, $t_{20} \approx \sqrt{273}\, t_{22} \lesssim o$. For high energy deuteron scattering these results were also obtained in impulse approximation, under the assumption that the deuteron is in a pure s-state (Saw 65).

In section 4.2, the generalised Rodberg relation for spin-$\frac{1}{2}$ particle polarisation was shown to follow if the phases of $H_\pm(\bar{\eta})$ and $H_\pm(\xi)$ differ by $\pm\frac{1}{2}\pi$. The same result holds for spin-1 particles. As an example we assume

$$H_\pm(\bar{\eta}) = H_\pm \quad = \text{real},$$
$$H_\pm(\xi) = i h_\pm \quad = \text{imaginary},$$
$$H_\pm(\psi) = H_\pm(\gamma) = o,$$

and obtain

$$\sigma(\theta) = |\lambda(\theta)|^2 \left[H_+^2 + H_-^2 + 2 H_+ H_- \sin(2T\theta) + \tfrac{1}{6} \{ h_+^2 + h_-^2 - 2 h_+ h_- \sin(2T\theta) \} \right] , \qquad (4.38)$$

$$\sigma(\theta)\, P(\theta) = \tfrac{2}{3} |\lambda(\theta)|^2 (H_+ h_- + H_- h_+) \cos(2T\theta) , \qquad (4.39)$$

$$\sigma(\theta)\, t_{20}(\theta) = \sqrt{2/3}\ \ \sigma(\theta)\, t_{22}(\theta)$$
$$= \frac{-1}{12\sqrt{2}}\ |\lambda(\theta)|^2 \left[h_+^2 + h_-^2 + 2 h_+ h_- \sin(2T\theta)\right] . \qquad (4.40)$$

For $\underset{\sim}{\ell}\cdot\underset{\sim}{s}$ interactions which produce a generalised Rodberg relation for the vector polarisation, it follows from eq. (4.40) that the tensor polarisations t_{20} and t_{22} oscillate in phase with the main contribution to the oscillations in the cross section.

For forward angles the experimental data and the OM fits for 22 MeV deuterons scattered by ^{40}Ca (Ray 63, Ray 65) qualitatively satisfy the main features of eqs. (4.38)-(4.40). Hüfner and de Shalit (Hüf 65) have described these data by means of a sharp-cutoff model. These authors introduced an angle-dependent radius (or cut-off value) to describe the observed "stretching" of the oscillation period. In section 5 it is shown (for inelastic scattering) that η_ℓ-functions of the form (4.3) have the same effect, but it has not been possible to fit the 22 MeV deuteron data by this method. Calculations with OM η_ℓ-coefficients showed that the irregular behaviour of the diffraction oscillations is due to the contributions from low ℓ-values. It is therefore amazing that the phase relations still hold qualitatively for a case of incomplete absorption. A similar situation occurs in 30-40 MeV proton scattering where the absorption of low-ℓ partial waves is far from complete and the radial integrals for low ℓ-values are sometimes even larger than those for surface ℓ-values. However, the experimental data are still in qualitative agreement with the Blair phase rule.

Our results are expected to increase in accuracy with increasing deuteron energy, because the absorption of low-ℓ partial waves increases with energy. Other light spin-1

nuclei are ^{6}Be and ^{14}N. Although little polarisation is expected for ^{14}N scattering by heavy targets (because the Coulomb interaction dominates) our relations are expected to be useful for the scattering of ^{14}N (with an energy of about 10 MeV/neucleon) by light target nuclei, such as ^{16}O. In such cases the strong absorption conditions are expected to be well satisfied.

5. CLOSED FORMULAE FOR INELASTIC SCATTERING AND POLARISATION OF SPIN-o AND SPIN-$\frac{1}{2}$ PARTICLES

Closed form expressions for the angular distribution of inelastic cross sections were first derived in Fraunhofer approximation (Dro 55, Ino 57, Bla 59). These expressions led to the Blair phase rule which states that for one-phonon excitations the diffraction oscillations in inelastic scattering to odd/even parity states are in-/out-of phase with the elastic diffraction oscillations. For multipolarity L = o,2, the inelastic scattering amplitude was later (Bla 62) expressed in terms of the elastic reflection coefficients in open form. Austern and Blair (Aus 65) have generalised this result for all L-values. However, the results become less accurate as L increases. It was shown in section 2.7 that the Austern-Blair (AB) relations can be extended to spin-$\frac{1}{2}$ particle scattering. A number of papers (Bas 65, Hah 66, Pot 66a, Dar 66) dealing with the closed form expressions for spin-o particles have appeared. Here we follow closely ref. (Hah 66).

5.1 Spin-o particles

For spin-o particles, expression (2.35) reduces to

$$T_L^M = \hat{L}\,\langle L \| \alpha_L \| 0 \rangle \frac{4\pi}{k_i k_f} \sum_{\ell\ell'} i^{\ell-\ell'} \beta_{\ell\ell'}(k_i k_f)\, e^{i(\sigma_\ell + \sigma_{\ell'})} \cdot \hat{\ell}'\, Y_{\ell'}^{-M}(\theta,0)\, \langle \ell' L\, -M\, M | \ell 0 \rangle \langle \ell' L\, 0\, 0 | \ell 0 \rangle \quad . \tag{5.1}$$

With the definitions

$$K \equiv \ell - \ell' \quad ,$$
$$\bar{\ell} \equiv \tfrac{1}{2}(\ell + \ell') = \ell' + \tfrac{1}{2}K \quad , \tag{5.2}$$

the radial integrals can be written in the form

$$\beta_{\ell\ell'} = -\tfrac{1}{2} i (E_i E_f)^{\frac{1}{2}} h_K(\bar{\ell}) \quad . \tag{5.3}$$

For Q = o and $h_K(\bar{\ell}) = dn_{\bar{\ell}}/d\bar{\ell}$, eq. (5.3) reduces to the AB expression. For Q = o, it follows that

$$h_K(\bar{\ell}) = h_{-K}(\bar{\ell}) \quad . \tag{5.4}$$

Expression (5.4) is important for the discussions in section 6.

Defining an amplitude B^{LM} by

$$T^M_L = \hat{L} \langle L \| \alpha_L \| 0 \rangle \frac{4\pi}{k_i k_f} i^{-(L+1)} \cdot \tfrac{1}{2}(E_i E_f)^{\frac{1}{2}} B^M_L \quad , \tag{5.5}$$

we have

$$\sigma(\theta) = C \sum_M |B^M_L|^2 \quad ,$$
$$C = \tfrac{1}{4}(2L+1) |\langle L \| \alpha_L \| 0 \rangle|^2 \frac{k_f}{k_i} \quad . \tag{5.6}$$

The presence of ℓ-space localisation of the radial integrals allows us to expand $h_K(\bar{\ell})$ in terms of derivatives of the Woods-Saxon function (3.2). The AB theory suggests the form

$$h_K(\bar{\ell}) = \sum_{j=1} a_{Kj} \frac{d^j q(\bar{\ell})}{d\bar{\ell}} + i \sum_{j=2} b_{Kj} \frac{d^j q(\bar{\ell})}{d\bar{\ell}} \quad . \tag{5.7}$$

We again require that the SAC (4.8), are satisfied. In addition we require

$$\ell_o - L - \Delta \gg 1 . \tag{5.8}$$

We can now approximate the Coulomb phase shifts by

$$\sigma_{\ell'}(f) + \sigma_{\ell}(i) \approx 2\sigma_{\ell_0} + (\bar{\ell} - \ell_0)\theta_c + \tfrac{1}{4} K \delta\theta_c \,. \qquad (5.9)$$

In eq. (5.9) the bar indicates the arithmetical average over the initial and final channels, and $\delta\theta_c = \theta_c(i) - \theta_c(f)$.

Since $h_K(\bar{\ell})$ is confined to a narrow region in ℓ-space and important contribution comes from ℓ-values, the Clebsch-Gordan coefficients in eq. (5.1) can be approximated by elements of the rotation matrices (Bru 57). We have, subject to condition (5.8),

$$\langle \ell' L \; -M \, M \,|\, \ell 0 \rangle \approx d^L_{KM}(-\tfrac{1}{2}\pi) \,. \qquad (5.10)$$

For the sign of the d-matrices the convention of ref. (Bri 62) is used.

From eqs. (5.1), (5.3), (5.5), (5.9) and (5.10), we find

$$B^M_L = e^{2i\sigma_{\ell_0}} \sum_K i^{K+L} d^L_{KM}(-\tfrac{1}{2}\pi)\, d^L_{K0}(-\tfrac{1}{2}\pi)\, e^{i\frac{1}{4}K\delta\theta_c} \cdot \sum_{\ell} e^{i(\ell + \frac{1}{2}K - \ell_0)\bar{\theta}_c} h_K(\ell + \tfrac{1}{2}K)\, Y^{-M}_{\ell}(\theta, 0) \,. \qquad (5.11)$$

From the symmetry properties of rotation matrices and the properties of the spherical harmonics it follows that

$$d^L_{KM}(-\tfrac{1}{2}\pi)\, d^L_{K0}(-\tfrac{1}{2}\pi)\, Y^{-M}_{\ell}(\theta, 0) = d^L_{KM}(\tfrac{1}{2}\pi)\, d^L_{K0}(\tfrac{1}{2}\pi)\, Y^{M}_{\ell}(\theta, 0) \qquad (5.12)$$

The second sum of eq. (5.11) may be replaced by an integral (Ven 63) and we define quantities A_{MK} by

$$A_{MK}(\theta) = \int_{-\infty}^{+\infty} dt\, \sqrt{t}\; Y_l^M(\theta,0)\, h_K(t+\tfrac{1}{2}K,T)\, e^{i(t+\frac{1}{2}K-T)\bar{\theta}_c} \tag{5.13}$$

By solving the appropriate differential equation in WKB approximation (Bru 57), the spherical harmonics can, for $l>>1$, $\varepsilon = M/l$ and $\varepsilon<<\theta<<\pi-\varepsilon$, be approximated by

$$Y_l^M(\theta,0) = \tfrac{1}{2}\pi^{-1}(\sin\theta)^{-\frac{1}{2}}\{e^{i\phi_M(t)} + e^{-i\phi_M(t)}\}\,, \tag{5.14}$$

$$\phi_M(t) = t\theta + \alpha + (2M-1)\tfrac{1}{4}\pi\,.$$

The phase correction α depends on M, l and θ, but it is a slowly varying function of l. We have approximated a factor $\lambda(\theta)$ by unity. This factor is, in WKB approximation, given by $\lambda(\theta) = (\sin\theta)^{\frac{1}{2}}\{\sin(\theta+\beta)\sin(\theta-\beta)\}^{-\frac{1}{4}}$ where β = arc sin (M/l).

By using eq. (5.14) in eq. (5.13), substituting l for $l+\frac{1}{2}K$, and neglecting terms of order $K/(2l+1)$ we obtain

$$A_{MK} = A^{+}_{MK} + A^{-}_{MK}\,, \tag{5.15}$$

$$A^{\pm}_{MK} = \left(\frac{T}{2\pi^2\sin\theta}\right)^{\frac{1}{2}} e^{\mp i\frac{1}{2}K\theta}\; G^{\pm}_{MK}\,, \tag{5.16}$$

$$G^{\pm}_{MK} = H^{\pm}_{K}\, e^{\pm i\phi_M(T)}\,, \tag{5.17}$$

$$H^{\pm}_{K} = \int_{-\infty}^{\infty} dt\; h_K(t,T)\, e^{\pm i(t-T)(\bar{\theta}_c \pm \theta)}\,. \tag{5.18}$$

For the differential cross section we have

$$\sigma(\theta) = \frac{T \cdot c}{2\pi^2 \sin\theta} \sum_M \Big| \sum_K i^{K+L} d^L_{KM}(\tfrac{1}{2}\pi)\, d^L_{K0}(\tfrac{1}{2}\pi)\, e^{i\frac{1}{4}K\delta\theta_c} \cdot \{ e^{-i\frac{1}{2}K\theta} G^+_{MK} + e^{+i\frac{1}{2}K\theta} G^-_{MK} \} \Big|^2 . \tag{5.19}$$

It is seen from eqs. (5.17)-(5.19) that the differential cross section is essentially a function of the Fourier transforms of the radial integrals.

In order to obtain explicit formulae for $H^{\pm}_K$, we introduce $f(x) = dg(x)/dx$ and denote the Fourier transforms of $f(x)$ by $F_{\pm}$. We then find

$$H^{\pm}_K \approx \sum_{j=0} (-i)^j a_{K,j+1} (\theta_c \pm \theta)^j F_{\pm} + i \sum_{j=1} (-i)^j b_{K,j+1} (\theta_c \pm \theta)^j F_{\pm} . \tag{5.20}$$

For the Woods-Saxon form (see eqs. (4.3) and (4.7))

$$F_{\pm} = \frac{\pi \Delta (\theta_c \pm \theta)}{\sinh [\pi \Delta (\theta_c \pm \theta)]} . \tag{5.21}$$

5.2 Adiabatic Approximation

We now introduce the AB relations (3.15) and (3.18) and take the form (4.1) for the reflection coefficients. Therefore, $a_{k1} = 1$, $b_{k2} = \mu$, $a_{kj} = 0$ for $j \neq 1$ and $b_{kj} = 0$ for $j \neq 2$. Eq. (5.20) reduces to

$$H^{\pm}_K = \{ 1 + \mu(\bar{\theta}_c \pm \theta) \} F_{\pm} . \tag{5.22}$$

In the present case $G^{\pm}_{MK}$ is independent of K and the index K is dropped. For $k_f = k_i$, we have $\delta\theta_c = o$. By introducing

$$E_{LM}(\pm\theta) = \sum_K i^{K+L} d^L_{KM}(\tfrac{1}{2}\pi)\, d^L_{KO}(\tfrac{1}{2}\pi)\, e^{\mp \frac{1}{2} i K\theta}, \qquad (5.23)$$

it follows that

$$B^M_L = \left(\frac{T}{2\pi^2 \sin\theta}\right)^{\frac{1}{2}} e^{2i\sigma_L} \left\{ E_{LM}(+\theta) G^+_M + E_{LM}(-\theta) G^-_M \right\}, \qquad (5.24)$$

$$\sigma(\theta) = \frac{T \cdot C}{2\pi^2 \sin\theta} \sum_M \left[|E_{LM}(\theta) G^+_M|^2 + |E_{LM}(-\theta) G^-_M|^2 \right. \qquad (5.25)$$

$$\left. + 2\,\mathrm{Re}\left\{ (E_{LM}(\theta) G^+_M)^* E_{LM}(-\theta) G^-_M \right\} \right].$$

In eq. (5.25) the first two terms are smooth functions of θ, while the last term is oscillatory. Eq. (5.18) shows that $|G^{\pm}_M|^2$ can be replaced by $|H^{\pm}|^2$. By using eq. (B.3) of appendix B, we see that the smooth contribution becomes

$$2\pi \sin\theta \left[\sigma(\theta)\right]_{av} = C T \pi^{-1} \left[|H^+|^2 + |H^-|^2 \right]. \qquad (5.26)$$

In a large number of reactions between complex nuclei the strong damping condition $F_+ << F_-$ (Fra 64b) holds in the relevant angular region. In this case

$$2\pi \sin\theta\ \sigma(\theta) = C T \pi^{-1} \left\{ 1 + \mu(\theta_c - \theta) \right\}^2 F_-^2 \qquad (5.27)$$

Eq. (5.27) has been obtained previously (Fra 64b, Bas 65) for $\mu = o$.

We now consider the oscillatory contribution to eq. (5.25). We restrict ourselves to functions f which are symmetric in (t-T) so that the Fourier transforms $F_\pm$ are real. By using eqs. (B.7) and (B.8) of appendix B we obtain

$$2\pi \sin\theta \, [\sigma(\theta)]_{osc.} = 2CT \, \pi^{-1} \, H^{+} H^{-} \sum_{M} (-)^{L+M} \left| E_{LM}(\theta) \right|^{2} \mathrm{Re}\, e^{-2i\phi(T)} \quad (5.28)$$

For $\varepsilon_1 << \theta << \pi - \varepsilon_1$, $\varepsilon_1 = M^2/T$, the phase correction α_o may be neglected. Under this assumption we have

$$2\pi \sin\theta \, \sigma(\theta) = CT\pi^{-1} \left[(H^{+})^2 + (H^{-})^2 + (-1)^{L} 2 H^{+} H^{-} \sin(2T\theta) \right] . \quad (5.29)$$

Comparison of eq. (5.29) with eq. (4.12) clearly demonstrates the Blair phase rule. From eqs. (4.9) and (5.20) it follows that $H^{\pm} = (\theta_c \pm \theta) H_{\pm}$. For $\theta > \theta_c$, the oscillations of eq. (5.29) for odd/even L are in-/out-of phase with those of eq. (4.12). The values of the minima of the quantity in square brackets in eq. (5.29) are given by $(H^{+} - H^{-})^2$. In the neutral limit $\theta_c = o$, the filling of the minima is due to the "nuclear" real phase shift parameter μ, since $(H^{+} - H^{-})^2 = 4 \left[\mu \theta F \right]^2$. In the case where the Coulomb interaction dominates, the filling is due to the fact that F_{+} and F_{-} have maximum value (=1) at $-\theta_c$ and θ_c , respectively. There is partial cancellation of the two contributions for positive μ.

Eq. (5.29) is a good approximation for L = o, and $\varepsilon_2 << \theta << \pi - \varepsilon_2$, $\varepsilon_2 = (4T)^{-1}$. For L≠o, the phase correction can be calculated in WKB approximation to various degrees of accuracy. The first order term is given by $\alpha \approx \frac{1}{2}(M^2/T) \cot g\, \theta$. We can also follow a different procedure. From eq. (5.14) we have

$$\left| Y_{l_o}^{M} \right|^{2} = (4\pi^2 \sin\theta)^{-1} \left\{ 2 + 2\,\mathrm{Re}\, e^{-2i\phi_M(T)} \right\} ,$$

therefore

$$2\pi \sin\theta\, \sigma(\theta) = C T \pi^{-1} \{ (H^+)^2 + (H^-)^2 + 2 H^+ H^- \sum_M (-1)^{L+M} |E_{LM}|^2 \cdot [\, 2\pi^2 \sin\theta\, |Y_{l_0}^M(\theta,0)|^2 - 1\,] \}. \qquad (5.30)$$

For small angles the spherical harmonics in eq. (5.30) can be approximated by cylindrical Bessel functions. Aside from the form factors, the result is similar to those obtained previously (Bla 59, Aus 65). In eq. (5.30) the terms with L+M odd contribute to the sum. The factor $(-1)^{L+M}$ compensates for the out-of-phase properties of the different spherical harmonics or Bessel functions. It will be shown in section 6 that the structure of our inelastic amplitude reproduces the general adiabatic predictions for $(\alpha,\alpha'\gamma)$ correlation functions.

5.3 Higher order terms

In this section we discuss the effect of higher order terms in eq. (5.7). In section 5.2 we have carried the term with coefficient $b_{K2} = \mu$. From eqs. (5.29) and (4.12) it follows that the phases of the inelastic and the elastic oscillations are inverted at $\theta = \theta_c + \mu^{-1}$. This is due to our special choice of the radial integrals. For the strong damping case the result is more interesting. Angular distributions of single nucleon transfer reactions (Fra 64b) and inelastic scattering (Bas 65) between complex nuclei have been obtained with $\mu = 0$. The "interaction radius" parameter was found to be appreciably larger than the one obtained in elastic scattering (Ven 64a). Eq. (5.27) shows

that for $\mu = 0$ the maximum of $2\pi \sin\theta\, \sigma(\theta)$ occurs at $\theta_m = \theta_c$. The parameter T is calculated from θ_c and n. However, for $\mu > 0$ it is seen that $\theta_m < \theta_c$. Therefore, one obtains a larger value T if one puts $\theta_m = 2 \operatorname{arctg}(n/T)$. The physical interpretation of this effect is that the real attractive nuclear force counteracts the repulsive Coulomb force and thereby produces an apparently larger radius. Potgieter (Pot 67a) has determined μ-values from the inelastic cross section by using the T-value obtained from elastic scattering analyses.

By using the form (4.3) for η_ℓ, we obtain from eq.(5.20)

$$H^{\pm} = F_{\pm} \left[\{1 + \mu_1(\theta_c \pm \theta)\}^2 + \{\gamma(\theta_c \pm \theta) + \mu_2(\theta_c \pm \theta)^2\}^2 \right]^{\frac{1}{2}} e^{-i\psi_{\pm}}, \quad (5.31)$$

$$\psi_{\pm} = \operatorname{arctg}\left[\frac{\gamma(\theta_c \pm \theta) + \mu_2(\theta_c \pm \theta)^2}{1 + \mu_1(\theta_c \pm \theta)} \right] . \quad (5.32)$$

For angles where α_o may be neglected the angular distribution is given by

$$2\pi \sin\theta\, \sigma(\theta) = C T \pi^{-1} \{ |H^+|^2 + |H^-|^2 + 2(-1)^L |H^+||H^-| \sin(2T\theta + \psi_- - \psi_+) \}. \quad (5.33)$$

In general there is no angle at which the diffraction amplitude vanishes and the phase changes by π. The phase varies continuously through the interplay of ψ_+ and ψ_-. We observe that, if the radial integrals have imaginary and real parts (up to a phase) which are symmetric and antisymmetric in (t-T), respectively, the oscillatory part of the angular distribution is proportional to sin (2Tθ) for angles such that α may be neglected. Deviations from these symmetries cause an angle-dependent change in the argument of the sine function. In this way, "stretching" of the oscillation period is obtained.

5.4 Numerical results

In order to test the accuracy of our approximations, the sum in eq. (5.1) was evaluated numerically. The results obtained by these calculations are referred to by SUM. Typical values of the parameters were chosen which, however, do not correspond to specific physical systems. Figs. 9 (i)-(iii) give results in which only the first term with coefficient $a_{K1} = 1$ is considered. An additional term with coefficient $b_{K2} = \mu$ was included in the calculation of the curves in figs. 9 (iv) and (v). The absolute value of the cross section is arbitrary.

Fig. 9(i) illustrates the structure of the inelastic amplitude for the strong damping case with L=2. It can be shown that $TC|B_L^M|^2 = |E_{LM}(\theta)|^2\ \sigma(\theta)$. The accuracy of this relation for the SUM calculations of fig. 9(i) was found to be of the order of 1%. At 71^o the value of $|B_2^0|^2$ was found to be 10^{-5} ($|B_2^1|^2 + |B_2^2|^2$).

Fig 9(ii) shows the SUM calculations of $2\pi\sin\theta\ \sigma(\theta)$ for L=o and L=2. The distribution with L=o agrees very well with the one obtained from eq. (5.29). As expected, eq.(5.29) does not reproduce the small-angle behaviour of the curve for L=2. For L=2, the distribution obtained by eq. (5.30) coincides with the SUM calculation of fig. 9(ii) even for $\theta < 2/\ell_o$. This can be understood by the following qualitative argument. For small angles, $|E_{21}(\theta)|^2$ is small and $|Y^2_{\ell_o}(\theta)|^2$ decreases rapidly if θ varies from $2/\ell_o$ to zero. Therefore, the main contribution comes from $|Y^0_\ell(\theta)|^2$ which is still treated quite accurately in our derivation. By using the spherical harmonics in eq. (5.30) we compensate, to some extent, for the error made in the amplitude.

The effect of large Coulomb parameters on the form factors is shown in fig. 9(iii). It is seen that the minima of the

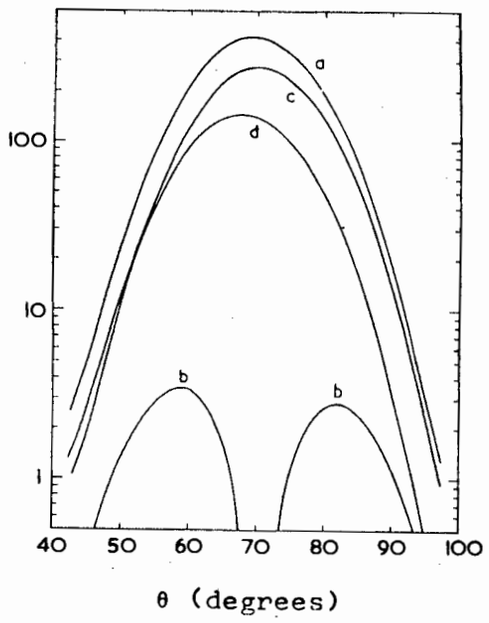

Fig. 9(i). Structure of inelastic scattering amplitude. Curves (a), (b), (c) and (d) show the result of SUM calculations of $\sigma(\theta)$, $C|B_2^0|^2$, $C(|B_2^1|^2 + |B_2^{-1}|^2)$ and $C(|B_2^2|^2 + |B_2^{-2}|^2)$, respectively. The parameters are $T = 60$, $\Delta = 3.5$, $n = 42.0$ and $\mu = 0$.

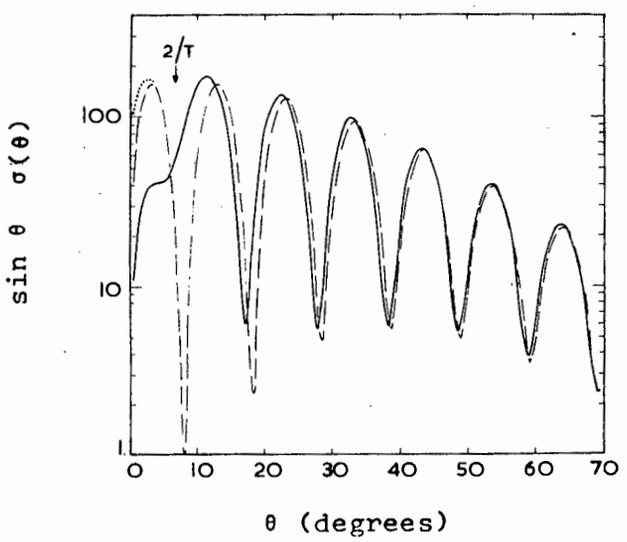

Fig. 9(ii). Angular distributions for inelastic scattering. The dashed and solid lines show the result of SUM calculations for $L = 0$ and $L = 2$, respectively. The dotted line is calculated from eq. (5.29) The parameters are $T = 17.5$, $\Delta = .82$, $n = 1.9$ and $\mu = 0$.

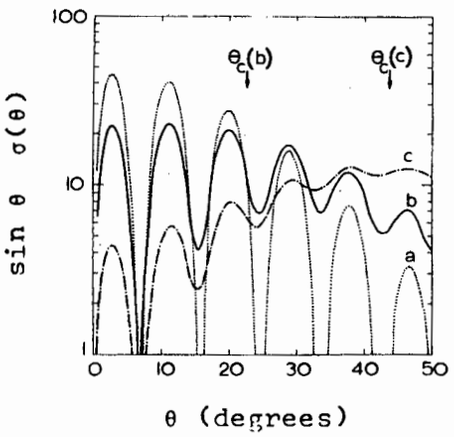

Fig. 9(iii). Effect of Coulomb parameter n on angular distribution. Curves (a), (b) and (c) correspond to cases n = o, 4 and 8, respectively. The parameters are T = 20, Δ = 1.25 and μ = o.

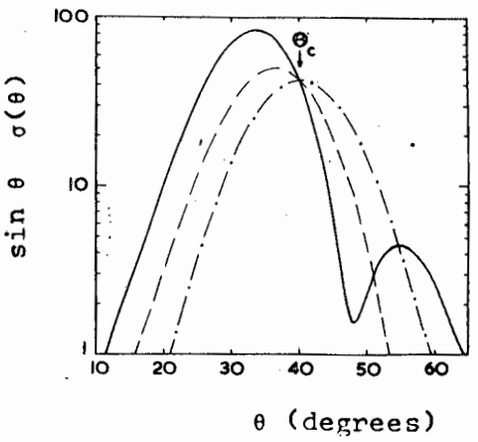

Fig. 9(iv). Effect of the real nuclear phase shift parameter μ in the strong damping case. The SUM calculations for μ/4Δ = o, 0.2 and 0.5 are given by the dashed-dotted, dashed and solid lines, respectively. The other parameters are T = 78.5, Δ = 3.85 and n = 28.7.

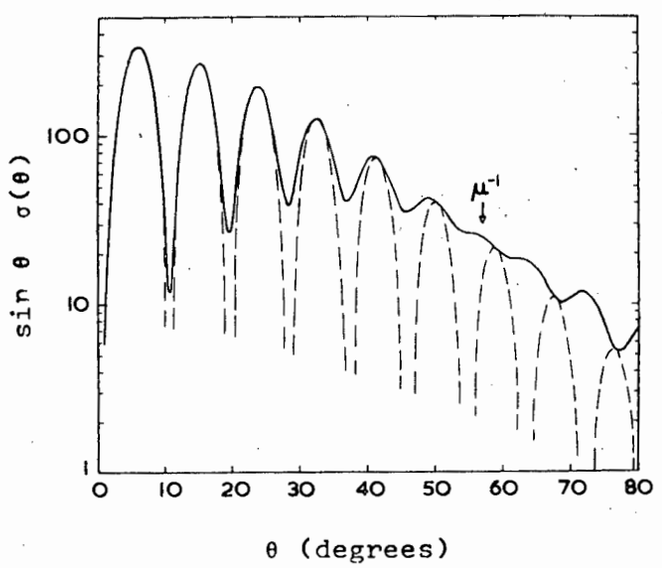

Fig. 9(v) Effect of the real nuclear phase shift parameter μ in the neutral case. The dashed and solid lines show the result of SUM calculations for μ/4Δ = o and 0.25, respectively. The other parameters are T = 20.5 and Δ = 1.0.

diffraction oscillations are filled in for increasing Coulomb parameters. For small angles the maximum of the angular distribution of $2\pi \sin\theta\ \sigma(\theta)$ is approximately proportional to $|F(\Delta\theta_c)|^2$. We can understand this effect qualitatively by a simple argument. In the absence of Coulomb interactions, the spherical harmonics for different ℓ' interfere constructively at small angles. However, the Coulomb interaction changes the relative phase of the partial waves and destructive interference results. The magnitude of this effect depends on the width Δ and the Coulomb parameter n contained in θ_c.

Fig. 9(iv) shows the effect of the real phase parameter μ. We note (i) that all distributions of $2\pi \sin\theta\ \sigma(\theta)$ have the same value at θ_c as predicted by eq. (5.27), (ii) that the maximum shifts towards smaller angles for increasing μ, and (iii) that a second maximum appears for larger μ values.

Fig. 9(v) illustrates the phase inversion at $\theta = \mu^{-1}$ in the neutral case $\theta_c = 0$. It follows from eq. (5.29) that, in the neutral case, $2\pi \sin\theta\ \sigma(\theta)$ is independent of μ for angles θ_1 defined by $\sin(2T\theta_1) = (-1)^L$.

5.5 Spin-$\frac{1}{2}$ particles

The inelastic transition amplitude for spin-$\frac{1}{2}$ particles is given by eq. (2.35) with $s=\frac{1}{2}$. We now introduce the AB approximation in an extended form which includes spin-orbit effects. An outline of this procedure was given in sections 2.3 and 3.7. Here we avoid the generality of section 5.1, since we shall not discuss γ-correlation functions for spin-$\frac{1}{2}$ particle scattering. Simultaneous measurements of γ-correlation functions and polarisation in inelastic scattering of

strongly absorbed spin-½ particles are not expected for some time.

For the radial integrals defined in eq. (2.36) we assume the form

$$\beta_{\ell\ell'}^{\ell+\lambda\ \ell'+\lambda'} \approx -\tfrac{1}{2}\, i E \left[\frac{\partial \bar{\eta}_{\bar{\ell}}}{\partial \bar{\ell}} + \lambda \delta_{\lambda\lambda'} \frac{\partial \xi_{\bar{\ell}}}{\partial \bar{\ell}}\right] , \tag{5.34}$$

where $\bar{\eta}_\ell$ and ξ_ℓ are defined by eqs. (4.14) and (4.18), respectively. The radial integrals with $\lambda = \lambda' = \pm\frac{1}{2}$ are thus expressed in terms of derivatives of $\eta^{\pm}$. This is analogous to the AB theory for spinless projectiles. For radial integrals with $\lambda = -\lambda'$ derivatives of $\bar{\eta}_\ell$ are taken. This convenient approximation may be open to criticism. However, it will be shown that terms with $\lambda = -\lambda'$ carry little weight if $\bar{\ell}$ is large.

By inserting eq. (5.34) in eq. (2.35), we can write the transition amplitude as a sum of two terms. For the first term, containing $\bar{\eta}$, the summation over j and j' can be performed exactly. We obtain

$$\begin{aligned} T_L^{M_f m_f m_i}{}_{(1)} &= \delta_{m_f m_i} \langle L \| \alpha_L \| 0 \rangle \hat{S}^{-1} \hat{L}\, \frac{4\pi}{k i k_f} \sum_{\ell\ell'} i^{\ell-\ell'} (-\tfrac{1}{2} i E)\, \frac{d\bar{\eta}_{\bar{\ell}}}{d\bar{\ell}}\, e^{i(\sigma_\ell + \sigma_{\ell'})} \\ &\cdot \langle \ell' L\ -M_f\ M_f | \ell 0 \rangle \langle \ell' L\ 0\ 0 | \ell 0 \rangle \cdot \hat{\ell}'\, Y_{\ell'}^{-M_f}(\theta, 0) \qquad (5.35) \\ &= C_1\, A_L^{M_f m_f m_i} , \end{aligned}$$

where

$$C_1 = (-i)^{L+1}\, \hat{L}\, \hat{S}^{-1} \langle L \| \alpha_L \| 0 \rangle\, \frac{4\pi}{k^2}\, E \ . \tag{5.36}$$

The spin-independent part has thus the same form as the spinless amplitude. It is the non-spin-flip amplitude ($m_i = m_f$).

For the calculation of the spin-dependent contribution (i.e. the term containing ξ_ℓ), we note that in eq. (2.35) we

always couple one small and two large j-values in the 3j- and 6j- coefficients. In such cases convenient approximations are possible. For the Racah coefficients we can easily show by direct calculation that

$$W(l+\lambda, l, l'+\lambda, l'; \tfrac{1}{2}L) \approx 2\lambda(-1)^{l+l'-L}\hat{l}^{-1}\hat{j}^{-1} \cdot \{1 + \frac{(K-L)(K+L+1)}{8\bar{l}^2} + O(\bar{l}^{-3})\}, \tag{5.37}$$

where $K = l-l'$.

If approximation (5.34) is used we do not need the Racah coefficients for $\lambda' = -\lambda$. However, we give an expression for $\lambda = \frac{1}{2} = -\lambda'$ in order to demonstrate that these terms carry little weight for large $\bar{l}$. We have

$$W(l+\tfrac{1}{2}, l, l'-\tfrac{1}{2}, l'; \tfrac{1}{2}L) = (-)^{2\bar{l}-L}\hat{l}\hat{j}\left[\frac{(K+L+1)(L-K)}{4\bar{l}^2+6\bar{l}-K+2}\right].$$

The term with $\lambda = -\frac{1}{2}$ has a similar magnitude.

Next we approximate the Clebsch-Gordan coefficients appearing in eq. (2.35) for the case $j-l = j'-l' = \lambda$ by

$$\begin{aligned} &\langle l'+\lambda\ L\ m_f-m\ m-m_f+m_i | l+\lambda\ m_i\rangle \approx -d^{L}_{K,m-m_f+m_i}(-\tfrac{1}{2}\pi), \\ &\langle l\ \tfrac{1}{2}\ 0\ m_i | l+\lambda\ m_i\rangle \approx (-1)^{m_i-\lambda} d^{\frac{1}{2}}_{\lambda m_i}(\tfrac{1}{2}\pi), \\ &\langle l'\ \tfrac{1}{2}\ -m\ m_f | l'+\lambda\ m_f-m\rangle \approx (-1)^{m_f-\lambda} d^{\frac{1}{2}}_{\lambda m_i}(\tfrac{1}{2}\pi). \end{aligned} \tag{5.38}$$

The third approximation is not as good as the other two. It deteriorates with increasing m, the error being of the order $\frac{1}{2}(m/l')$. However, the maximum value of m is L+1 and therefore the approximations (5.38) are quite accurate for small angular momentum transfer and large cut-off value.

By inserting approximations (5.37), (5.38) and the second term of eq. (5.34) in eq. (2.35), we have

$$T_L^{M_f m_f m_i}{}_{(2)} = -\delta_{m_i,-m_f}\,\hat{S}^{-1}\hat{L}\,\langle L\|\mathcal{Q}_L\|0\rangle\,\frac{i\pi}{k_i k_f}\,E$$
$$\cdot\sum_{\ell\ell'} i^{\ell-\ell'}\frac{\partial\xi_{\bar{\ell}}}{\partial\bar{\ell}}\,e^{i(\sigma_\ell+\sigma_{\ell'})}\,d^L_{KM_f}(-\tfrac{1}{2}\pi)\,d^L_{K0}(-\tfrac{1}{2}\pi)\,\hat{\ell}'\,Y_{\ell'}^{-M-2m_f} \qquad (5.39)$$
$$= C_1\,B_L^{M_f m_f m_i}\,.$$

The total transition amplitude is given by the sum of the terms of eqs. (5.35) and (5.39). In our present approximation, $d\xi_\ell|d\ell$ contributes only to the spin-flip part of the inelastic amplitude. We note that there is a close resemblance between the elastic and inelastic amplitudes. This is best demonstrated for L=o.

The use of approximation (5.10) in eq. (5.35) and relation (5.12) yields

$$A_L^{M_f m_f m_i} = \delta_{m_f m_i}\sum_{\ell\ell'} i^{K+L}\,d^L_{KM_f}(\tfrac{1}{2}\pi)\,d^L_{K0}(\tfrac{1}{2}\pi)$$
$$\cdot\,(d\bar{\eta}_{\bar{\ell}}|d\bar{\ell})\,e^{i(\sigma_\ell+\sigma_{\ell'})}\,\hat{\ell}'\,Y_{\ell'}^{M_f}(\theta,0)\,;$$
$$B_L^{M_f m_f m_i} = -\tfrac{1}{2}\,\delta_{m_f,-m_i}\sum_{\ell\ell'} i^{K+L}\,d^L_{KM_f}(\tfrac{1}{2}\pi)\,d^L_{K0}(\tfrac{1}{2}\pi) \qquad (5.40)$$
$$\cdot\,(d\xi_{\bar{\ell}}|d\bar{\ell})\,e^{i(\sigma_\ell+\sigma_{\ell'})}\,Y_{\ell'}^{M_f+2m_\ell}(\theta,0)\,.$$

The amplitudes A and B of eqs. (5.40) are similar to the spin-o amplitude of section 5.1. The methods of sections 5.1 and 5.2 can thus be used to calculate these quantities. Alternatively, the approximation procedure of ref. (Pot 66a) can be followed. To illustrate the extended Blair phase rule, we only consider the asymptotic angular region, i.e. we approximate the spherical harmonics as indicated in eq. (5.14) and take α = o. We then obtain

$$A_L^{M_f m_f m_i} = \delta_{m_f m_i} \left(\frac{T}{2\pi^2 \sin\theta}\right)^{\frac{1}{2}} e^{2i\sigma_{l_0}} \left[E_{LM_f}^{(\theta)} G_{M_f}^{+(1)} + E_{LM_f}^{(-\theta)} G_{M_f}^{-(1)}\right] , \tag{5.41}$$

$$B_L^{M_f m_f m_i} = -\tfrac{1}{2} \delta_{m_f, -m_i} \left(\frac{T}{2\pi^2 \sin\theta}\right)^{\frac{1}{2}} e^{2i\sigma_{l_0}} \left[E_{LM_f}^{(\theta)} G_{M_f+2m_f}^{+(2)} + E_{LM_f}^{(-\theta)} G_{M_f+2m_f}^{-(2)}\right] ,$$

where

$$G_m^{\pm}(1,2) = H^{\pm}(1,2)\, e^{\pm i[T\theta + (2m-1)\frac{1}{4}\pi]} ,$$

$$H^{\pm}(1) = \int_{-\infty}^{+\infty} (d\bar{\eta}(t)/dt)\, e^{\pm i(t-T)(\theta_c \pm \theta)}\, dt , \tag{5.42}$$

$$H^{\pm}(2) = \int_{-\infty}^{+\infty} (d\xi(t)/dt)\, e^{\pm i(t-T)(\theta_c \pm \theta)}\, dt ,$$

and $E_{LM}(+\theta)$ is given by eq. (5.23).

By inserting the expressions (5.41) into eqs. (2.38) and (2.39) and performing the summations over M_f with the aid of eqs. (B.3) and (B.7) of appendix B, we obtain

$$\sigma(\theta) = \frac{C \cdot T}{2\pi^2 \sin\theta} \left[|H^+(1)|^2 + |H^-(1)|^2 + (-1)^L 2\,\mathrm{Im}\left(H^+(1) H^{-*}(1) e^{2iT\theta}\right) \right.$$
$$\left. + \tfrac{1}{4} \left\{ |H^+(2)|^2 + |H^-(2)|^2 - (-1)^L 2\,\mathrm{Im}\left(H^+(2) H^{-*}(2) e^{2iT\theta}\right) \right\} \right] , \tag{5.43}$$

$$\sigma(\theta) P(\theta) = \frac{CT}{2\pi^2 \sin\theta} \left\{ \mathrm{Re}\left[H^+(1) H^{+*}(2) - H^-(1) H^{-*}(2) \right] \right.$$
$$\left. - (-)^L \mathrm{Im}\left[H^+(1) H^{-*}(2) e^{2iT\theta} + H^-(1) H^{+*}(2) e^{-2iT\theta} \right] \right\} , \tag{5.44}$$

where $C = \frac{1}{4}(2L+1)\,|\langle L||a_L||o\rangle|^2 = \frac{1}{4}(\delta^{(L)})^2$.

By comparing eqs. (4.20) and (4.21) with eqs. (5.43) and (5.44), respectively, we clearly see the very close connection between elastic and inelastic angular distributions of the cross section

and the polarisation. The extended Blair phase rule is demonstrated by noting that

$$H^{\pm}(1,2) = (\theta_c \pm \theta) H_{\pm}(\bar{\eta}, s) \qquad (5.45)$$

where $H_{\pm}$ and $H^{\pm}$ appear in the elastic and inelastic expressions, respectively. The cross section and polarisation angular distributions for elastic scattering and inelastic scattering to odd/even parity states by one-phonon excitations oscillate in- /out-of-phase. As pointed out in section 2.3, only transitions to natural parity states are described by these expressions.

The assumption $|\eta_o| \approx o$ is expected to be quite good for ^{3}He and ^{3}H scattering from about 30 MeV upwards. At present, experimental data are only available for proton scattering (Fri 66, Hay 64). For the scattering of 40 MeV protons by ^{60}Ni, calculations from OM potentials (Fri 66) give $|\eta_o| = 0.37$, and the radial integrals are also by no means localized. However, surprisingly the experimental data for polarisations and cross sections qualitatively satisfy the Blair phase rule. Quite good DWBA fits to these data have been obtained by deforming the complex central and the spin-orbit potentials (Fri 66).

Finally, it should be pointed out that suitable approximations for the "geometry" (i.e. the coupling coefficients) are possible for the case where spin is transferred in the inelastic process (i.e., where there is an interaction depending on the coupling of the internal coordinates of the target and the projectile spin). However, it is not clear how the "physics" (i.e. the radial integrals) should be approximated in such a case. Such a contribution to the polarisation is expected to depend strongly on the Q-value of the reaction. We recall that for spin-independent distortions the polarisation vanishes for

vanishing Q-value (Sat 60b). For spin transfer reactions an additional term thus enters for $Q \neq 0$. It may be possible to determine its presence or absence by systematic measurements of polarisation from nuclei with different inelastic Q-values, as well as for different beam energies.

6. MODIFIED AUSTERN-BLAIR THEORY AND $(\alpha,\alpha'\gamma)$ CORRELATION FUNCTIONS

In the previous section the Austern-Blair theory was used to calculate inelastic cross sections in closed form. Quantitative fits with fixed SAM parameters have been obtained for elastic and inelastic scattering of spin-o particles by methods similar to section 5 (Pot 66a, Pot 66b, Pot 67b). Analyses by means of the Austern-Blair theory in open form were also performed by several authors (Dar 64, Spr 65, Hor 65, Pet 65, Als 66, Mer 66). In all these cases the theory gives a satisfactory description of the differential cross sections for the scattering by low-lying levels. However, the deformation parameter obtained in this theory is normally somewhat smaller than the corresponding DWBA value (Pot 67a).

A sensitive test for the assumptions underlying the Austern-Blair theory is provided by the correlation functions in the $(\alpha,\alpha'\gamma)$ reaction. The AB predictions for these correlation functions coincide, of course, with general adiabatic expressions which were first derived by Blair (Bla 59) in Fraunhofer approximation, then by Satchler (Sat 60b) in DWBA with $k_i = k_f$, and finally, quite generally, by Blair and Wilets (Bla 61). However, measurements of these functions often (McD 62, Eid 64, Bla 65) show characteristic deviations from the adiabatic predictions, and the nonvanishing of $\delta k = k_i - k_f$, though small, becomes very important. It has been pointed out (Bla 65) that only potential sets which produce fairly strong S-matrix surface localisation give the observed angular correlation behaviour. This suggests the use of SAM methods.

Inglis (Ing 64, Ing 66, Ing 67) has described the observed behaviour of the correlation functions by modifying the

Fraunhofer approach. In this section we modify the Austern-Blair theory to describe the main features of $(\alpha,\alpha'\gamma)$ correlation functions and to obtain deformation parameters which are in better agreement with the values obtained in DWBA.

6.1 Modified Austern-Blair theory

Austern and Blair (Aus 65) have derived, in the adiabatic limit, the relationship (3.15) between the diagonal radial integrals and the reflection coefficients. In addition, these authors assume equality of the diagonal and off-diagonal radial integrals. They have also pointed out that the second approximation is not as good as the first, and that it deteriorates rapidly with increasing $K = \ell-\ell'$.

In order to obtain an idea of how Q-value effects change the results and how off-diagonal elements are related to diagonal elements, DWBA calculations for 64.3 MeV α-particles scattered by ^{58}Ni were performed for Q = o and Q = -5 MeV. (The potential parameters were taken from ref. (Dar 64).) Fig. 10 shows curves for $-\mathrm{Im}\beta_{\ell\ell'}$, as a function of $\bar{\ell}$. For Q = o (indicated in fig. 10 by (k_1,k_1)), the curves for K = -2 and K = 2 coincide, and they have a lower maximum value and a greater "width" than the curve for K = o. (This can also be seen in fig. 6 for similar curves of $|\beta_{\ell\ell'}|$.) For Q = -5 MeV (indicated in fig. 10 by (k_1, k_2)) the curve for K = 2 has an increased maximum value and a decreased width compared to the Q = o case. The opposite holds for the K = -2 curve. We note also that the curve for Q = -5 MeV has maximum value at an ℓ-value which is smaller than the corresponding ℓ-value for the Q = o curve. The adiabatic radial integrals for the

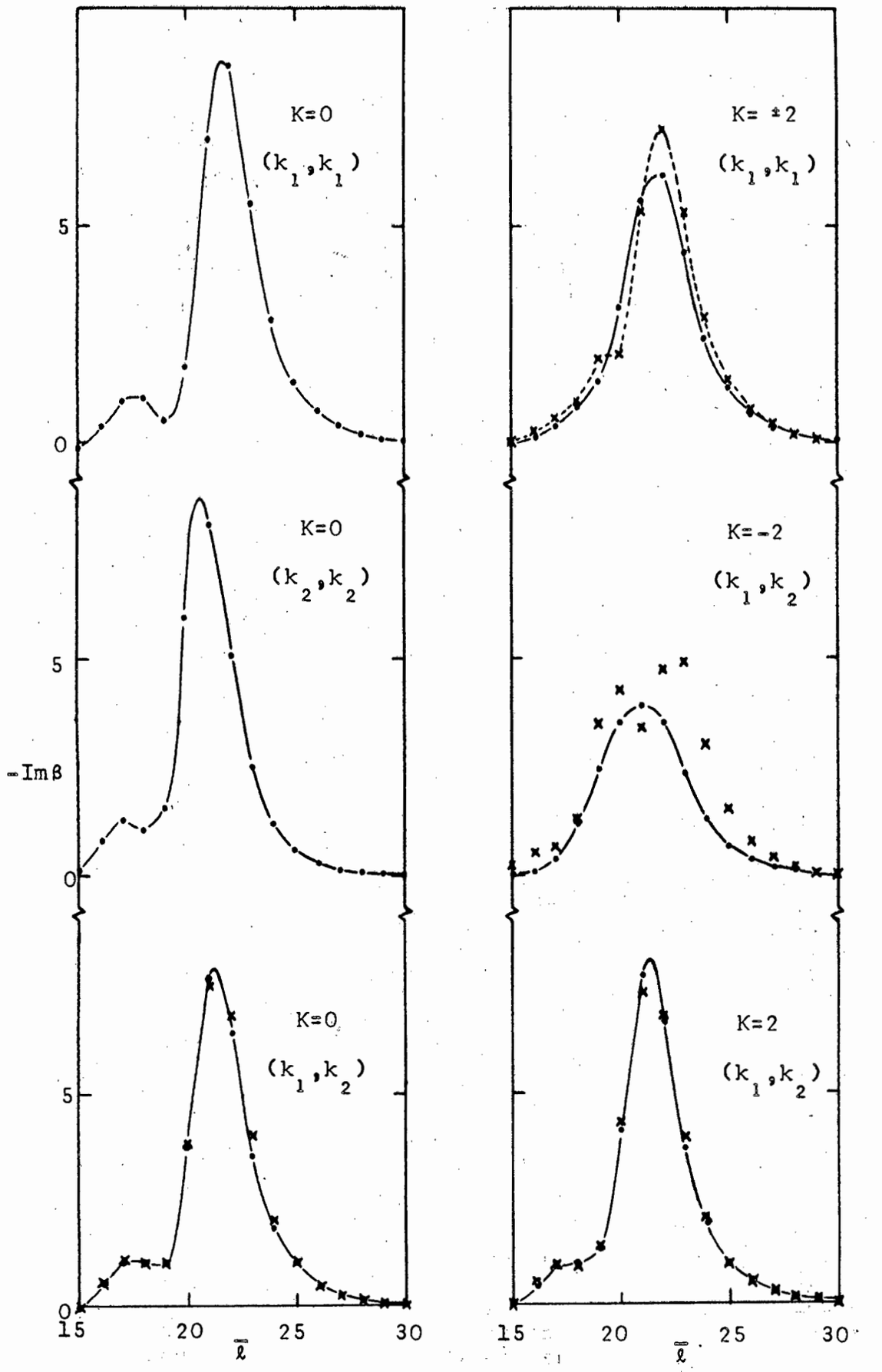

Fig.10. DWBA radial integrals for 64.3 MeV α-particles scattered by ^{58}Ni. Taking Q=-5 MeV, gives $k_i=k_f=3.282$fm , $k_f=k_2=3.142$fm . (k_i,k_f) denotes k-values in the initial and final channels. The results of calculations by eq.(6.2) are shown by crosses.

exit channel (denoted by (k_2, k_2)) are also shown in fig.10 and it is seen that, for K = o, the maximum of the (k_1,k_2) curve appears between those of the (k_1, k_1) and (k_2, k_2) curves.

To obtain an approximation which reproduces these effects, we consider a radial inelastic interaction potential of the form

$$V(r) = V_0 \, \delta(r-R) \, . \qquad (6.1)$$

It can then be shown that

$$\beta_{ll'}(k_i k_f) = \left[\beta_{ll}(k_i k_i) \, \beta_{l'l'}(k_f k_f) \right]^{\frac{1}{2}} , \qquad (6.2)$$

i.e. the off-diagonal radial integrals are given by the geometrical mean (GM) of the adiabatic diagonal radial integrals in the entrance and exit channels.

The main draw-back of the delta function interaction is that it produces radial integrals with poor localisation (Ros 62). However, this does not disturb us here because good localisation of the off-diagonal elements is guaranteed by the localisation of the diagonal elements.

To investigate the extent to which relation (6.2) depends on the range of the potential, we consider a Gaussian interaction

$$V(r) = V_0 \, (a^2 \pi)^{-\frac{1}{2}} \exp\left\{ -\left(\frac{r-R}{a} \right)^2 \right\} \, . \qquad (6.3)$$

We define a measure of the accuracy of eq. (6.2) by

$$D = \left\{ \beta_{ll'}(k_i k_f) \right\}^2 - \beta_{ll}(k_i k_i) \, \beta_{l'l'}(k_f k_f) \, . \qquad (6.4)$$

By expanding the integrands of the radial integrals in a power series in the range a, and neglecting terms of order a^4, we obtain under the assumption V(r=o) = o

$$D = -\frac{a^2}{2} V_o^2 \left\{ \int_o^R u_\ell(k_i r)\, u_{\ell'}(k_f r)\left[2\bar{k}\,\delta k - (2\bar{\ell}+1)K/r^2\right] dr \right\}^2 \qquad (6.5)$$

where $\bar{k} = \frac{1}{2}(k_i + k_f)$ and $\delta k = k_i - k_f$. For large ℓ-values, the only significant contribution to the integral in eq. (6.5) comes from the region $r \approx R$. We can then approximate eq. (6.5) to obtain

$$D \approx -\left(\frac{a V_o}{R^2}\right)^2 (T\,\delta T - tK)^2 \left\{ \int_o^R u_\ell(k_i r)\, u_{\ell'}(k_f r)\, dr \right\}^2 \qquad (6.6)$$

where $T = \bar{k}R$, $\delta T = \delta k\, R$ and $t = \bar{\ell}+\frac{1}{2}$. For $t \approx T$, a further approximation gives

$$D \approx -\left(\frac{ka V_o}{R}\right)^2 (\delta T - K)^2 \left\{ \int_o^R u_\ell(k_i r)\, u_{\ell'}(k_f r)\, dr \right\}^2 \qquad (6.7)$$

We note that for real V_o and real elastic potentials (i.e. real wave functions), D is always negative. This result also follows from Schwarz inequalities, but it can not be extended to the case of complex potentials.

We now return to the numerical calculations. In fig. 10 the radial integrals calculated from eq. (6.2) are shown by crosses. First of all, we note the very satisfactory results for the (k_1, k_2) curves with K = o and K = 2. The agreement in the two cases is of the same order. This follows from eq. (6.7) and the fact that in this case, $\delta T \approx 1$. As $(\delta T - K)^2$ increases, the quality of eq. (6.2) deteriorates (see for instance the (k_1, k_2) curve with K = -2). However, there is one consolation. As the quality of approximation (6.2)

deteriorates, the maximum values of the radial integrals decrease and the widths of the curves increase. This implies that such contributions to the cross section decrease rapidly with increasing angles. (The irregularity of the curves for off-diagonal radial integrals calculated by eq. (6.2) is due to the irregularity of the diagonal elements below the cut-off. Smooth diagonal elements produce smooth off-diagonal elements.)

As a second example of the quality of eq. (6.2), the radial integrals for the scattering of 28 MeV α-particles by ^{58}Ni were calculated. The OM parameters were taken from ref. (Sat 65). For low ℓ-values the sign was determined by using eq. (3.20). Considering the difference in shape between the DWBA curves for K = o and K = ±2, the quality of approximation (6.2) is surprisingly good.

In what follows we shall assume the validity of eq. (6.2).

6.2 Parameterised reflection coefficients

We now insert into the GM approximation (6.2) the adiabatic result of Austern and Blair, eq. (3.15). We then obtain

$$\beta_{\ell\ell'}(k_i k_f) = -\frac{i}{2}\left\{E_i E_f \frac{\partial\eta(\ell-\ell_i)}{\partial\ell}\frac{\partial\eta(\ell'-\ell_f)}{\partial\ell'}\right\}^{\frac{1}{2}}, \tag{6.8}$$

$$\ell_{i,f}+\tfrac{1}{2} = T_{i,f} = k_{i,f}R\left\{1-2\eta_{i,f}/(k_{i,f}R)\right\}^{\frac{1}{2}}.$$

A disadvantage of eq. (6.8) is the difficulty of obtaining Fourier transform of $\beta_{\ell\ell'}$ for general η_ℓ-functions. However, the calculations in open form are manageable even on a small

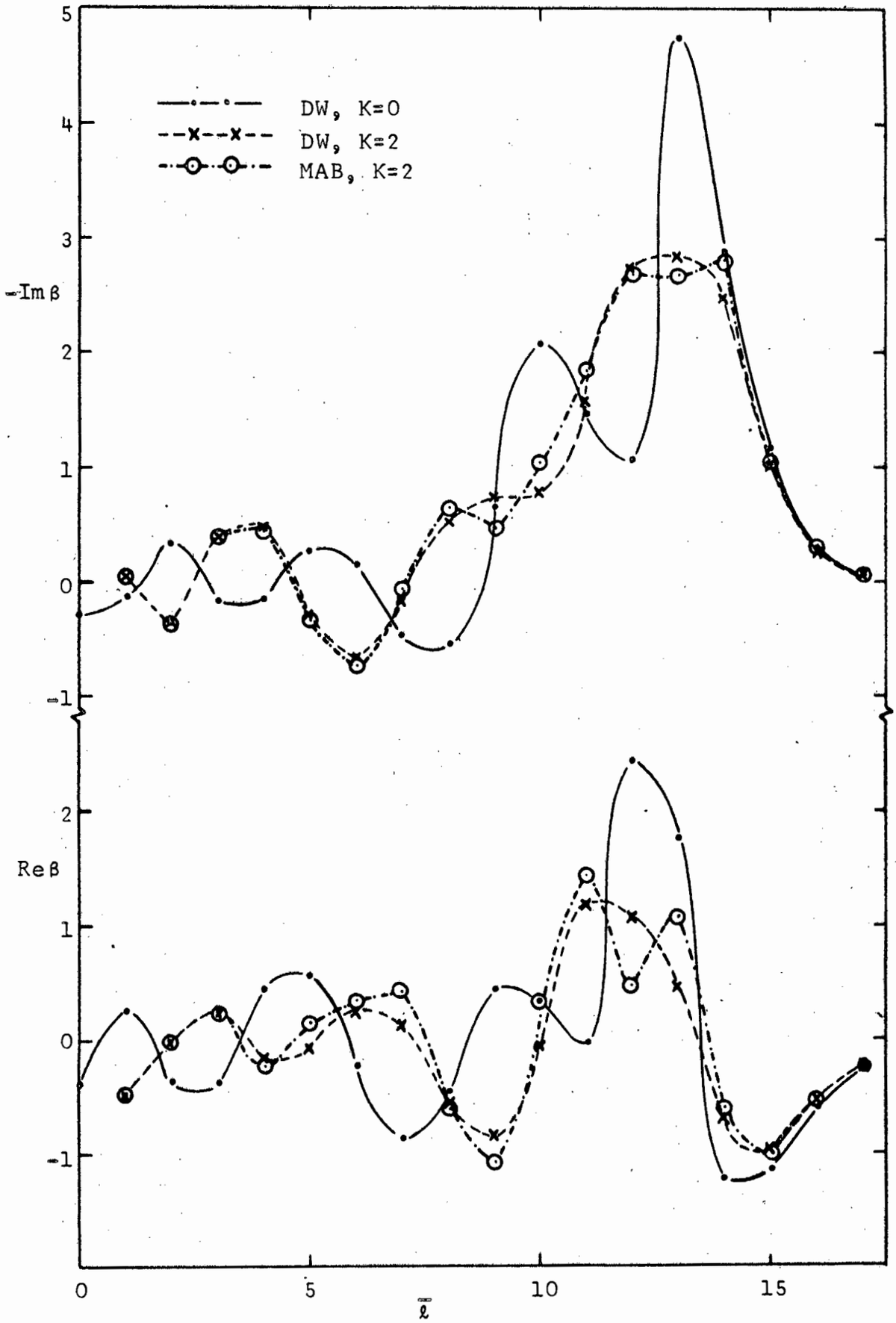

Fig.11. Radial integrals for 28 MeV α-particle scattering calculated in DWBA and by eq.(6.2).

computer. Here we give closed form expressions for the "error function" parameterisation (Fra 63)

$$\eta_\ell = \tfrac{1}{2}\left(1 + i\mu\frac{\partial}{\partial t}\right)\left\{1 + 2\pi^{-\frac{1}{2}}\, erf\left(\frac{t-T}{\Delta}\right)\right\} . \qquad (6.9)$$

By using eqs. (5.3), (6.7) and (6.18) we obtain to first order in μ

$$h_K(t) = \exp\left\{-\left(\frac{K-\delta T}{2\Delta}\right)^2\right\}\left(1+i\mu\frac{\partial}{\partial t}\right)\exp\left\{-\left(\frac{t-T}{\Delta}\right)^2\right\} . \qquad (6.10)$$

Taking Fourier transforms gives

$$H_K^{\pm} = \exp\left\{-\left(\frac{K-\delta T}{2\Delta}\right)^2\right\}\left(1+\mu(\theta_c \pm \theta)\right)\exp\left\{-\frac{\Delta^2}{4}(\theta_c \pm \theta)^2\right\} . \qquad (6.11)$$

where $\delta T = T_i - T_f = \ell_i - \ell_f$.

In eq. (6.10) all the functions $h_K(t)$ have the same width. This is due to the fact that we have used the Gauss form for the diagonal elements. For forms which tend to zero more slowly, the width of the off-diagonal terms is increased. We also note that (i), for $\delta T = 0$, $|h_0(t)| > |h_2(t)|$ and (ii), for $\delta T \neq 0$, $|h_{+2}(t)| > |h_{-2}(t)|$. This is in agreement with the results of section 6.1.

Closed formulae for $\sigma(\theta)$ can again be obtained by redefining

$$E_{LM}(\theta) = \alpha_{LM}(\theta) - i\,\beta_{LM}(\theta) \qquad (6.12)$$

$$= \sum_K i^{K-L}\, d^L_{KM}(\tfrac{1}{2}\pi)\, d^L_{K0}(\tfrac{1}{2}\pi)\, e^{-\frac{1}{2}iK\theta} e^{\frac{1}{4}iK\delta\theta_c} \exp\left\{-\left(\frac{K-\delta T}{2\Delta}\right)^2\right\}.$$

With this definition the expression (5.25) for $\sigma(\theta)$ or the corresponding expression of ref. (Pot 66a) remain unchanged However, we now have $\sum_M |E_{LM}|^2 \neq 1$, for $L \neq 0$. Eq. (6.12) can

also be used, as a first approximation, for "Woods-Saxon" η_ℓ-function with $\Delta(\text{Gauss}) = 2.1\Delta$ (Woods-Saxon).

6.3 Correlation functions

So far, for spin-o particles, we have considered only the inelastic differential cross section

$$\sigma(\theta) \propto \sum_M |T_L^M|^2$$

Much information is lost by the summation over M. In order to investigate the reaction mechanism more closely, it is necessary to establish the extent to which the different M-states of the excited level are populated, and to determine the relative phases. Experimentally, this is done by measuring the γ-rays, emitted in the subsequent decay of the excited level, in coincidence with the inelastically scattered α-particles.

The general formalism for correlation functions has been given by Cramer and Eidson (Cra 64). These authors also give references to earlier treatments and other relevant literature.

First of all, we transform the scattering amplitude to a new system of axes. In section 5 we chose $\underset{\sim}{z}$ along $\underset{\sim}{k}_i$, and $\underset{\sim}{y}$ along $\underset{\sim}{k}_i \times \underset{\sim}{k}_f$. In this section it is convenient to consider $\underset{\sim}{z}$ along $\underset{\sim}{k}_i \times \underset{\sim}{k}_f$ and $\underset{\sim}{x}$ along $\underset{\sim}{k}_i$. In this system of axes we denote the transition matrix elements by T^{LM}. Remembering that T_L^M transforms under rotation like $Y_L^{M\,*}$ (Sat 64a), it can easily be shown that

$$T^{LN} = (-1)^N \sum_M T_L^M \, i^M \, d^L_{MN}(\tfrac{1}{2}\pi) \,, \qquad (6.13)$$

and $T^{LN} = 0$ for L + N odd.

Most of the following discussions will concern the L = 2 transition for which the parameters a_0, a_2, δ_0 and δ_2 are defined (Cra 64) through

$$a_0 e^{i\delta_0} = T^{20}/T^{22} \quad , \quad a_2 e^{i\delta_2} = T^{2-2}/T^{22}. \tag{6.14}$$

These parameters appear in the correlation functions, and a_2 and δ_2 can be obtained from the correlation function in the scattering plane (Cra 64)

$$W(\varphi) \propto (1-a_2)^2 + 4a_2 \sin^2\{2(\varphi - \tfrac{1}{4}\delta_2)\} . \tag{6.15}$$

A computer programme, containing eqs. (5.1), (6.8), (6.13) and (6.14), was written. The calculations of section 6.4 were performed with the aid of this programme.

In order to discuss the main features of the correlation parameters, we insert the asymptotic expressions of section 5.1 (i.e. with $\alpha = 0$) into eq. (6.13) and obtain

$$B^{LN} = \left(\frac{T}{2\pi^2 \sin\theta}\right)^2 e^{2i\sigma_{l_0}} (-1)^N \sum_{MK} i^{K-L} d^L_{KM}(\tfrac{1}{2}\pi)\, d^L_{MN}(\tfrac{1}{2}\pi) \cdot d^L_{K0}(\tfrac{1}{2}\pi) \cdot \{(-1)^M e^{-i\frac{1}{2}iK\theta} H^+_K e^{i\phi} + e^{\frac{1}{2}iK\theta} H^-_K e^{-i\phi}\}. \tag{6.16}$$

where $\phi = T\theta - \frac{1}{4}\pi$.

The summation over M and K can be performed, giving

$$B^{LM} = \left(\frac{T}{2\pi^2 \sin\theta}\right)^{\frac{1}{2}} e^{2i\sigma_{l_0}}\, d^L_{0K}(\tfrac{1}{2}\pi)\, i^L\, e^{i\frac{1}{2}M(\pi-\theta)} \cdot \{H^+_M e^{i\phi} + (-1)^M H^-_{-M} e^{-i\phi}\} . \tag{6.17}$$

In approximation (6.17), the only contribution to T^{LM} comes from radial integrals with $l - l' = \pm M$. This result is due to the fact that we have used semi-classical expressions

for the coupling of angular momenta. By drawing classical trajectories we see, for instance, that the radial integrals with $\ell'-\ell = o$ cannot contribute to T^{LM} with $M \neq o$. For $L = 2$, this implies that the parameters a_2 and δ_2 depend only on the off-diagonal radial integrals as expressed by

$$a_2 e^{i\delta_2} = \frac{H^+_{-2} e^{i\phi} + H^-_{+2} e^{-i\phi}}{H^+_{+2} e^{i\phi} + H^-_{-2} e^{-i\phi}} \; e^{2i\theta} \qquad (6.18)$$

For $k_i = k_f$ (i.e. $H^{\pm}_{+2} = H^{\pm}_{-2}$), we have

$$a_2 = 1 \quad , \quad \delta_2 = 2\theta \; , \qquad (6.19)$$

in agreement with the general adiabatic result (Bla 61).

For $k_i \neq k_f$, we define

$$H^{\pm}_2 = \mathcal{H}^{\pm} + h^{\pm} \quad , \quad H^{\pm}_{-2} = \mathcal{H}^{\pm} - h^{\pm} \; , \qquad (6.20)$$

and

$$\begin{aligned} Y &= \mathcal{H}^+ + \mathcal{H}^- \quad , \quad y = h^+ + h^- \; , \\ Z &= \mathcal{H}^+ - \mathcal{H}^- \quad , \quad z = h^+ - h^- \; , \end{aligned} \qquad (6.21)$$

and obtain

$$a_2 e^{i\delta_2} = e^{2i\theta} \cdot \frac{(Y-z)\cos\phi + i(Z-y)\sin\phi}{(Y+z)\cos\phi + i(Z+y)\sin\phi} \; . \qquad (6.22)$$

If we neglect Coulomb and real nuclear phase shifts in eq. (6.11) (i.e., we take $\theta_c = o$ and $\mu = o$), we have $Z = z = o$. It then follows from eq. (6.22) that δ_2 varies through $2(\pi-\theta)$ for variations of ϕ through π. At a diffraction maximum in the cross section (i.e. $\sin\phi = o$), δ_2 cuts the adiabatic line. This behaviour of δ_2 is confirmed experimentally (McD 62, Eid 64, Bla 65) as shown in section 6.4. However, in this special case we obtain $a_2 = 1$. By assuming that $|y| \gtrsim |Z|$ and $|z| << |Y|$,

the result for δ_2 is unchanged but now $a_2 \approx 1$ at the maximum of $\sigma(\theta)$ and a_2 is large or small (depending on the relative signs of Z and y) at the minimum of $\sigma(\theta)$. The experimental curves for a_2 do not follow this pattern consistently.

In cases where the Coulomb interaction dominates and strong damping occurs ($H^- >> H^+$), we have from eq. (6.18) for real $H_K^{\pm}$

$$\alpha_2 = H_2^- / H_{-2}^- \quad , \quad \delta_2 \approx 2\theta . \qquad (6.23)$$

The effects of a nonvanishing Q-value thus show up most strongly (i) in δ_2 for oscillatory differential cross sections and (ii) in a_2 for damped curves.

6.4 Analyses of correlation measurements

Measurements of the correlation parameters a_2 and δ_2 have been reported (i) for 42 MeV α-particles scattered by ^{12}C (McD 62) and (ii) for 22.5 MeV α-particles scattered by ^{24}Mg (Eid 64) and ^{28}Si (Bla 65). In all these cases the elastic and inelastic cross section data are also given.

Because in case (i) the target nucleus is light and in case (ii) the α-particle energies are low, difficulties are encountered in the fitting of the elastic cross sections by SAM methods. For the five-parameter model, eq. (4.3), several parameter sets of comparable quality are obtained. They are found to depend strongly on the angular region selected for fitting, and it was not possible to obtain good fits for the entire angular region.

As an illustration of our methods we analyze data from refs. (McD 62), (Bla 65) and (Eid 64). The results are shown

in figs. 12-17. The elastic cross sections given in figs. 12, 14 and 16 are analyzed by the three-parameter version (3.1) of SAM. The parameters so obtained are shown in table 2.

Table 2 SAM parameters for correlation analysis.

Nucleus	^{12}C	^{24}Mg	^{28}Si
Lab. energy (MeV)	42	22.5	22.5
Q (MeV)	-4.43	-1.37	-1.77
T_i	10.86	10.01	10.49
Δ	0.607	0.432	0.509
$\mu/4\Delta$	0.25	0.24	0.45

With these parameter values, the correlation functions a_2 (or $A/B = (1-a_2)^2/4a_2$) and δ_2 are calculated from eqs. (6.14), (6.13) and (5.1), using the modified AB expressions (6.8). The results are compared with the experimental data in figs. 13, 15 and 17.

Also shown in figs. 12, 14 and 16 are the inelastic cross sections for the lowest 2^+ states, calculated from eq. (5.1) with the parameters of table 2.

The quality of our fits to the δ_2 measurements is compariable with those obtained in DWBA (McD 62, Bla 65). For a_2 (or A/B), however, there are still discrepancies between the calculated and the experimental values, especially at small angles.

In DWBA, the characteristic variation of δ_2 is obtained for one in every six potential sets (Ing 66). In our model

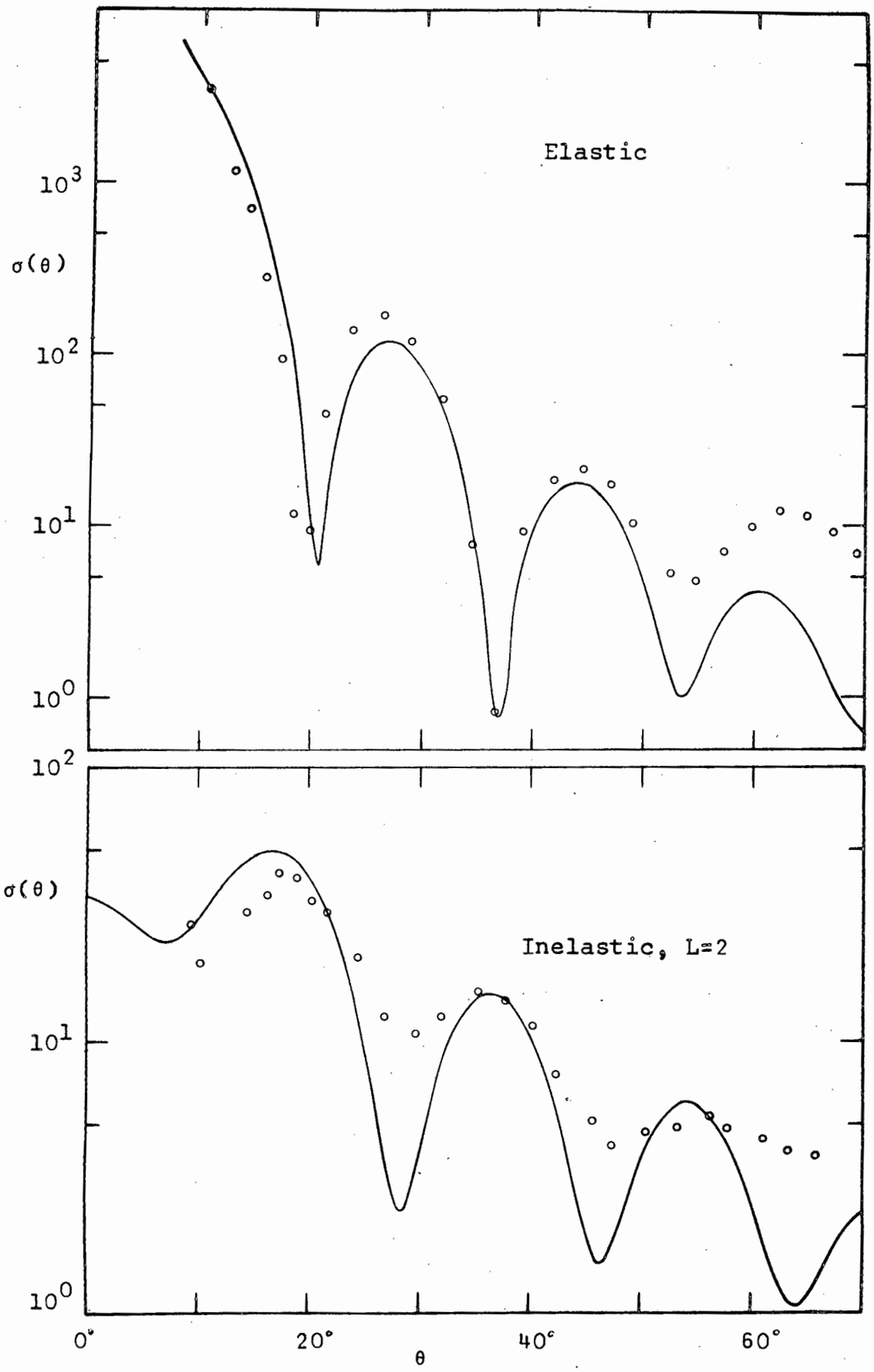

Fig.12. Differential cross sections for elastic and inelastic scattering of 42 MeV α-particles by ^{12}C . The experimental points are taken from ref. (McD 62) and the SAM parameters are shown in table 2.

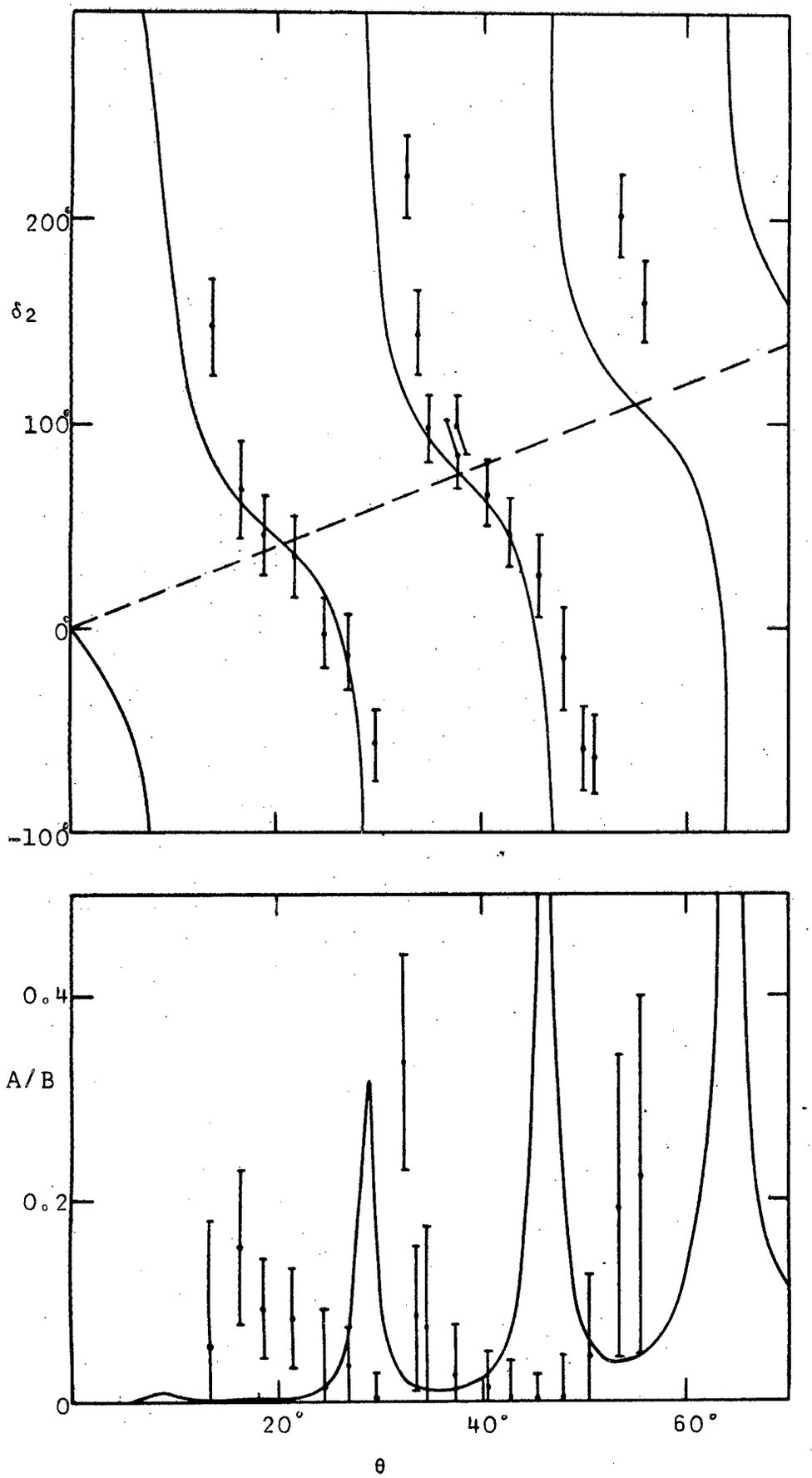

Fig.13. Correlation parameters δ_2 and A/B for the inelastic scattering shown in fig.12. The dashed line shows the adiabatic prediction.

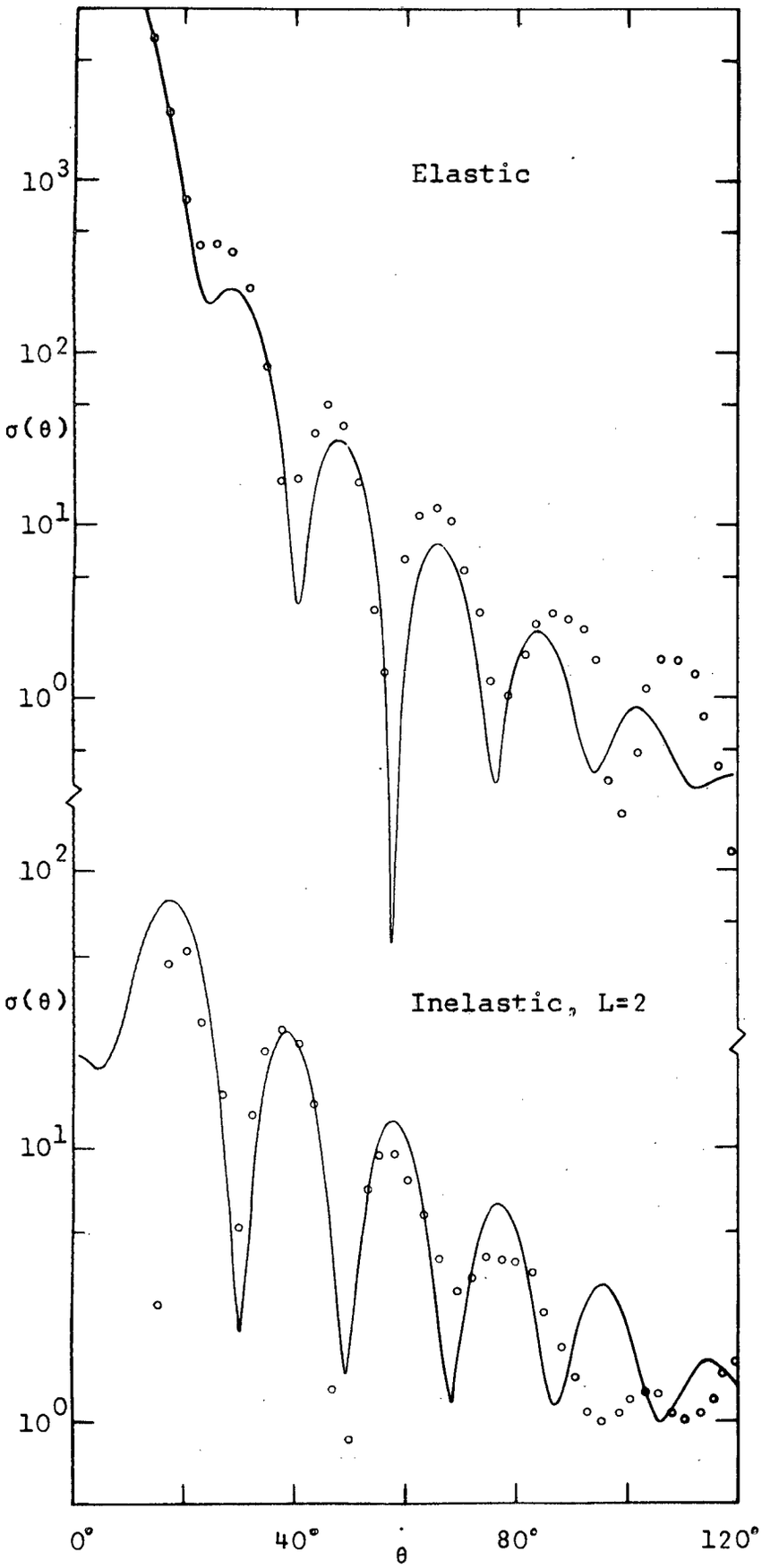

Fig. 14. Differential cross sections for elastic and inelastic scattering of 22.5 MeV α-particles by ^{24}Mg. The experimental points are taken from ref. (Eid 64) and the SAM parameters are shown in table 2.

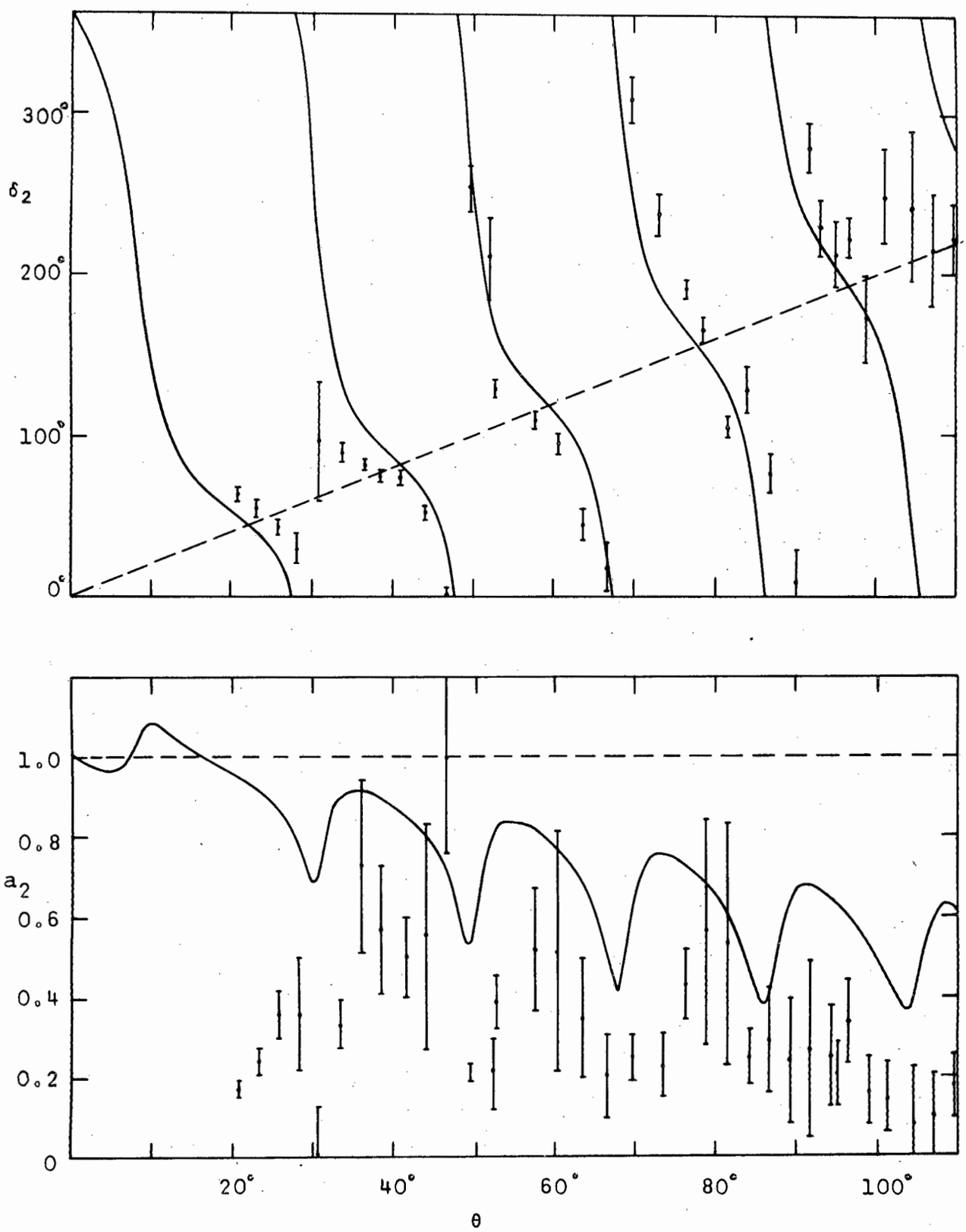

Fig.15. Correlation parameters δ_2 and a_2 for inelastic scattering shown in fig.14. The dashed lines show the adiabatic predictions.

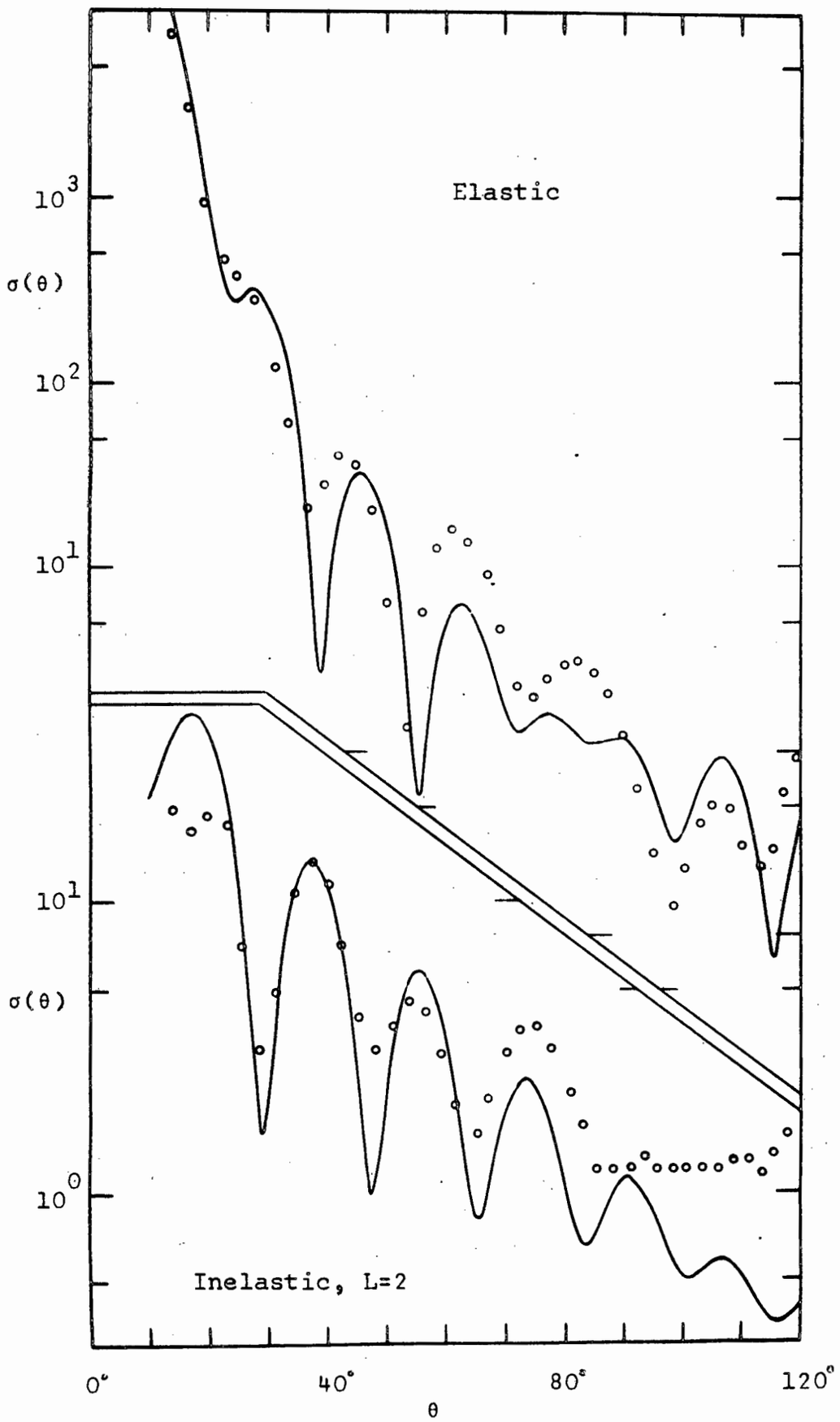

Fig.16. Differential cross sections for elastic and inelastic scattering of 22.5 MeV α-particles by ^{28}Si. The experimental points are taken from ref. (Bla 65) and the SAM parameters are shown in table 2.

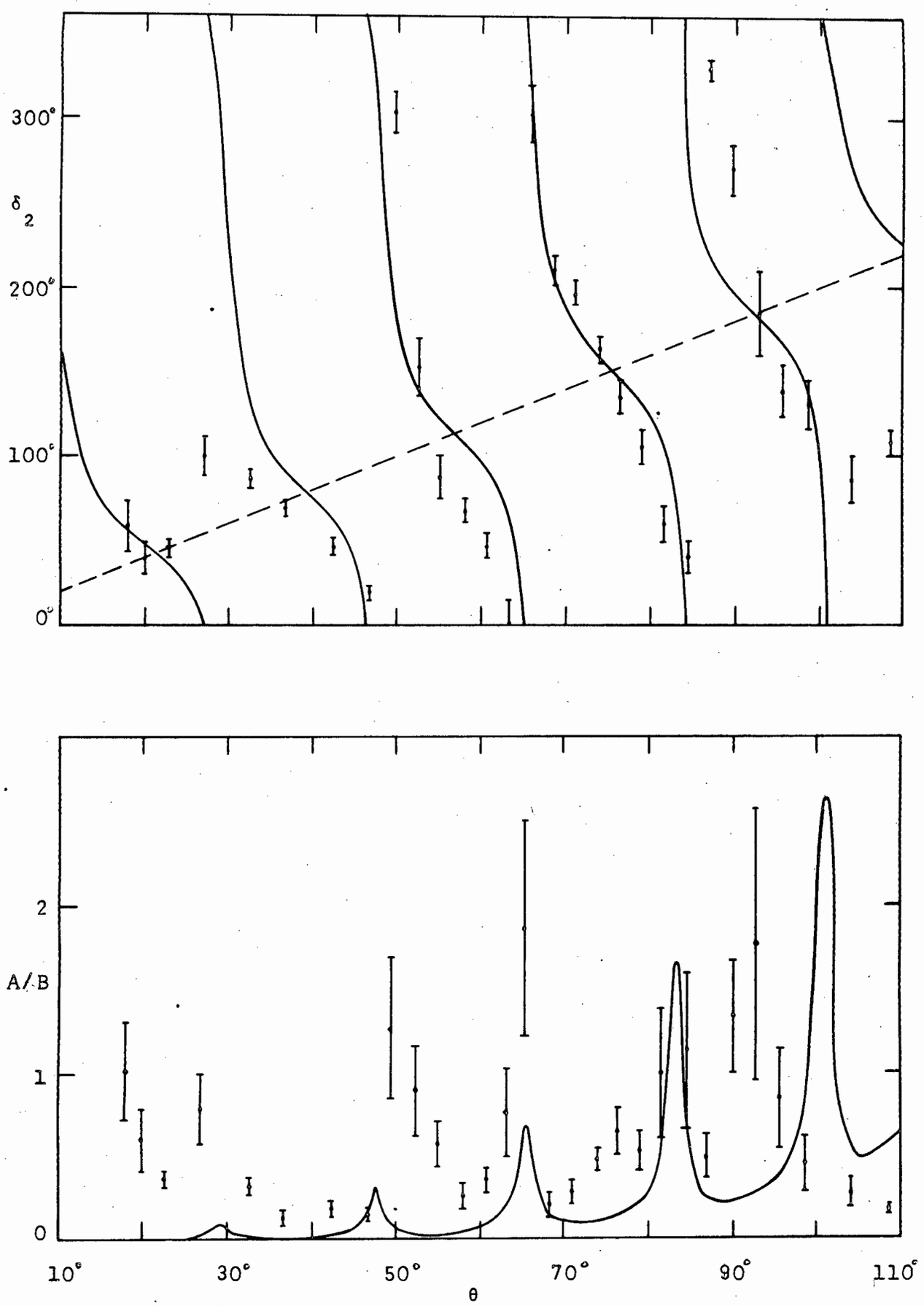

Fig.17. Correlation parameters δ_2 and a_2 for inelastic scattering shown in fig.16. The dashed line shows the adiabatic prediction.

this behaviour is reproduced for practically all parameter sets in the cases considered. We are committed to these phase variations and cannot break them off at any point as Inglis does for small (Ing 67) and large (Ing 66) angles in the modified Fraunhofer approximation. Nevertheless, we obtain reasonable fits to the correlation function and inelastic cross section without the use of free parameters.

Improved agreement can be expected for correlation measurements at energies and for target nuclei for which SAM methods are better applicable. Measurements of a_o and δ_o are of particular interest because they will provide a measure of the ratios of diagonal to off-diagonal radial integrals. As pointed out above, a_2 and δ_2 contain, approximately, only off-diagonal radial integrals, while a_o and δ_o contain both diagonal and off-diagonal elements.

6.5 Comparison of deformation distances

One of our objectives in modifying the Austern-Blair theory is to obtain deformation parameters $\delta(L) = \hat{L}\langle L||\alpha_L||o\rangle$ which are in better agreement with the values obtained from DWBA.

For the sake of comparison the radial integrals for the reaction $^{58}Ni(\alpha,\alpha')\ ^{58}Ni^*$ are calculated at 64.3 MeV and 28 MeV from OM potentials of refs. (Dar 64) and (Sat 65), respectively. The inelastic cross sections $\sigma(\theta)$ are calculated for (i) the DWBA radial integrals (ii) all off-diagonal radial integrals equal to the corresponding diagonal DWBA radial integrals, eq. (3.18) (referred to as AB), and (iii) the off-diagonal radial integrals calculated from the diagonal radial integrals by eq. (6.2) (referred to as MAB).

By taking the deformation δ(DWBA) = 1, the AB and MAB cross sections were normalised at the first asymptotic diffraction maximum to extract δ(AB) and δ(MAB). The results are summarized in table 3.

Table 3 Comparison of deformation distances

E	64.3 MeV			28 MeV	
Q	o		-5 MeV	o	
	δ(AB)	δ(MAB)	δ(MAB)	δ(AB)	δ(MAB)
L= 1	0.95	0.97	0.94		
2	0.88	0.95	0.97	1.01	1.01
3	0.80	0.94	0.92		0.99
4	0.72	0.91	0.93	0.76	0.98
5	0.71	0.94	0.94		1.03
6	0.68	0.95			

Table 3 shows that the MAB deformation distances are close to unity and have no systematic L-dependence. At 64.3 MeV, the MAB method underestimates the deformation only by about 5%, while the AB values are strongly L-dependent and deviate considerably from unity for L>1. At 28 MeV, the AB cross section was calculated for L=2 and 4 only, because interpolation of radial integrals for odd L-values (we need $\beta_{\bar{\ell}\bar{\ell}}$ with $\bar{\ell} = n+\frac{1}{2}$, n integer) is not straightforward (see fig. 11). Again, the MAB method gives very good results.

Unnormalised angular distributions $\sigma(\theta)$ calculated by the three methods are shown in fig. 18 for 64.3 MeV α-particles with L = 2, 4, 6 and Q = o, and in fig. 19 for 28 MeV α-particles with L = 2,4 and Q = o. The agreement between the DW and MAB methods is again satisfactory.

We now enquire into what happens if SAM η_ℓ-functions are used in the modified Austern-Blair expression (6.8). For this purpose the experimental data (Bro 65) of 43-MeV α-particle scattering are chosen. A SAM analysis of the elastic cross section was performed with the η-functions given by eqs. (4.2) and (4.3). The parameters are found to be T = 17.14, Δ = 0.766, $\gamma/(4\Delta)$ = -0.166, $\mu_1/(4\Delta)$ = 0.297 and $\mu_2/(6\sqrt{3}\Delta^2)$ = -0.148. For the DWBA calculations, two of the four-parameter sets of ref. (Bro 65), referred to by set (1) and set (2), are used. A third potential (set (3)) is obtained by increasing the absorption of set (2). Set (3) gives a reasonable fit to the elastic angular distribution. The three potentials are summarized in table 4.

Table 4 OM potentials for 43-MeV α-particles

set	V (MeV)	W (MeV)	r_o (fm)	a (fm)
1	70	16.3	1.501	0.555
2	141.9	21.5	1.409	0.549
3	141.9	30	1.409	0.549

Taking Q = o and L = 2, relative deformation distances are extracted. The values are summarized in table 5.

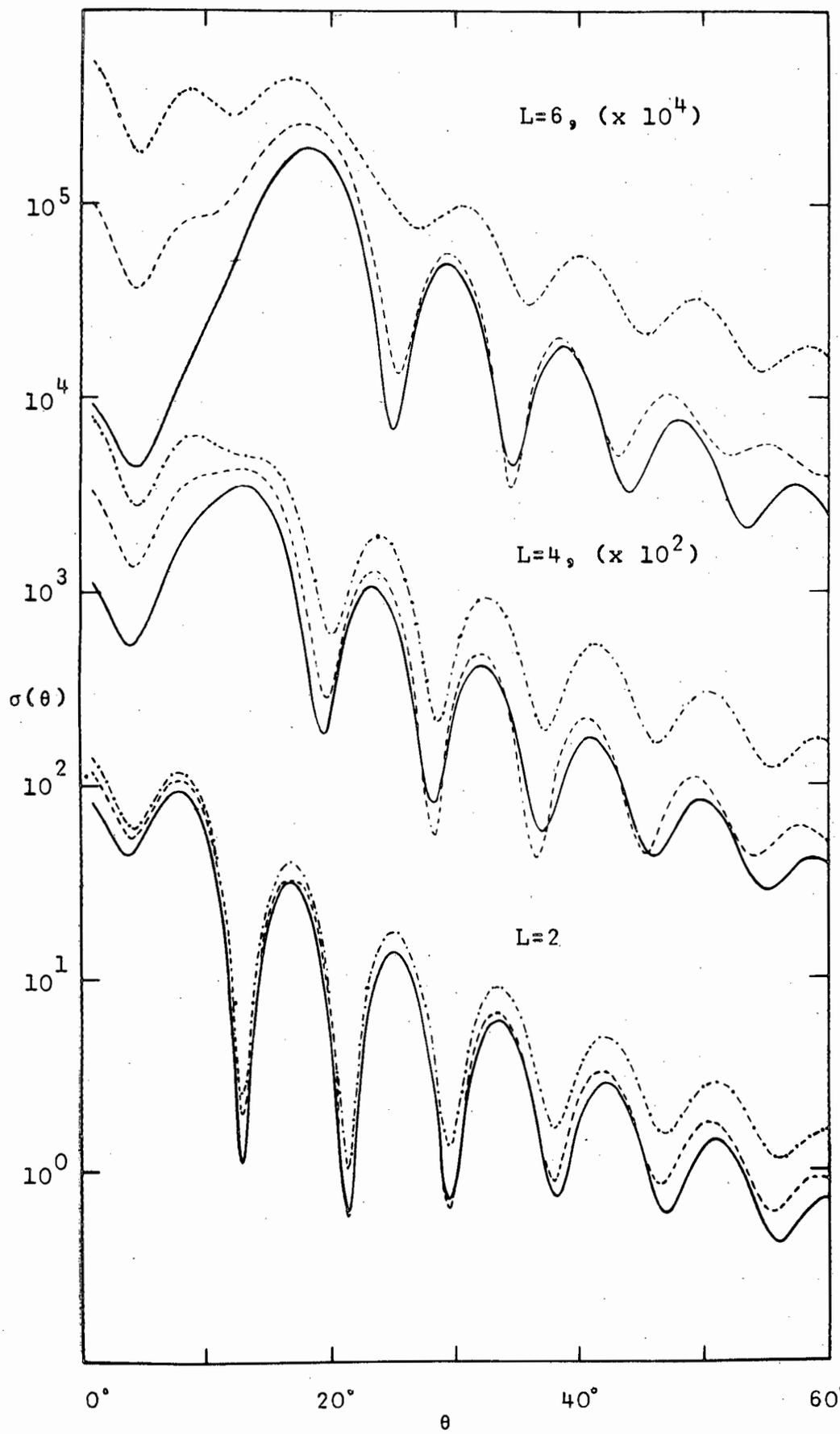

Fig.18. Inelastic differential cross sections for 64.3 MeV α-particles. The DWBA, MAB and AB calculations are shown by solid, dashed and dashed-dotted lines, respectively.

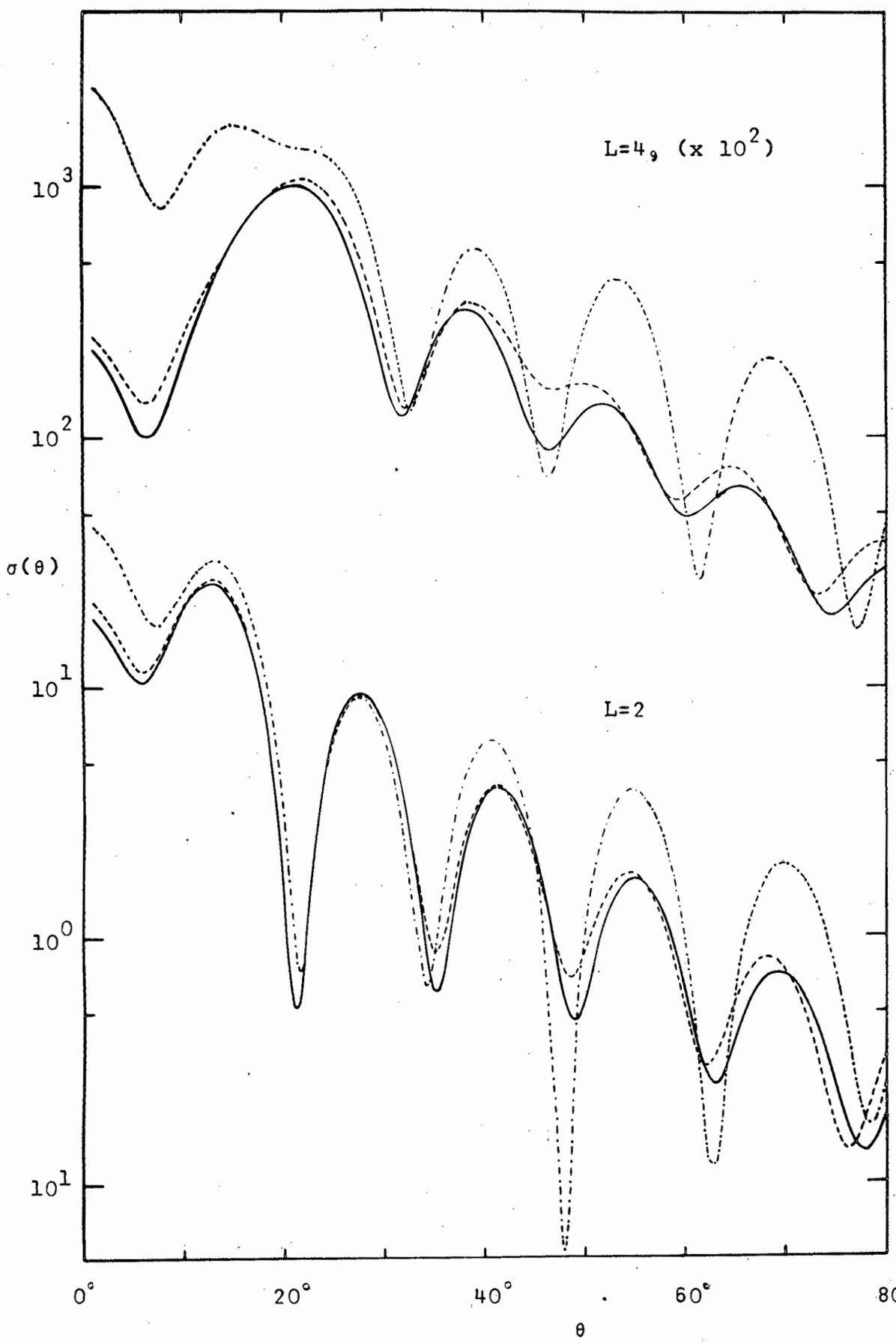

Fig.19. Inelastic differential cross sections for 28 MeV α-particles. The DWBA, MAB and AB calculations are shown by solid, dashed and dashed-dotted lines, respectively.

Table 5 Relative deformation distances

Method	DWBA			SAM	
	set (1)	set (2)	set (3)	AB	MAB
δ	1	1.025	1.03	0.85	0.99

We see from table 5 that the MAB again gives a very satisfactory result. We also see that the deformation distance is not very sensitive to the potential in DWBA calculations, even if the potential produces only a reasonable fit to the elastic cross section (set (3)).

As a further example, we have used the SAM parameters of ref. (Pot 66b) for the reaction $^{40}Ca\ (\alpha,\alpha')\ ^{40}Ca^{*}$, $L = 3$, $Q = -3.73$ MeV, and obtain $\delta(MAB) = 1.06$ fm. In ref. (Pot 66b) the value $\delta(AB) = 0.83$ fm is given. At 31 MeV the value $\delta(DW) = 1.08$ is obtained (Ber 66). This is in good agreement with our result.

For all cases studied the geometrical mean approximation (6.2) for off-diagonal radial integrals is found to be a satisfactory modification of the Austern-Blair theory for single excitation. In experiments to which SAM parameterisation can be applied we find agreement within about 5% between deformation parameters obtained by DWBA and by the modified Austern-Blair theory for all multipolarities.

7. SUMMARY

We have attempted to describe various aspects of elastic and inelastic scattering of strongly absorbed particles in terms of S-matrix rather than potential properties. However, optical model calculations were performed to enable us to make reasonable assumptions concerning the S-matrix elements.

At high energies, optical model calculations show that the elastic S-matrix elements η_ℓ are sufficiently smooth functions of ℓ to allow a simple parameterisation. This is particularly true for strongly absorptive potentials.

The cross section and polarisation for elastic scattering are expressed in terms of Fourier transforms of the derivatives of η_ℓ-functions. For a suitable choice of parameters in the assumed analytic forms of η_ℓ-functions, a Rodberg-type relation between the vector polarisation and the cross section is obtained. For spin-1 particles it is found, in the absence of tensor interactions, that the tensor polarisations t_{20} and t_{22} are related by $t_{20} = \sqrt{2/3}\, t_{22} \leq 0$ and that the tensor component t_{21} vanishes. Furthermore, for a Rodberg-type relation between the vector polarisation and the cross section, the oscillations in the angular distributions of the tensor components t_{20} and t_{22} and the cross section are shown to be in phase.

For one-phonon excitations the inelastic radial integrals are given in terms of the η_ℓ-coefficients by means of a suitable extension of the Austern-Blair theory which includes spin-orbit interactions. Approximations for the 3j- and 6j-symbols which appear in the partial wave expansions of the inelastic scattering amplitudes, enable us to express the angular distributions of the inelastic cross section and polarisation, again in terms of Fourier transforms of the derivatives of η_ℓ-functions.

A close resemblance between the elastic and inelastic angular distributions is observed. The Blair phase rule is shown to follow explicitly from the expressions for elastic and inelastic cross sections. The expressions for polarisation of spin-$\frac{1}{2}$ particles show, for instance, that a Rodberg-type relation for the polarisation of elastically scattered particles implies a similar relation for inelastic scattering. This means that we can extend the Blair phase rule to polarisation. This we state as follows. The oscillations in the angular distribution of the polarisation of elastically scattered strongly absorbed spin-$\frac{1}{2}$ particles are in-/out-of-phase for one-phonon excitations to odd/even parity levels.

The Austern-Blair theory, which is based on the adiabatic approximation, gives a satisfactory description of the differential cross sections for inelastic scattering from low-lying excited states. However, a number of experimental measurements of $(\alpha,\alpha'\gamma)$ correlation functions show characteristic deviations from the general adiabatic predictions. In order to describe these experiments, the Austern-Blair theory is modified by assuming that the radial integrals are given by the geometrical mean of the adiabatic diagonal radial integrals in the entrance and exit channels. The resulting expressions give an improved description of the experimental correlation functions. At the same time the modified expressions give nuclear deformation parameters which are in better agreement with the values obtained in distorted wave Born approximation.

APPENDIX A

In this appendix we briefly summarise the optical model programme which was used to calculate the η_ℓ-coefficients and radial integrals. The programme was coded in EMA for the Orion-II computer.

First, we consider the numerical integration of the Schrödinger equation (6.26) in the form

$$u_\ell''(\rho) + A_\ell(\rho)\, u_\ell(\rho) = 0 \,,$$
$$A_\ell(\rho) = 1 - \{U(r) + V(r)\}/E - \{\ell(\ell+1)\}/\rho^2 \,, \qquad \text{(A.1)}$$

where $\rho = kr$. Taking a constant integration step length h, we calculate $u(\rho+h)$ from

$$u_\ell(\rho+h) = \frac{\{2 - \frac{5}{6}h^2 A_\ell(\rho)\}\, u_\ell(\rho) - \{1 + \frac{1}{12}h^2 A_\ell(\rho-h)\}\, u_\ell(\rho-h)}{1 + \frac{1}{12}h^2 A_\ell(\rho+h)} \,. \qquad \text{(A.2)}$$

by starting at $\rho = h$, where we have

$$u_\ell(0) = 0 \quad , \quad u_\ell(h) = h^{\ell+1} \,. \qquad \text{(A.3)}$$

For very large ℓ-values, this starting point is advanced to larger values of ρ (Mel 65).

At the matching radius r_M (normally we take $r_M = R + 7a$) the interior wave function $u_\ell(\rho)$ is matched to the exterior wave function, eq. (2.27); thereby η_ℓ is determined.

The Coulomb functions are calculated in essentially the same way as described by Hodgson (Hod 63). The functions $F_\ell(\rho)$ and $G_\ell(\rho)$ are required to satisfy the Wronskian

$$F_\ell'(\rho)\, G_\ell(\rho) - F_\ell(\rho)\, G_\ell'(\rho) = 1 \,, \qquad \text{(A.4)}$$

to one part in 10^5 for all relevant ℓ-values.

The radial integrals were calculated by

$$\beta_{\ell\ell'}(k_i k_f) = \sum_{\lambda} h\, u_\ell(k_i r_\lambda)\, V(r_\lambda)\, u_{\ell'}(k_f r_\lambda) \quad . \qquad (A.5)$$

The interior wave functions are, of course, normalised.

APPENDIX B

In this appendix we derive relations for the quantities $E_{LM}(\pm\theta)$ defined by eq. (5.23) using properties of the rotation matrices $d^{L}_{MK}(\frac{1}{2}\pi)$ as given for instance in ref. (Bri 62).

From the definition of $E_{LM}(\pm\theta)$ eq. (5.23) we have

$$\sum_{M} \left| E_{LM}(\pm\theta) \right|^2 = \sum_{M,K,K'} i^{K-K'} d^{L}_{K'M}(\tfrac{1}{2}\pi)\, d^{L}_{K'0}(\tfrac{1}{2}\pi)\, d^{L}_{KM}(\tfrac{1}{2}\pi)\, d^{L}_{K0}(\tfrac{1}{2}\pi)\, e^{\pm i(K'-K)\theta/2} .$$

The summation over M can be performed by using the symmetry relation

$$d^{L}_{MK}(\tfrac{1}{2}\pi) = (-1)^{M-K} d^{L}_{KM}(\tfrac{1}{2}\pi) \qquad (B.1)$$

and the sum rule

$$\sum_{M} d^{L}_{MK'}(\tfrac{1}{2}\pi)\, d^{L}_{MK}(\tfrac{1}{2}\pi) = \delta_{K'K} . \qquad (B.2)$$

Afer summation K and K' we obtain

$$\sum_{M} \left| E_{LM}(\pm\theta) \right|^2 = 1 \qquad (B.3)$$

From eqs. (5.23) and (B.1) we have

$$E^{*}_{LM}(\theta)\, E_{LM}(-\theta) = \sum_{KK'} \left\{ i^{K-K'} d^{L}_{MK}(\tfrac{1}{2}\pi)\, d^{L}_{0K}(\tfrac{1}{2}\pi) \cdot d^{L}_{0K'}(\tfrac{1}{2}\pi)\, d^{L}_{MK'}(\tfrac{1}{2}\pi)\, e^{i\frac{1}{2}(K+K')\theta} \right\} . \qquad (B.4)$$

Applying the symmetry relation

$$d^{L}_{MK}(\tfrac{1}{2}\pi) = (-1)^{L+M} d^{L}_{M-K}(\tfrac{1}{2}\pi) \qquad (B.5)$$

to the first two d-matrix elements in eq. (B.4), and replacing -K by K, gives

$$E^{*}_{LM}(+\theta)\, E_{LM}(-\theta) = (-1)^{M} \sum_{KK'} (-1)^{K}\, i^{K'-K}\, d^{L}_{MK}(\tfrac{1}{2}\pi)\, d^{L}_{OK}(\tfrac{1}{2}\pi) \cdot d^{L}_{MK'}(\tfrac{1}{2}\pi)\, d^{L}_{OK'}(\tfrac{1}{2}\pi)\, e^{-i(K-K')\frac{1}{2}\theta} \,. \tag{B.6}$$

Due to the presence of $d^{L}_{OK}(\frac{1}{2}\pi)$, only terms with L + K even contribute to the sum. It follows that

$$E^{*}_{LM}(\theta)\, E_{LM}(-\theta) = (-1)^{L+M}\, |E_{LM}(-\theta)|^{2} \,. \tag{B.7}$$

Furthermore,

$$|E_{LM}(-\theta)|^{2} = |E_{LM}(\theta)|^{2} \,. \tag{B.8}$$

We finally list explicit expressions for $|E_{LM}(\theta)|^{2}$ for L = 0, 1, 2.

$$|E_{00}(\theta)|^{2} = 1 \,,$$

$$|E_{10}(\theta)|^{2} = \sin^{2}(\tfrac{1}{2}\theta) \,,$$

$$|E_{11}(\theta)|^{2} = |E_{1-1}(\theta)|^{2} = \tfrac{1}{2}\cos^{2}(\tfrac{1}{2}\theta) \,,$$

$$|E_{20}(\theta)|^{2} = \tfrac{1}{16}\{3\cos\theta - 1\}^{2} \,,$$

$$|E_{21}(\theta)|^{2} = |E_{2-1}(\theta)|^{2} = \tfrac{3}{8}\sin^{2}\theta \,,$$

$$|E_{22}(\theta)|^{2} = |E_{2-2}(\theta)|^{2} = \tfrac{3}{32}\{\cos\theta + 1\}^{2} \,.$$

REFERENCES

Als 66 : J. Alster, Phys. Rev. 141 (1966) 1138
J. Alster, D.C. Shreve and R.J. Peterson, Phys. Rev. 144 (1966) 999

Aus 61 : N. Austern, Ann. Phys. 15 (1961) 299

Aus 65 : N. Austern and J.S. Blair, Ann. Phys. 33 (1965) 15

Bas 65 : W.H. Bassichis and A. Dar, Phys. Rev. Lett. 14 (1965) 648

Ber 66 : A.M. Bernstein and E.P. Lippincott, Phys. Lett. 17 (1966) 321

Bin 66 : C.R. Bingham, M.L. Halbert and R.H. Bassel, Phys. Rev. 148 (1966) 1174

Bla 52 : J.M. Blatt and L.C. Biedenharn, Revs. Mod. Phys. 24 (1952) 258

Bla 54 : J.S. Blair, Phys. Rev. 95 (1954) 1218

Bla 59 : J.S. Blair, Phys. Rev. 115 (1959) 928

Bla 61 : J.S. Blair and L. Wilets, Phys. Rev. 121 (1961) 1493

Bla 62 : J.S. Blair, D. Sharp and L. Wilets, Phys. Rev. 125 (1962) 1625

Bla 65 : D.E. Blatchley and R.D. Bent, Nuclear Physics 61 (1965) 641

Bri 62 : D.M. Brink and G.R. Satchler, Angular Momentum (Clarendon Press, Oxford 1962)

Bro 65 : H.W. Broek, J.L. Yntema, B. Buck and G.R. Satchler, Nuclear Physics 64 (1965) 259

Bru 57 : P.J. Brussaard and H.A. Tolhoek, Physica 23 (1957) 955

Buc 61 : B. Buck and P.E. Hodgson, Phil. Mag. 6 (1961) 1371

Cal 63 : F. Calogero, Nuovo Cimento 27 (1963) 261

Cra 64 : J.G. Cramer, Jr. and W.W. Eidson, Nuclear Physics 55 (1964) 593

Dar 64 : P. Darriulat, G. Igo, H.G. Pugh, J.M. Meriwether and S. Yamabe, Phys. Rev. 134 (1964) B42

Dar 66 : A. Dar, Nuclear Physics 82 (1966) 354

Dri 63 : R.M. Drisko, G.R. Satchler and R.H. Bassel, Phys. Lett. 5 (1963) 347

Dro 55 : S.I. Drozdov, J. Exptl. Theoret. Phys. 28 (1955) 734 and 736 (translation : Soviet Phys. - JETP 1 (1955) 588 and 591)

Eid 64 : W.W. Eidson, J.G. Cramer, Jr., D.E. Blatchley and R.D. Bent, Nuclear Physics 55 (1964) 613

Fra 63 : W.E. Frahn and R.H. Venter, Ann. Phys. 24 (1963) 243

Fra 64a : W.E. Frahn and R.H. Venter, Ann. Phys. 27 (1964) 135

Fra 64b : W.E. Frahn and R.H. Venter, Nuclear Physics 59 (1964) 651

Fra 65a : W.E. Frahn and G. Wiechers, Nuclear Physics 74 (1965) 65

Fra 65b : W.E. Frahn, Nuclear Physics 75 (1965) 577

Fra 66a : W.E. Frahn, Proc. Second Int. Conference on Polarisation Phenomena of Nucleons, Karlsruhe, September 1965 (Birkhauser Verlag, Basel 1966)

Fra 66b : D.M. Fradkin and F. Calogero, Nuclear Physics 75 (1966) 475

Fri 66 : M.P. Fricke, R.M. Drisko, R.H. Bassel, E.E. Gross, B.J. Morton and A. Zucker, Phys. Rev. Lett. 16 (1966) 746

Frö 55 : C.E. Fröberg, Revs. Mod. Phys. 27 (1955) 399

Gol 64 : M.L. Goldberger and K.M. Watson, Collision Theory (John Wiley and Sons Inc. New York, London, Sydney 1964)

Hah 66 : F.J.W. Hahne, Nuclear Physics 80 (1966) 113

Hay 64 : R.M. Haybron, H. McManus, A. Werner, R.M. Drisko and G.R. Satchler, Phys. Rev. Lett. 12 (1964) 249

Hod 63 : P.E. Hodgson, The Optical Model of Elastic Scattering (Clarendon Press, Oxford 1963)

Hor 65 : D.J. Horen, J.R. Meriwether, G.B. Harvey, A. Bussiere de Nercy and J. Mahoney, Nuclear Physics 72 (1965) 97

Hüf 65 : J. Hüfner and A. de Shalit, Phys. Lett. 15 (1965) 52

Igo 59 : G. Igo, Phys. Rev. 115 (1959) 1665

Ing 64 : D.R. Inglis, Phys. Lett. 10 (1964) 336

Ing 66 : D.R. Inglis, Phys. Rev. 142 (1966) 591

Ing 67 : D.R. Inglis, preprint

Ino 57 : E.V. Inopin, J. Expt. Theoret. Phys. (U.S.S.R.) 31 (1956) 901 (translation: Soviet Phys. -JETP 4 (1957) 784)

Kla 66 : H. Klar and H. Krüger, Zeitschrift für Physik 191 (1966) 409

McD 62 : K.K. McDaniels, D.L. Hendrie, R.H. Bassel and G.R. Satchler, Phys. Lett 1 (1962) 295

Mel 65 : M.A. Melkanoff, J. Raynal and T. Sawada in Methods of Computational Physics Vol. 5 (Academic Press, New York and London, 1965)

Mer 66 : J.R. Meriwether, I. Gabrielli, D.L. Hendrie, J. Mahoney and B.G. Harvey, Phys. Rev. 146 (1966) 804

Mes 62 : A. Messiah, Quantum Mechanics Vol. 2 (North-Holland Publishing Co., Amsterdam 1962)

Pet 65 : R.J. Peterson, Phys. Rev. 140 (1965) B1479

Pot 66a : J.M. Potgieter and W.E. Frahn, Nuclear Physics 80 (1966) 434

Pot 66b : J.M. Potgieter and W.E. Frahn, Phys. Lett. 21 (1966) 211

Pot 66c : J.M. Potgieter, Private Communication

Pot 67a : J.M. Potgieter, PhD. thesis, University of Cape Town (unpublished)

Pot 67b : J.M. Potgieter and W.E. Frahn, Nuclear Physics, to be published

Raw 66 : G.H. Rawitscher, Nuclear Physics 85 (1966) 337

Ray 63 : J. Raynal, Phys. Lett. 7 (1963) 281

Ray 65 : J. Raynal, Rapport CEA-R2511, Centre D'Études Nucleaires de Scalay 1965

Rod 59 : L.S. Rodberg, Nuclear Physics 15 (1959) 72

Ros 62 : E. Rost, Phys. Rev. 128 (1962) 2708

Sat 60a : G.R. Satchler, Nuclear Physics 16 (1960) 674

Sat 60b : G.R. Satchler, Nuclear Physics 18 (1960) 110

Sat 60c : G.R. Satchler, Nuclear Physics 21 (1960) 116

Sat 64a : G.R. Satchler, Nuclear Physics 55 (1964) 1

Sat 64b : G.R. Satchler and R.M. Haybron, Phys. Lett. 11 (1964) 313

Sat 65 : G.R. Satchler, Nuclear Physics 70 (1965) 177

Saw 65 : T. Sawada, Nuclear Physics 74 (1965) 289

Spr 65 : A. Springer and B.G. Harvey, Phys. Lett. 14 (1965) 116

Ven 63 : R.H. Venter, Ann. Phys. 25 (1963) 405

Ven 64a : R.H. Venter and W.E. Frahn, Ann. Phys. 27 (1964) 385

Ven 64b : R.H. Venter and W.E. Frahn, Ann. Phys. 27 (1964) 401

Wol 54 : L. Wolfenstein, Phys. Rev. 96 (1954) 1654